POLITECNICO DI TORINO

CORSO DI LAUREA MAGISTRALE IN INGEGNERIA CIVILE

FUNICULARITY IN ELASTIC DOMES:

COUPLED EFFECTS OF SHAPE AND THICKNESS

Tesi di Laurea Magistrale

Relatore

Chiar.mo Prof. Ing. Alberto Carpinteri

Correlatori

Ill.mo Dr. Ing. Federico Accornero

Candidata

Ludovica Palma

22 Luglio 2021

CONTENTS

ABSTRACT

The present work aims to analyse the behaviour of thin or shallow shells in order to find a simple way for defining quantitatively the concept of Funicularity.

The first mention in the scientific literature about the condition of Funicularity was due to Dermot O'Dwyer, from Trinity College in Dublin, who describe the funicular analysis of masonry vaults. He started by studying arches in which the stress state can be represented with a line of thrust defined by a funicular polygon. This calculation procedure is quite simple when we deal with 2-D structures, i.e., arches, but it becomes more difficult when we deal with 3-D structures like shells. O'Dwyer proposes a method to evaluate the surface of thrust and to determinate the ultimate load of collapse This method consists of seven different steps that allow to find the force network by imposing two sets of constraints: the first set is related to the height of the structural nodes that should lie into the thickness of the element; the second set of constraints concerns the vertical equilibrium of the forces in each node. The method proposed by O'Dwyer allows the user to identify the collapse load factor, i.e., the geometric safety factor.

Then, O'Dwyer's idea has been improved by John A. Ochsendorf and his student Philippe Block, from MIT in Boston. Ochsendorf and Block designed a new type of analysis, the Thrust Network Analysis (TNA), starting from Maxwell's concept of reciprocal figures: "*Two plane figures are reciprocal when they consist of an equal number of lines, so that corresponding lines in the two figures are parallel, and corresponding lines which converge to a point in one figure form a closed polygon in the other".* Thus, there will be two figures, the primal grid Γ (the horizontal projection of the final solution, *G*, which will be the thrust network) and the dual grid Γ*, which can be considered the reciprocal of the former. As a matter of fact, the equilibrium of a node in Γ can be represented by a closed polygon in Γ* and vice versa.

Another approach to mention is the one proposed by Francesco Marmo and Luciano Rosati, from Federico II University in Naples. Their method is analogous to TNA, but they tried to simplify the process by considering only the primal grid and not the dual one. Consequently, they deleted some geometric hypothesis. Furthermore, they studied the problem of shells loaded by horizontal loads, in order to apply their method also in seismic areas. It is worth noting that in TNA, all the loads have to be vertical ones.

The abovementioned approaches are quite complex and tricky, employing a large number of equations to be solved. Therefore, the aim of the present thesis is to propose a simple and effective method to describe the surface of thrust governing the static behaviour of shell structures.

Our studies have been implemented by "SAP2000" FEM software: at first, it has been necessary to define the radius R, the height H, the number of divisions along the vertical axes Z, and the angular divisions of the shell mesh; then, the element type has been adopted by choosing "thick shell", which has been characterized by Concrete C28/35 material with E=32308 MPa and ν=0.2.

Thus, the parametric analysis has been performed by varying the shell relative thickness, t/2R, and the shallowness ratio, H/R, as in the following:

$H/R = \frac{5}{5}\ ; \frac{4}{5}\ ; \frac{3}{5}\ ; \frac{2}{5}\ ; \frac{1}{5}\ ,$

$t/2R = \frac{1}{15} ; \frac{1}{25} ; \frac{1}{40} ; \frac{1}{70} ; \frac{1}{100} ; \frac{1}{200} ; \frac{1}{500}.$

Finally, 35 finite element models have been obtained from the combination of these two dimensionless parameters.

From the SAP models, in which the shell structures are subjected to dead load only, we have obtained the bending moments and axial forces M_x, M_y, N_x and N_y for each shell node, from which it is possible to derive the eccentricities of the surface of thrust:

$e_x = \frac{M_x}{N_x}$,

$e_y = \frac{M_y}{N_y}$,

$e_{av} = \frac{e_x + e_y}{2}$,

From the analysis of the obtained surfaces of thrust, it is possible to observe that, by decreasing the shell relative thickness, the surface of thrust tends to overlap with the geometrical axis of the structure, particularly in the boundary constraint region: it means that, for each shallowness ratio, the bending moment acting at the shell supports tends to vanish.

1. THEORY OF SHELLS

1.1 Introduction

The theory of the modern shell developed in the nineteenth century. Cauchy, in 1828, was the first to study thin cylindrical shell. Poisson, the year after, started to analyse the shells of revolution and he defined the equations of a thin shell stressed by forces tangential to its surface. Then Lamé and Clapeyron studied the thin shell subjected to axially symmetrical loading.

Afterward many others analysed the shell elements: the mathematician Aron, on the basis of Kirchhoff's studies was the first to solve the problem of shell subjected by bending in a general term, Mathieu used the Poisson's equation to solve the problem of a shell of revolution and then, in 1993 Donnell defined a stress analysis of cylindrical shell.

1.1.1 Plate elements

To study the shell elements, we have to start by the definition of the plate elements.

Plates are structural elements where one dimension, the thickness, is negligible in comparison with the other two. Let us take into account a plate, characterized by a thickness *h,* constrained at the edges and with a distributed load *q* orthogonally applied to the faces (Fig. 1.1).

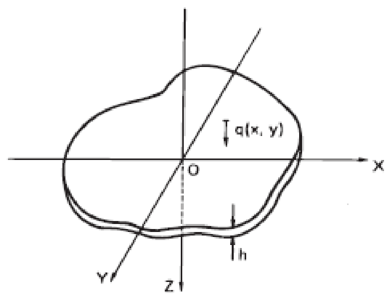

Figure 1.1

XY represents the middle plane of the plate and Z is the orthogonal axis. According to the Kirchoff's kinematic hypothesis, all the segments orthogonal to the middle plane, after a deformation, remain orthogonal to the deformed middle plane. If we consider a generic point P of the plate, whose coordinates are *x,y,z,* we observe that the displacement will have the following three components:

$$u = \varphi_x z = -\frac{\partial w}{\partial x} z \tag{1.1a}$$

$$v = \varphi_y z = -\frac{\partial w}{\partial y} z \tag{1.1b}$$

$$w = w(x, y) z \tag{1.1c}$$

Where: φ_x is the angle of rotation about the Y axis;

φ_y is the angle of rotation about the X axis.

With a derivation of the displacements, we can obtain the strain field:

$$\varepsilon_x = \frac{\partial u}{\partial x} = \frac{\partial \varphi_x}{\partial x} z = -\frac{\partial^2 w}{\partial x^2} z \tag{1.2a}$$

$$\varepsilon_y = \frac{\partial u}{\partial y} = \frac{\partial \varphi_y}{\partial y} z = -\frac{\partial^2 w}{\partial y^2} z \tag{1.2b}$$

$$\varepsilon_z = \frac{\partial w}{\partial z} = 0 \tag{1.2c}$$

$$\gamma_{xy} = \frac{\partial u}{\partial y} + \frac{\partial v}{\partial x} = \left(\frac{\partial \varphi_x}{\partial y} + \frac{\partial \varphi_y}{\partial x}\right) z = -2 \frac{\partial^2 w}{\partial x \partial y} z \tag{1.2d}$$

$$\gamma_{yz} = \frac{\partial v}{\partial z} + \frac{\partial w}{\partial y} = 0 \tag{1.2e}$$

$$\gamma_{xz} = \frac{\partial u}{\partial z} + \frac{\partial w}{\partial x} = 0 \tag{1.2f}$$

It is noticed, from previous equations that there is a condition of plane strain, which derives from the Kirchoff's kinematic hypothesis. The three components of the strain, different from zero, can be expressed as follows:

$$\varepsilon_x = \chi_x z \tag{1.3a}$$

$$\varepsilon_y = \chi_y z \tag{1.3b}$$

$$\gamma_{xy} = \chi_{xy} z \tag{1.3c}$$

Where χ_x and χ_y are the flexural curvatures of the middle plane, respectively, in *x* and *y* directions, and χ_{xy} is twice the unit angle of torsion of the middle plane in the *x* and *y* directions.

For the condition of plane stress, the constitutive relations become

$$\varepsilon_x = \frac{1}{E}\left(\sigma_x - \nu\sigma_y\right) \tag{1.4a}$$

$$\varepsilon_y = \frac{1}{E}\left(\sigma_y - \nu\sigma_x\right) \tag{1.4b}$$

$$\gamma_{xy} = \frac{1}{G}\tau_{xy} \tag{1.4c}$$

In these equations the stress σ_z is neglected, because the thickness *h* is small and so this one become so little to be negligible. By a simple addition, and considering the Equations 1.3 we can obtain the final expressions of the stress field of the plate:

$$\sigma_x = \frac{E}{1-\nu^2} \tag{1.5a}$$

$$\sigma_y = \frac{E}{1-\nu^2}\left(\chi_y + \nu\chi_x\right)z \tag{1.5b}$$

$$\tau_{xy} = \frac{E}{2(1-\nu)}\chi_{xy} z \tag{1.5c}$$

Then, to obtain the characteristics of the internal reaction, it is necessary to integrate the stresses σ_x, σ_y and τ_{xy} over the thickness :

$$M_x = \int_{-h/2}^{h/2} \sigma_x z \, dz \tag{1.6a}$$

$$M_y = \int_{-h/2}^{h/2} \sigma_y z \, dz \tag{1.6b}$$

$$M_{xy} = M_{yx} = \int_{-h/2}^{h/2} \tau_{xy} z \, dz \tag{1.6c}$$

M_x and M_y are the bending moments per unit length and M_{xy} is the twisting moment per unit length.

Substituting the definition of the stress field in the Equations 1.6, and considering D, as the flexural rigidity of the plate, we have:

$$M_x = D(\chi_x + \nu\chi_y) \tag{1.7a}$$

$$M_y = D(\chi_y + \nu\chi_x) \tag{1.7b}$$

$$M_{xy} = M_{yx} = \frac{1-\nu}{2} D\chi_{xy} \tag{1.7c}$$

Where

$$D = \frac{Eh^3}{12(1-\nu^2)} \tag{1.8}$$

Let us consider an infinitesimal element of the plate loaded by an external load q. The indefinite equations of equilibrium can be obtained by imposing the equilibrium with regard to rotation about the y axis (Figure 1.2a) and the equilibrium with regard to translation in the direction of the z axis (Figure 1.2b). Considering that the plate is not loaded by forces that belong to the middle plane, the remaining three conditions of equilibrium, the rotation about the z axis and the translation in the x and y direction are identically satisfied.

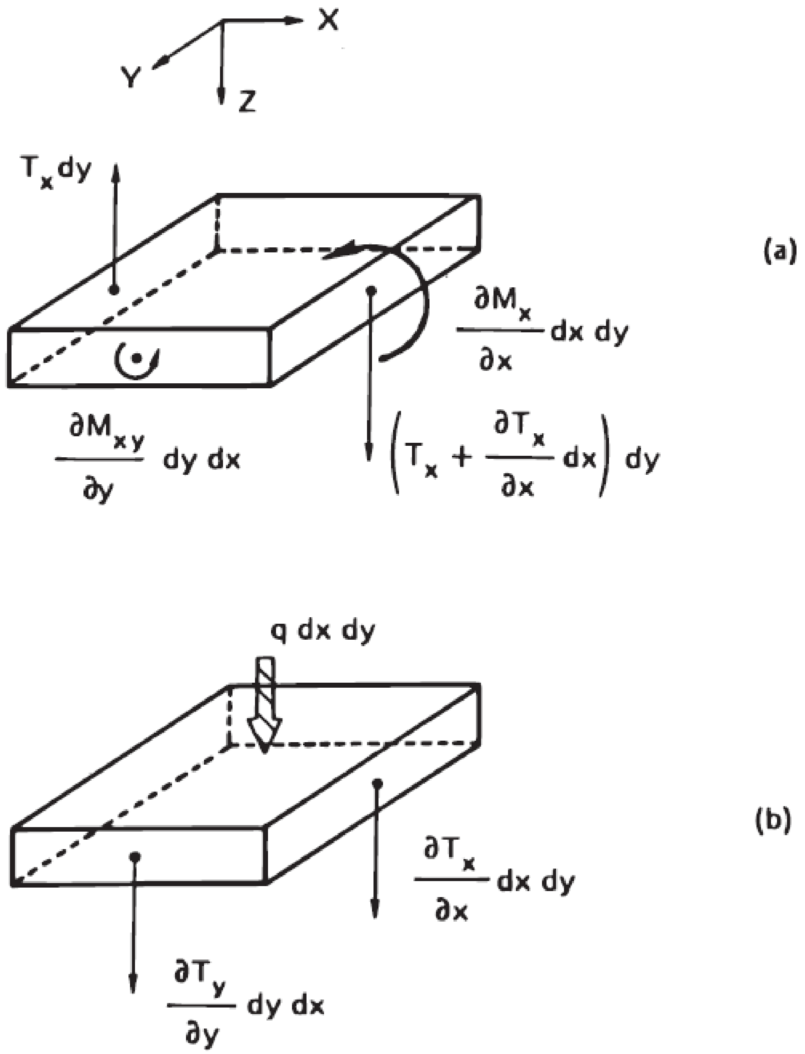

Figure 1.2

$$\frac{\partial M_x}{\partial x} + \frac{\partial M_{xy}}{\partial y} - T_x = 0 \tag{1.9a}$$

$$\frac{\partial M_{xy}}{\partial x} + \frac{\partial M_y}{\partial y} - T_y = 0 \tag{1.9b}$$

$$\frac{\partial T_x}{\partial x} + \frac{\partial T_y}{\partial y} + q = 0 \tag{1.9a}$$

The static equations can be presented in the following matrix form

$$\begin{bmatrix} \frac{\partial}{\partial x} & \frac{\partial}{\partial y} & 0 & 0 & 0 \\ -1 & 0 & \frac{\partial}{\partial x} & 0 & \frac{\partial}{\partial y} \\ 0 & -1 & 0 & \frac{\partial}{\partial y} & \frac{\partial}{\partial x} \end{bmatrix} \begin{bmatrix} T_x \\ T_y \\ M_x \\ M_y \\ M_{xy} \end{bmatrix} + \begin{bmatrix} q \\ 0 \\ 0 \end{bmatrix} = \begin{bmatrix} 0 \\ 0 \\ 0 \end{bmatrix} \tag{1.11}$$

Moreover, also the kinematic equations can be expressed in a matrix form, in which the deformations are defined as functions of generic displacements

$$\begin{bmatrix} \gamma_x \\ \gamma_y \\ \chi_x \\ \chi_y \\ \chi_{xy} \end{bmatrix} = \begin{bmatrix} \frac{\partial}{\partial x} & +1 & 0 \\ \frac{\partial}{\partial y} & 0 & +1 \\ 0 & \frac{\partial}{\partial x} & 0 \\ 0 & 0 & \frac{\partial}{\partial y} \\ 0 & \frac{\partial}{\partial y} & \frac{\partial}{\partial x} \end{bmatrix} \begin{bmatrix} w \\ \varphi_x \\ \varphi_y \end{bmatrix} \tag{1.12}$$

So, analysing the two matrixes, we can observe a duality between the static and kinematic matrix operators, expressed by the fact that the static matrix is the transpose of the kinematic matrix and vice versa (with the only exception of the algebraic sign of the unity terms).

It is also possible to express the constitutive equations in a matrix form:

$$\begin{bmatrix} T_x \\ T_y \\ M_x \\ M_y \\ M_{xy} \end{bmatrix} = \begin{bmatrix} \frac{5}{6}Gh & 0 & 0 & 0 & 0 \\ 0 & \frac{5}{6}Gh & 0 & 0 & 0 \\ 0 & 0 & D & \nu D & 0 \\ 0 & 0 & \nu D & D & 0 \\ 0 & 0 & 0 & 0 & \frac{1-\nu}{2}D \end{bmatrix} \begin{bmatrix} \gamma_x \\ \gamma_y \\ \chi_x \\ \chi_y \\ \chi_{xy} \end{bmatrix} \tag{1.13}$$

Where 5/6 is the inverse of the shear factor evaluated for a rectangular cross section, characterised by a height *h* and a unit base.

The kinematic, static and the constitutive equations can be defined in the following compact form:

$$\{q\} = [\partial]\{\eta\} \tag{1.14a}$$

$$[\partial]^{*}\{Q\} + \{\mathcal{F}\} = \{0\} \tag{1.14b}$$

$$\{Q\} = [H]\{q\} \tag{1.14c}$$

1.1.2 Shell elements

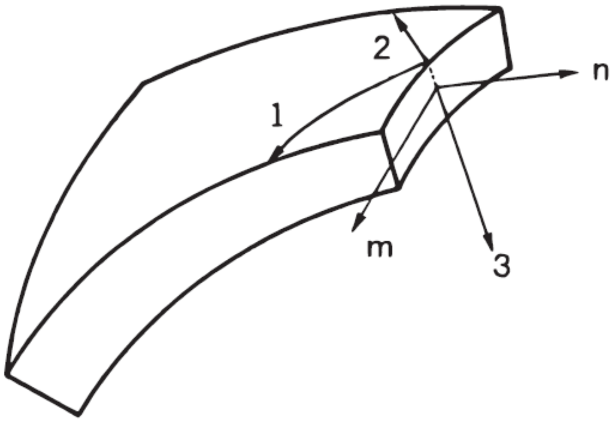

Figure 1.3

Let us consider the shell in the figure 1.3, which is characterized by a thickness h and a double curvature. It is possible to identify a system of principal curvilinear coordinates s_1 and s_2 (Figure 1.3).

We can consider two different regimes: the membrane and the flexural ones. In the membrane regime we have the presence of normal forces N_1 and N_2 (Figure 1.4a), with the correspondent dilatations ε_1 and ε_2, the shearing force N_{12} with the shearing strain ε_{12} between the principal directions of curvature. In the flexural regime is possible to identify the shearing forces T_1 and T_2, perpendicular to the tangent plane, the bending moments M_1 and M_2 and the twisting moment M_{12} (Figure 1.4b), with the correspondent shearing strains γ_1 and γ_2 between each principal direction of the curvature and the direction normal to the plane, the flexural curvatures χ_1, χ_2 and twice the unit angle of torsion χ_{12}.

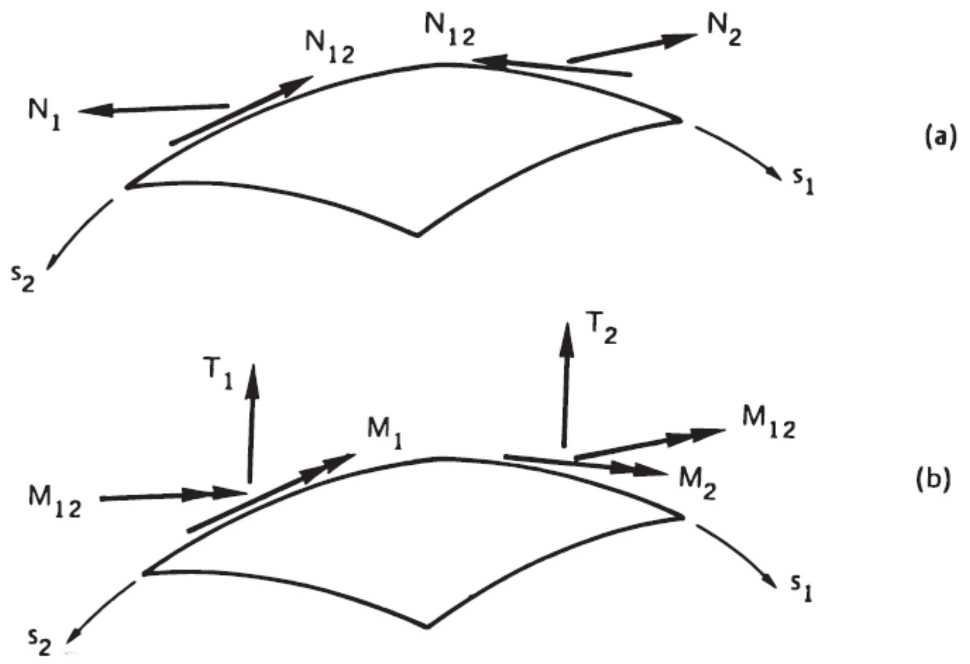

Figure 1.4

The characteristics of deformations that can be described as a function of the generalized displacements by the kinematic equations, are expressed by the following matrix form:

$$\begin{bmatrix} \varepsilon_1 \\ \varepsilon_2 \\ \varepsilon_{12} \\ \gamma_1 \\ \gamma_2 \\ \chi_1 \\ \chi_2 \\ \chi_{12} \end{bmatrix} = \begin{bmatrix} \dfrac{\partial}{\partial s_1} & +\dfrac{R_2}{R_1(R_2-R_1)}\dfrac{\partial R_1}{\partial s_2} & +\dfrac{1}{R_1} \\ +\dfrac{R_1}{R_2(R_1-R_2)}\dfrac{\partial R_2}{\partial s_1} & \dfrac{\partial}{\partial s_2} & +\dfrac{1}{R_2} \\ \dfrac{\partial}{\partial s_2}-\dfrac{R_2}{R_1(R_2-R_1)}\dfrac{\partial R_1}{\partial s_2} & \dfrac{\partial}{\partial s_1}-\dfrac{R_1}{R_2(R_1-R_2)}\dfrac{\partial R_2}{\partial s_1} & 0 \\ -\dfrac{1}{R_1} & 0 & \dfrac{\partial}{\partial s_1} \\ 0 & \dfrac{1}{R_2} & \dfrac{\partial}{\partial s_2} \\ 0 & 0 & 0 \\ 0 & 0 & 0 \\ 0 & 0 & 0 \end{bmatrix}$$

$$
\left.\begin{array}{cc}
0 & 0 \\
0 & 0 \\
0 & 0 \\
+1 & 0 \\
0 & +1 \\
\dfrac{\partial}{\partial s_1} & +\dfrac{R_2}{R_1(R_2-R_1)}\dfrac{\partial R_1}{\partial s_2} \\
+\dfrac{R_1}{R_2(R_1-R_2)}\dfrac{\partial R_2}{\partial s_1} & \dfrac{\partial}{\partial s_2} \\
\dfrac{\partial}{\partial s_2}-\dfrac{R_2}{R_1(R_2-R_1)}\dfrac{\partial R_1}{\partial s_2} & \dfrac{\partial}{\partial s_1}-\dfrac{R_1}{R_2(R_1-R_2)}\dfrac{\partial R_2}{\partial s_1}
\end{array}\right]
\begin{bmatrix} u_1 \\ u_2 \\ u_3 \\ \varphi_1 \\ \varphi_2 \end{bmatrix}
\tag{1.15}
$$

Where u are the components of displacement in the direction 1,2 and 3; φ are the rotation about the directions of curvature 1,2 and R_1 and R_2 are the two principal radii of curvature.

Through the equilibrium to the translation in the directions 1,2,3 and the equilibrium to the rotation about the axes 1,2 we obtain five equations that express the indefinite equations of equilibrium (1.16).

$$
\left[\begin{array}{ccc}
\dfrac{\partial}{\partial s_1}+\dfrac{R_1}{R_2(R_1-R_2)}\dfrac{\partial R_2}{\partial s_1} & -\dfrac{R_1}{R_2(R_1-R_2)}\dfrac{\partial R_2}{\partial s_1} & \dfrac{\partial}{\partial s_2}+\dfrac{2R_2}{R_1(R_2-R_1)}\dfrac{\partial R_1}{\partial s_2} \\
-\dfrac{R_2}{R_1(R_2-R_1)}\dfrac{\partial R_1}{\partial s_2} & \dfrac{\partial}{\partial s_2}+\dfrac{R_2}{R_1(R_2-R_1)}\dfrac{\partial R_1}{\partial s_2} & \dfrac{\partial}{\partial s_1}+\dfrac{R_1}{R_2(R_1-R_2)}\dfrac{\partial R_2}{\partial s_1} \\
-\dfrac{1}{R_1} & -\dfrac{1}{R_2} & 0 \\
0 & 0 & 0 \\
0 & 0 & 0
\end{array}\right.
$$

$$
\begin{array}{ccc}
+\dfrac{1}{R_1} & 0 & 0 \\
0 & +\dfrac{1}{R_2} & 0 \\
\dfrac{\partial}{\partial s_1}+\dfrac{R_1}{R_2(R_1-R_2)}\dfrac{\partial R_2}{\partial s_1} & \dfrac{\partial}{\partial s_2}+\dfrac{R_2}{R_1(R_2-R_1)}\dfrac{\partial R_1}{\partial s_2} & 0 \\
-1 & 0 & \dfrac{\partial}{\partial s_1}+\dfrac{R_1}{R_2(R_1-R_2)}\dfrac{\partial R_2}{\partial s_1} \\
0 & -1 & -\dfrac{R_2}{R_1(R_2-R_1)}\dfrac{\partial R_1}{\partial s_2}
\end{array}
$$

$$
\left.\begin{matrix}
0 & 0 \\
0 & 0 \\
0 & 0 \\
-\dfrac{R_1}{R_2(R_1-R_2)}\dfrac{\partial R_2}{\partial s_1} & \dfrac{\partial}{\partial s_2}+\dfrac{2R_2}{R_1(R_2-R_1)}\dfrac{\partial R_1}{\partial s_2} \\
\dfrac{\partial}{\partial s_2}+\dfrac{R_2}{R_1(R_2-R_1)}\dfrac{\partial R_1}{\partial s_2} & \dfrac{\partial}{\partial s_1}+\dfrac{2R_1}{R_2(R_1-R_2)}\dfrac{\partial R_1}{\partial s_1}
\end{matrix}\right]
\begin{bmatrix} N_1 \\ N_2 \\ N_{12} \\ T_1 \\ T_2 \\ M_1 \\ M_2 \\ M_{12} \end{bmatrix}
+\begin{bmatrix} p_1 \\ p_2 \\ q \\ m_1 \\ m_2 \end{bmatrix}
=\begin{bmatrix} 0 \\ 0 \\ 0 \\ 0 \\ 0 \end{bmatrix}
\tag{1.16}
$$

At last, to completely describe the problem, we can define the constitutive equations in the following matrix form:

$$
\begin{bmatrix} N_1 \\ N_2 \\ N_{12} \\ T_1 \\ T_2 \\ M_1 \\ M_2 \\ M_{12} \end{bmatrix}
=\begin{bmatrix}
\frac{12D}{h^2} & \nu\frac{12D}{h^2} & 0 & 0 & 0 & 0 & 0 & 0 \\
\nu\frac{12D}{h^2} & \frac{12D}{h^2} & 0 & 0 & 0 & 0 & 0 & 0 \\
0 & 0 & \frac{1-\nu}{2}\frac{12D}{h^2} & 0 & 0 & 0 & 0 & 0 \\
0 & 0 & 0 & (1-\nu)\frac{5D}{h^2} & 0 & 0 & 0 & 0 \\
0 & 0 & 0 & 0 & (1-\nu)\frac{5D}{h^2} & 0 & 0 & 0 \\
0 & 0 & 0 & 0 & 0 & D & \nu D & 0 \\
0 & 0 & 0 & 0 & 0 & \nu D & D & 0 \\
0 & 0 & 0 & 0 & 0 & 0 & 0 & \frac{1-\nu}{2}D
\end{bmatrix}
\begin{bmatrix} \varepsilon_1 \\ \varepsilon_2 \\ \varepsilon_{12} \\ \gamma_1 \\ \gamma_2 \\ \chi_1 \\ \chi_2 \\ \chi_{12} \end{bmatrix}
\tag{1.17}
$$

1.1.3 Shell of revolution

A shell of revolution is generated by a complete rotation of the plane curve *r(z)* about the axis of symmetry Z (Figure 1.5).

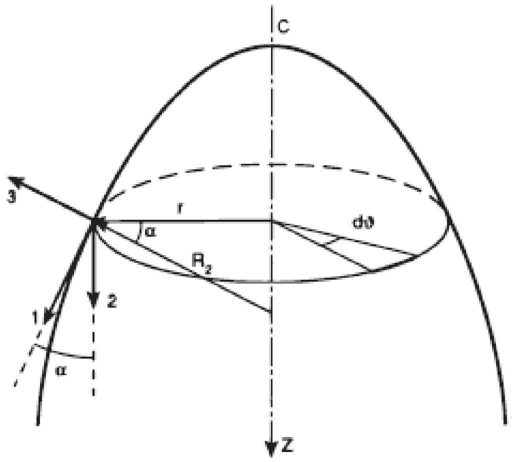

Figure 1.5

In the shell of revolution we identify the meridians and the parallels: the meridians are generated by the rotation of the generating curve *r(z),* the parallels are generated by the circular trajectories, described by each point of the shell. Considering the meridian and the parallels we can define a system of principal curvilinear coordinates s_1 and s_2, where s_1 is the curvilinear coordinate along the meridians and s_2 is the curvilinear coordinate along the parallels.

The kinematic equations of non-symmetrically loaded shell of revolution can be represented as follows:

$$\begin{bmatrix} \varepsilon_s \\ \varepsilon_\vartheta \\ \gamma_s \\ \gamma_\vartheta \\ \gamma_{s\vartheta} \\ \chi_s \\ \chi_\vartheta \\ \chi_{s\vartheta} \end{bmatrix} = \begin{bmatrix} \frac{\partial}{\partial s} & 0 & +\frac{1}{R_1} & 0 & 0 \\ +\frac{\sin\alpha}{r} & \frac{1}{r}\frac{\partial}{\partial\vartheta} & +\frac{1}{R_2} & 0 & 0 \\ \frac{1}{r}\frac{\partial}{\partial\vartheta} & \left(\frac{\partial}{\partial s}-\frac{\sin\alpha}{r}\right) & 0 & 0 & 0 \\ -\frac{1}{R_1} & 0 & \frac{\partial}{\partial s} & +1 & 0 \\ 0 & -\frac{1}{R_2} & \frac{1}{r}\frac{\partial}{\partial\vartheta} & 0 & +1 \\ 0 & 0 & 0 & \frac{\partial}{\partial s} & 0 \\ 0 & 0 & 0 & +\frac{\sin\alpha}{r} & \frac{1}{r}\frac{\partial}{\partial\vartheta} \\ 0 & 0 & 0 & \frac{1}{r}\frac{\partial}{\partial\vartheta} & \left(\frac{\partial}{\partial s}-\frac{\sin\alpha}{r}\right) \end{bmatrix} \begin{bmatrix} u \\ v \\ w \\ \varphi_s \\ \varphi_\vartheta \end{bmatrix} \tag{1.18}$$

Also the static equations can be represented in the following matrix form:

$$\begin{bmatrix} \left(\frac{\partial}{\partial s}+\frac{\sin\alpha}{r}\right) & -\frac{\sin\alpha}{r} & \frac{1}{r}\frac{\partial}{\partial\vartheta} & +\frac{1}{R_1} & 0 & 0 & 0 & 0 \\ 0 & \frac{1}{r}\frac{\partial}{\partial\vartheta} & \left(\frac{\partial}{\partial s}+\frac{2\sin\alpha}{r}\right) & 0 & +\frac{1}{R_2} & 0 & 0 & 0 \\ -\frac{1}{R_1} & -\frac{1}{R_2} & 0 & \left(\frac{\partial}{\partial s}+\frac{\sin\alpha}{r}\right) & \frac{1}{r}\frac{\partial}{\partial\vartheta} & 0 & 0 & 0 \\ 0 & 0 & 0 & -1 & 0 & \left(\frac{\partial}{\partial s}+\frac{\sin\alpha}{r}\right) & -\frac{\sin\alpha}{r} & \frac{1}{r}\frac{\partial}{\partial\vartheta} \\ 0 & 0 & 0 & 0 & -1 & 0 & \frac{1}{r}\frac{\partial}{\partial\vartheta} & \left(\frac{\partial}{\partial s}+\frac{2\sin\alpha}{r}\right) \end{bmatrix}$$

$$\begin{bmatrix} N_s \\ N_\vartheta \\ N_{s\vartheta} \\ T_s \\ T_\vartheta \\ M_s \\ M_\vartheta \\ M_{s\vartheta} \end{bmatrix} + \begin{bmatrix} p_s \\ p_\vartheta \\ q \\ m_s \\ m_\vartheta \end{bmatrix} = \begin{bmatrix} 0 \\ 0 \\ 0 \\ 0 \\ 0 \end{bmatrix} \tag{1.19}$$

From the equation 1.19 we can notice that we have five equations of equilibrium in eight static unknowns, so the elastic problem has three degrees of internal redundancy.

1.1.4 Symmetrically loaded shell of revolution

Now we take into account the case of a shell of revolution, symmetrically loaded with respect to axis Z.

With regards to static equations, the conditions of equilibrium to translation along the parallels and to rotation around the meridians disappear, because they are identically satisfied, for reason of symmetry. So we can obtain the following static equations considering the conditions of the Figure 1.6.

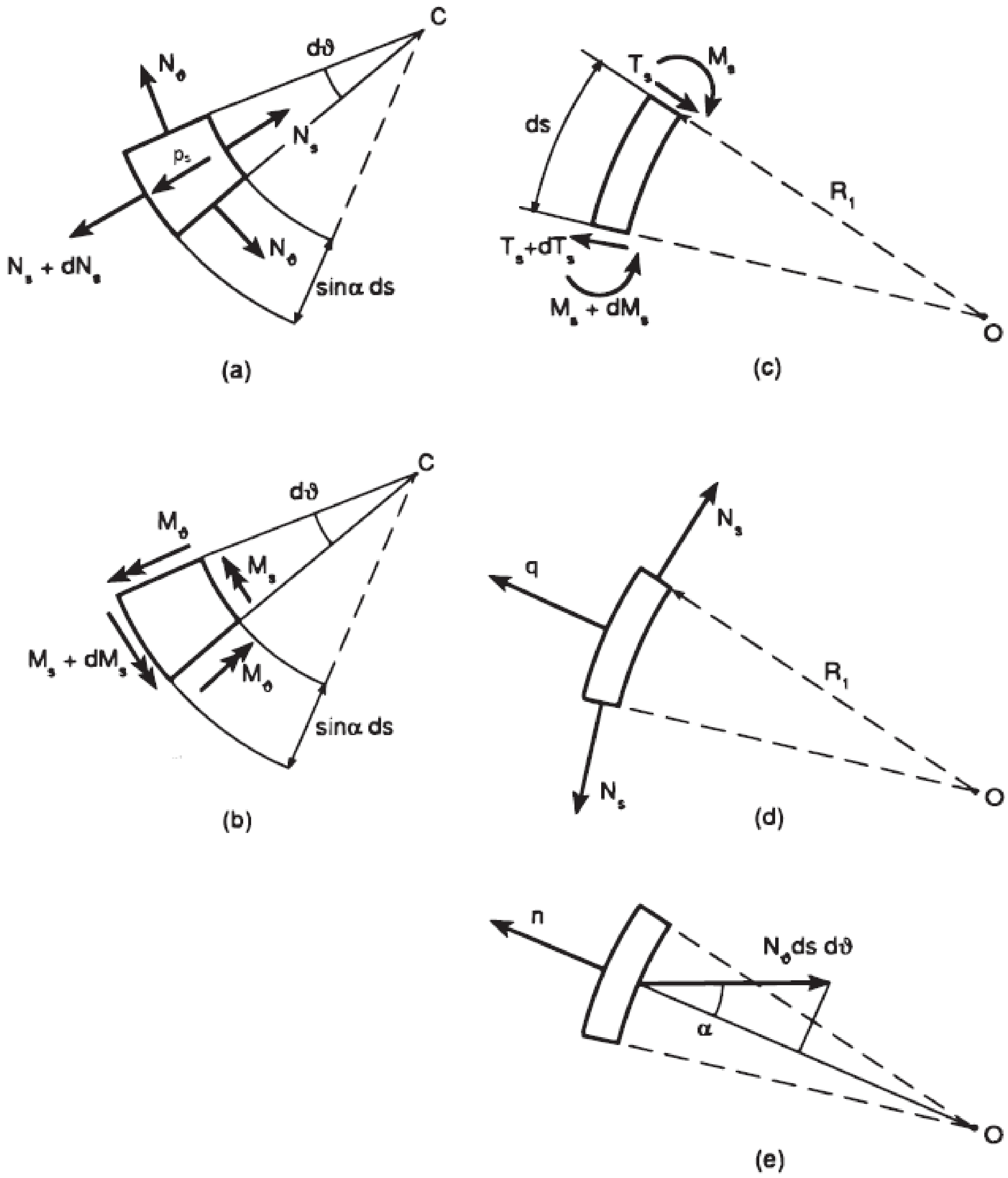

Figure 1.6

First, we impose the equilibrium to translation along the meridians

$$dN_s r \mathrm{d}\vartheta + N_s \mathrm{d}r\mathrm{d}\vartheta - N_\vartheta \sin\alpha \mathrm{d}s\mathrm{d}\vartheta + T_s \frac{\mathrm{d}s}{R_1} r\mathrm{d}\vartheta + p_s r\mathrm{d}s\mathrm{d}\vartheta = 0 \qquad (1.20a)$$

Secondly, imposing the equilibrium with regard to translation along the normal *n* we will have:

$$-N_s \frac{\mathrm{d}s}{R_1} r\mathrm{d}\vartheta - N_\vartheta \mathrm{d}s\mathrm{d}\vartheta\cos\alpha + dT_s r\mathrm{d}\vartheta + T_s \mathrm{d}r\mathrm{d}\vartheta + qr\mathrm{d}s\mathrm{d}\vartheta = 0 \qquad (1.20b)$$

For the third equation we can impose the equilibrium with regard to rotation about the parallels:

$$-T_s r \mathrm{d}\vartheta \mathrm{ds} + dM_s r \mathrm{d}\vartheta + M_s \mathrm{d}r \mathrm{d}\vartheta - M_\vartheta \sin\alpha \mathrm{ds} \mathrm{d}\vartheta + m_s r \mathrm{d}\vartheta \mathrm{ds} = 0 \tag{1.20c}$$

If we divide the Equations 1.20 by $r\mathrm{d}s\mathrm{d}\vartheta$ and represent these ones in a matrix form, we obtain the static equations:

$$\begin{bmatrix} \left(\frac{\mathrm{d}}{\mathrm{d}s} + \frac{\sin\alpha}{r}\right) & -\frac{\sin\alpha}{r} & \frac{1}{R_1} & 0 & 0 \\ -\frac{1}{R_1} & -\frac{1}{R_2} & \left(\frac{\mathrm{d}}{\mathrm{d}s} + \frac{\sin\alpha}{r}\right) & 0 & 0 \\ 0 & 0 & -1 & \left(\frac{\mathrm{d}}{\mathrm{d}s} + \frac{\sin\alpha}{r}\right) & -\frac{\sin\alpha}{r} \end{bmatrix} \begin{bmatrix} N_s \\ N_\vartheta \\ T_s \\ M_s \\ M_\vartheta \end{bmatrix} + \begin{bmatrix} p_s \\ q \\ m_s \end{bmatrix} = \begin{bmatrix} 0 \\ 0 \\ 0 \end{bmatrix} \tag{1.21}$$

in this case of symmetry, it is possible to observe that we have three equations in five unknowns, so introducing the symmetry, the redundancy is reduced from three to two degrees.

However, the kinematic equations can be obtained by applying the principle of virtual work.

$$\begin{bmatrix} \varepsilon_s \\ \varepsilon_\vartheta \\ \gamma_s \\ \chi_s \\ \chi_\vartheta \end{bmatrix} = \begin{bmatrix} \frac{\mathrm{d}}{\mathrm{d}s} & \frac{1}{R_1} & 0 \\ +\frac{\sin\alpha}{r} & \frac{1}{R_2} & 0 \\ -\frac{1}{R_1} & \frac{\mathrm{d}}{\mathrm{d}s} & +1 \\ 0 & 0 & \frac{\mathrm{d}}{\mathrm{d}s} \\ 0 & 0 & \frac{\sin\alpha}{r} \end{bmatrix} \begin{bmatrix} u \\ w \\ \varphi_s \end{bmatrix} \tag{1.22}$$

We will see how to obtain kinematic equations from the static ones in the Paragraph 1.4 “Static-kinematic duality”.

1.1.5 Thin shells and membranes

Thin shells are shells of such a small thickness that they have a negligible flexural rigidity, which can sustain only compressive forces contained in the tangent plane, so they have a zero tensile stiffness. Whereas membranes are two-dimensional structural elements without flexural rigidity, that can sustain only tensile forces contained in the tangent plane, so they have a zero compressive stiffness. Consequently, we can say that the thin shells and the membranes are one the opposite of the other, but, for different reasons, they both have a zero flexural rigidity.

These two elements are also similar, because they both present only forces along the meridians and the parallels N_s and N_ϑ, and only the displacement along the meridians, u and the displacements w, perpendicular to the middle surface.

Considering these assumptions, the kinematic and static equations of the membranes and thin shells of revolution are simpler than the 1.21 and 1.22

$$\begin{bmatrix} \varepsilon_s \\ \varepsilon_\vartheta \end{bmatrix} = \begin{bmatrix} \frac{\mathrm{d}}{\mathrm{d}s} & \frac{1}{R_1} \\ \frac{\sin\alpha}{r} & \frac{1}{R_2} \end{bmatrix} \begin{bmatrix} u \\ w \end{bmatrix} \tag{1.23a}$$

$$\begin{bmatrix} \left(\frac{\mathrm{d}}{\mathrm{d}s} + \frac{\sin\alpha}{r}\right) & -\frac{\sin\alpha}{r} \\ -\frac{1}{R_1} & -\frac{1}{R_2} \end{bmatrix} \begin{bmatrix} N_s \\ N_\vartheta \end{bmatrix} + \begin{bmatrix} p_s \\ q \end{bmatrix} = \begin{bmatrix} 0 \\ 0 \end{bmatrix} \tag{1.23b}$$

The foregoing matrix shows us that the problem of the thin domes is statically determinated.

From the second equation of the 1.23b we can link the forces along the meridians to the forces along the parallels:

$$\frac{N_s}{R_1} + \frac{N_\vartheta}{R_2} = q \tag{1.24}$$

and from the first (1.23a) we obtain a differential equation

$$\frac{\mathrm{d}N_s}{\mathrm{ds}} + \frac{\sin\alpha}{r} N_s - \frac{\sin\alpha}{r} N_\vartheta + p_s = 0 \tag{1.25}$$

Expressing N_ϑ in function of N_s we can obtain the following equation in the only unknown force N_s

$$\frac{dN_s}{ds} + \left(\frac{1}{R_1} + \frac{1}{R_2}\right) \tan\alpha\, N_s = q \tan\alpha - p_s \tag{1.26}$$

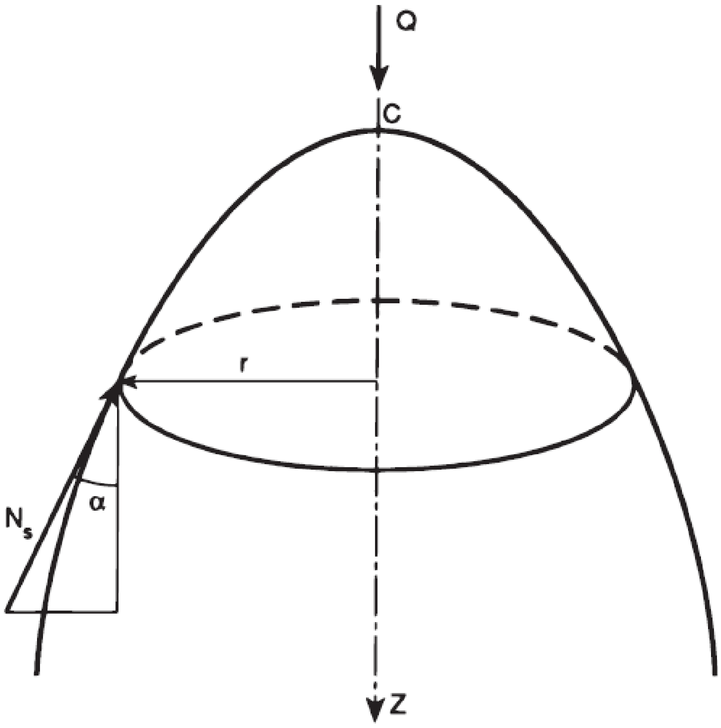

Figure 1.7

Let us consider a thin dome loaded by *Q*, that is the integral of the vertical loads acting on a portion, identified by a generic parallel (figure 1.7);instead of resolving the equation 1.26, we impose the equilibrium to translation in the *Z* direction of the portion of the shell considering:

$$Q = N_s \cos\alpha\,(2\pi r) \tag{1.27}$$

so we can express N_s as

$$N_s = \frac{Q}{2\pi r \cos\alpha} \tag{1.28}$$

And through the 1.24 we can extract the force along the parallel N_ϑ.

The equation 1.24 can be transformed as follows:

$$\frac{\sigma_s}{R_1} + \frac{\sigma_\vartheta}{R_2} = \frac{p}{h} \tag{1.29}$$

Where σ_s and σ_ϑ are the internal forces per unit area of the cross section, p is the pressure acting perpendicularly to the middle surface and h is the thickness of the thin shell.

1.2 The German school

The first analysis of the shells studied the shell with a plane frame approach, instead of analysing the problem in the three dimensions. Only in 1863 Schwedler performed a three-dimensional structural analysis of dome, the so called "Schwedler dome". Thanks to this approach, in 1875 he designed the roof of a gasometer for the Imperial Continental Gas Association in Berlin; this structure, still existing today, is an iron dome with a span of 55m. He became the first engineer to consider a three-dimensional load.

The Schwedler dome was described by him in the Zeitschrift für Bauwesen journal, in which he explained the theory of the 3D analysis: "Existing dome theory and construction practice took account of radial resistances only … However, in considering the dome equilibrium it is necessary to dispense with elastic member theory and instead use thin elastic plate double curvature as a basis" [Schwedler,1866, p.8]

In the figure 1.8 it is possible to see a typical scheme of the Schwedler dome.

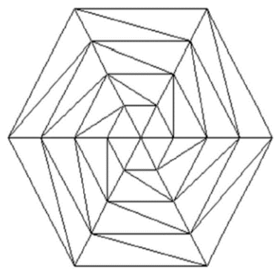

Figure 1.8- Schwedler dome

The contribution of the Zeitschrift journal was fundamental for the future developments. Indeed, after the Schwedler's studies, lot of spatial framework theories were developed.

In 1889 Hermann Zimmermann designed the dome over the German parliament building ("Zimmermann dome"), that is a statically determinate structure located in Berlin. Zimmermann based his studies on some basic hypothesis (Figure 1.9):

- All the vertical forces are supported by the four upper corners (figure 1.9a);
- The dome uses the structural plate effect to sustain the horizontal forces;
- The figure 1.9b shows all the forces of the spatial framework, which are the unknowns. Totally there are 40 unknowns in 40 equations. The equations are defined by considering that for each nodes it is possible to write three equations of equilibrium; there are 12 nodes so there will be 36 conditions, plus four more equations for the four supports.

The foregoing discussion is for a dome with four joints in the upper ring, but 11 years later Zimmerman extended his theory to other type of spatial frameworks and dome with any number of corners.

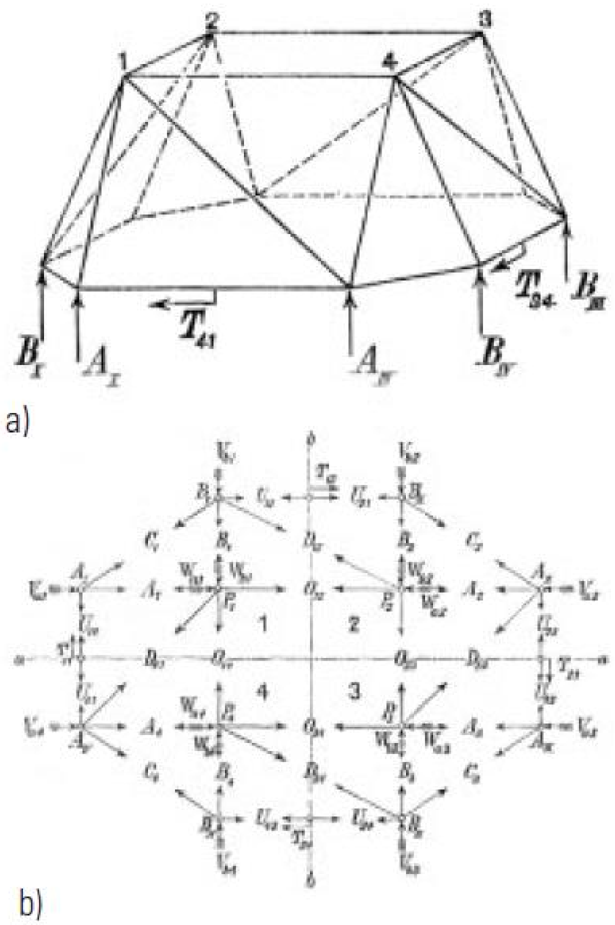

Figure 1.9

August Föppl (1854-1924) started his studies of the three-dimensional structures in 1880 in the book *Theories des Fachwerks*. In 1888 he published a paper in the *Schweizerische Bauzeitung,* in which he introduced a new type of dome: the lattice dome. Föppl used this dome system for the first time for the roof of the central market hall in Lipsia, which has a span of about 20 m and it is a statically determinate structure, that can be solved using the force diagrams.

In 1891 there was a collapse of the trussed railway bridges over the River Birs in München, and Föppl was the first engineer to say: "The bridge collapsed, because -as a spatial trussed framework – it was unstable". The collapse was the reason why Föppl decided to write his masterpiece *Das Fachwerk im Raume*, published in 1892. In this book he changed the definition of the spatial frameworks of the 1880: ".. a system composed of material points and certain connecting lines combined in such a away that no movement of system components relative to each other is possible without changing the length of the connecting lined" [Foppl,1892, p.2].

In Foppl's idea, a three-dimensional structure that is a stable trussed framework, is also statically determinate, and vice versa. Moreover, in his book August Föppl introduced new structural forms for the 3D structures, as trussed shells or lattice domes and established a new approach for analysing the classical dome.

Another important German engineer to be mentioned, is Muller-Breslau, who made a statics-constructional analysis of the Zimmermann dome. Between 1891 and 1892 he wrote the book *Beitrag zur Theorie des raumlichen Fachwerks,* in which he discussed about the theory of three dimensions structures. This book differed from the *Das Fachwerk im Raume* written by Föppl, because Muller-Breslau used an inductively method, analysing some examples, as the dynamic problem of certain domes and from these, he deducted his theory of the spatial framework.
First of all, Muller-Breslau is remembered for the substitute member method explained in the book mentioned foregoing: "By removing members and adding the same number of new members, referred to as substitute members, the trussed framework can be transformed into a very simple structure, possibly a structure with tension forces that can be determined by repeatedly solving the task of resolving a given force in three directions. The tension forces of the members removed are applied to new trussed framework as external forces, referred to as $Z_a, Z_b, Z_c,.., Z_n$. The tension forces of the members removed are applied to new trussed frameworks are then presented as a function of the given loads *P* and the initially unknown forces *Z.* They appear in the form $S = S_0 + S_a \cdot Z_a + S_b \cdot Z_b + S_c \cdot Z_c + \ldots + S_n \cdot Z_n$, where S_0 represents the value of S for the case when all loads *P* and forces $Z_b, Z_c, \ldots , Z_n$ are zero, whereas the two forces Z_a take a value of one. This load state is referred to as $Z_a = 1$; $S_b, S_c, \ldots , S_n$ can be interpreted as the tension forces for states $Z_b = 1, Z_c =1, \ldots , Z_n =1$. $S_a, S_b, S_c \ldots$ are independent of the loads *P,* whereas the tension forces S_0 have to be calculated for each load case to be examined. Setting the tension forces in the substitute members to zero results in the same number of linear equations as there are forces *Z* present, which means the latter can be calculated, provided the denominator determinant is not equal to zero. Otherwise the trussed framework is unusable, despite

the fact that the equation $s = 3k$ I satisfied" [Muller-Breslau, *Beitrag zur Theorie des raumlichen Fachwerks,* p.439].

In the Figure 1.11 it is possible to see the main differences between the force method and the substitute member method: the force method is used for statically indeterminate structure, while the substitute member method is used for statically determinate structure highly complex.

Force method	**Substitute member method**
System with n degrees of static indeterminacy (initial system)	Statically determinate system (initial system)
Transformation into a statically determinate basic system through release of n ties	Transformation into a statically determinate substitute system through replacement of n members
Calculation of the displacement steps δ_{i0} and δ_{ik} in the statically determinate basic system:	Calculation of the member forces S_{i0} and S_{ij} in the substitute system:
– δ_{i0}: Displacement step at point i due to initial state (given load) – δ_{ik}: Displacement step at point i due to the force parameter $X_k = 1$	– S_{i0}: Member force at point i in the member inserted at this point due to the initial state (given load) – S_{ij}: Member force at point i in the member inserted at this point due to the member force $Z_j = 1$ resulting from the removal of the member at point j
Compliance with the n elasticity conditions of the statically indeterminate system (continuity statements for deformation variables):	Compliance with the n equilibrium conditions of the statically determinate initial system (continuity statements for force variables):
$[\delta_{ik}] \cdot [X_k] + [\delta_{i0}] = [0]$	$[S_{ij}] \cdot [Z_j] + [S_{i0}] = [0]$
Calculation of the n released statically indeterminates X_k of the initial system from n elasticity equations	Calculation of the n removed member forces Z_j of the initial system from n equilibrium conditions
	Sufficient stability criterion:
	det $[S_{ij}] \neq 0 \longrightarrow$ initial system is not kinematic det $[S_{ij}] = 0 \longrightarrow$ initial system is kinematic

Figure 1.11

Dischinger, another student of Mohr, as Föppl, developed a new way to calculate and construct the shell and thanks to this, he is considered one of the pioneers in the construction of thin domes. In 1992, together with Walther Bauersfeld, he designed the Zeiss Planetarium dome in Jena (Fig 1.12), an hemispherical shell with a 30 mm thickness and a 16 m diameter. This dome was the first shell structure with prestressed reinforcement, the first Zeiss-Dywidag shell.

The prestressed reinforcement in the shell elements is not so common because of the over costs of the material used.

Figure 1.12

1.3 The Russian school

The most important authors of the twentieth century in terms of theory of shell were two Russian scientists: Timoshenko (1878-1972) and Viktor Valentinovich Novozhilov (1892-1970).

Timoshenko in 1940, published the "Theory of Plates and Shells", that was the first book that describes the shell theory, this work is very important especially because is a gather of all the previous scientific results on shell theory. The chapter 16 of his book called "Shells having the form of a surface of revolution and loaded symmetrically with respect to their axis" is of a great importance for our studies.

In the chapter above mentioned he considered the following portion of the shell of revolution (Figure 1.13), defined by two meridians, defined by the angle ϑ, and the two parallels orthogonal to the meridians, defined by the angle φ. In the meridians will act the forces N_ϑ and the moments M_ϑ. In contrast, in the upper parallel will act the force N_φ, the moment M_φ and a shearing force Q_φ acting in a plane perpendicular to the shell; in the shallow parallel there will be the same actions but incremented.

The shell is subjected to an external load contained in the meridian plane, that can be divided in two components: Y and Z, acting in the respectively axes. So there will be $Yr_1r_2\sin\varphi d\varphi d\vartheta$ in the direction of the meridian and $Zr_1r_2\sin\varphi d\varphi d\vartheta$ orthogonal to the shell element.

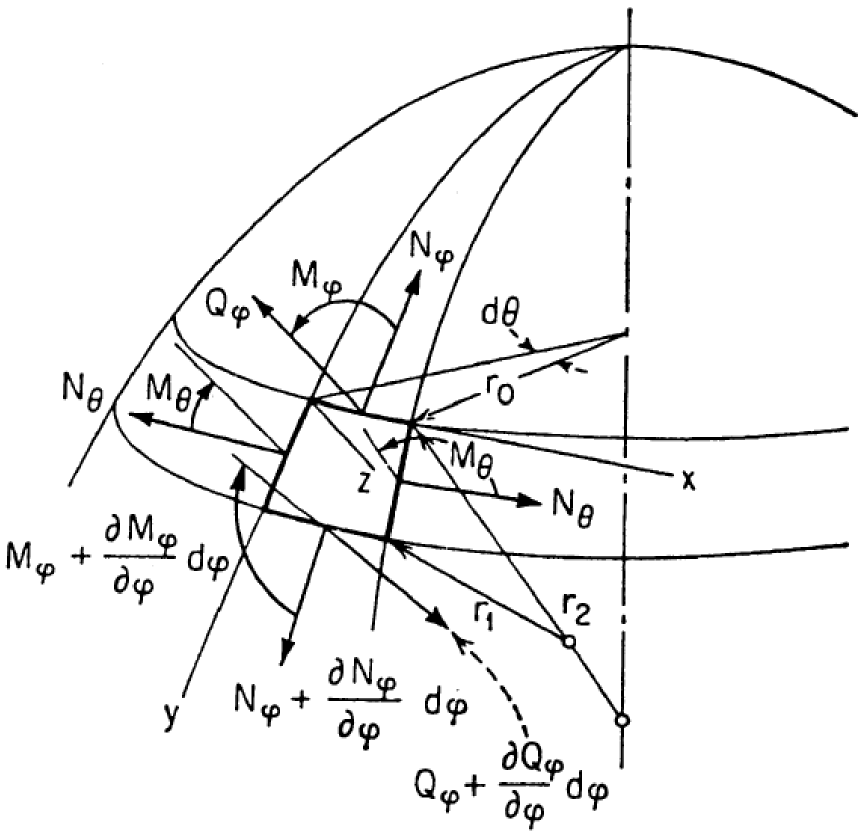

Figure 1.13

It is now possible to write the first equation of equilibrium in the direction orthogonal to the meridian:

$$\frac{\mathrm{d}}{\mathrm{d}\varphi}\left(N_\varphi r_0\right) - N_\vartheta r_1 \cos\varphi + Y r_1 r_0 - Q_\varphi r_0 = 0 \tag{1.30}$$

Where: - r_0 is the radius of the parallel;

-r_1 and r_2 are the principal radii of curvature.

The second equation is obtained by imposing the equilibrium about the normal to the surface of the shell:

$$N_\varphi r_0 + \ N_\varphi r_1 \sin\varphi + Z r_1 r_0 + \ \frac{d(Q_\varphi r_0)}{d\varphi} \ = 0 \tag{1.31}$$

The third and last equation is obtained by imposing the equilibrium to the rotation about the orthogonal to the considered parallel:

$$\left((M_\varphi + \frac{\mathrm{d}M_\varphi}{\mathrm{d}\varphi} d\varphi\right)\left(r_0 + \frac{dr_0}{d\varphi}\right) d\theta - \ M_\varphi r_0 \mathrm{d}\theta - M_\theta r_1 \cos\varphi \ \mathrm{d}\varphi \ \mathrm{d}\theta -$$

$$Q_\varphi r_2 \sin\varphi \ r_1 \mathrm{d}\varphi \mathrm{d}\theta = 0 \tag{1.32}$$

So we have a system of three equations in five unknowns: N_φ, N_θ, Q_φ, M_θ and M_φ.

The problem can be simplified in three equations, if we express the forces N_φ and N_θ in function of the displacements v and w as follows

$$N_\varphi = \frac{Eh}{1-\nu^2}\left[\frac{1}{r_1}\left(\frac{\mathrm{d}v}{\mathrm{d}\varphi} - w\right) + \frac{v}{r_2}(v \cot\varphi - \ w)\right] \tag{1.33a}$$

$$N_\theta = \frac{Eh}{1-\nu^2}\left[\frac{1}{r_2}(v \cot\varphi - w) + \frac{v}{r_1}\left(\frac{\mathrm{d}v}{\mathrm{d}\varphi} - \ w\right)\right] \tag{1.33b}$$

For the two moments $M_\varphi$and M_θ it is possible also to express this two in means of the components v and w

$$M_\varphi = -D\left[\frac{1}{r_1}\frac{\mathrm{d}}{\mathrm{d}\varphi}\left(\frac{v}{r_1} + \frac{\mathrm{d}w}{r_1 \mathrm{d}\varphi}\right) + \frac{v}{r_2}\left(\frac{v}{r_1} + \frac{\mathrm{d}w}{r_1 \mathrm{d}\varphi}\right)\cot\varphi\right] \tag{1.34a}$$

$$M_\theta = -D\left[\left(\frac{v}{r_1} + \frac{\mathrm{d}w}{r_1 \mathrm{d}\varphi}\right)\frac{\cot\varphi}{r_2} + \frac{v}{r_1}\frac{\mathrm{d}}{\mathrm{d}\varphi}\left(\frac{v}{r_1} + \frac{\mathrm{d}w}{r_1 \mathrm{d}\varphi}\right)\right] \tag{1.34b}$$

Obtained by expressing the curvature in this way:

$$\chi_\varphi = \frac{1}{r_1}\frac{\mathrm{d}}{\mathrm{d}\varphi}\left(\frac{v}{r_1} + \frac{\mathrm{d}w}{r_1\mathrm{d}\varphi}\right) \tag{1.35a}$$

$$\chi_\theta = \left(\frac{v}{r_1} + \frac{\mathrm{d}w}{r_1\mathrm{d}\varphi}\right)\frac{\cot\varphi}{r_2} \tag{1.36b}$$

Finally, substituting the equations 1.33 and 1.34 in the equations of equilibrium, we obtain a statically determinate system, with three equations in three unknowns.

To evaluate the displacements of the shell, according to Timoshenko, we have to come back to our notations and consider the shell of the Figure 1.14. In the figure is represented a shell of revolution defined by the curvilinear coordinate *s* and symmetrically loaded with respect to the axis of symmetry

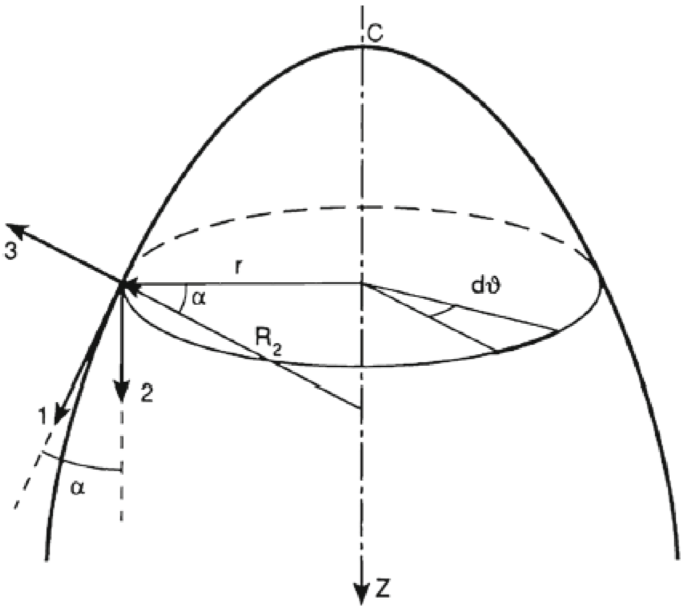

Z.

Figure 1.14

The kinematic equations, defined by Timoshenko, can be expressed in the following matrix form:

$$\begin{bmatrix} \varepsilon_s \\ \varepsilon_\vartheta \\ \gamma_s \\ \chi_s \\ \chi_\vartheta \end{bmatrix} = \begin{bmatrix} \frac{\mathrm{d}}{\mathrm{d}s} & \frac{1}{R_1} & 0 \\ +\frac{\sin\alpha}{r} & \frac{1}{R_2} & 0 \\ 0 & 0 & 0 \\ 0 & 0 & \frac{\mathrm{d}}{\mathrm{d}s} \\ 0 & 0 & +\frac{\sin\alpha}{r} \end{bmatrix} \begin{bmatrix} u \\ w \\ \varphi_s \end{bmatrix} \tag{1.37}$$

It is important to note that Timoshenko did not consider the deformation γ_s, the shearing strain, so we will see that in this way is not obeyed the static-kinematic duality.

In 1947, Novozhilov published a study of the thin shell, that in was translated in English during the following years. According to his theory, the kinematic equations are proposed like in (1.41).

1.4 Static kinematic duality

The static kinematic duality leads to a simple and direct demonstration of the principle of virtual work for deformable bodies, and vice versa. The two concepts implied each other [..]. The duality can be demonstrated considering the indefinite equation of equilibrium, the kinematic equations and the constitutive equation.

We can notice this duality in the shell of revolution, in which the kinematic matrix operator is the adjoint of the corresponding static matrix operator, and vice versa.

$$\begin{bmatrix} \varepsilon_s \\ \varepsilon_\vartheta \\ \gamma_s \\ \chi_s \\ \chi_\vartheta \end{bmatrix} = \begin{bmatrix} \frac{\mathrm{d}}{\mathrm{d}s} & \frac{1}{R_1} & 0 \\ +\frac{\sin\alpha}{r} & \frac{1}{R_2} & 0 \\ -\frac{1}{R_1} & \frac{\mathrm{d}}{\mathrm{d}s} & +1 \\ 0 & 0 & \frac{\mathrm{d}}{\mathrm{d}s} \\ 0 & 0 & \frac{\sin\alpha}{r} \end{bmatrix} \begin{bmatrix} u \\ w \\ \varphi_s \end{bmatrix} \tag{1.38}$$

$$\begin{bmatrix} \left(\frac{\mathrm{d}}{\mathrm{d}s} + \frac{\sin\alpha}{r}\right) & -\frac{\sin\alpha}{r} & \frac{1}{R_1} & 0 & 0 \\ -\frac{1}{R_1} & -\frac{1}{R_2} & \left(\frac{\mathrm{d}}{\mathrm{d}s} + \frac{\sin\alpha}{r}\right) & 0 & 0 \\ 0 & 0 & -1 & \left(\frac{\mathrm{d}}{\mathrm{d}s} + \frac{\sin\alpha}{r}\right) & -\frac{\sin\alpha}{r} \end{bmatrix} \begin{bmatrix} N_s \\ N_\vartheta \\ T_s \\ M_s \\ M_\vartheta \end{bmatrix} + \begin{bmatrix} \mathcal{F}_s \\ \mathcal{F}_n \\ 0 \end{bmatrix} = \begin{bmatrix} 0 \\ 0 \\ 0 \end{bmatrix} \tag{1.39}$$

As for the kinematic equations (1.38) they can be easily obtained by applying the virtual work principle. In these equations we have the displacements u, w and φ_s that are respectively, the displacement along the meridian, the normal displacement and the rotation about the parallel; ε_s and ε_ϑ which are the membrane dilations, γ_s is the shearing strain along the meridian, χ_s and χ_ϑ are the curvatures.

In the equation (1.39) N_s and N_ϑ are, respectively, the membrane forces along the meridian and the parallel, T_s is the shearing force along the meridian, M_s and M_ϑ are the bending moments about the parallel and the meridian.

As we can notice from the equations (1.39) we have three equations of equilibrium in the five unknows N_s, N_ϑ, T_s, M_s, M_ϑ so the problem presents two degrees of internal redundancy, whereas the more general problem of shells with double curvature presents three degrees of internal redundancy.

If we consider beams, plates and 3D solids is really simple to demonstrate the static-kinematic duality, because we will have that the static matrix operator will be the transpose of the kinematic one and vice versa, except for the sign. For the shell of revolution is not so direct, because due to Green's theorem, the area of a surface element cannot be expressed by the product of two differentials, but it will be $r d\vartheta ds$.

To demonstrate it, we will consider a portion of a shell of revolution, with a surface S and a contour C formed by two parallels and two meridians.

For the principle of virtual work, the external virtual work is equal to the internal one, so we can define the following equation:

$$\int_S (p_s u + q w + m_s \varphi_s) r \mathrm{d}\vartheta \mathrm{ds} + \oint_C (N_s u + T_s w + M_s \varphi_s) r \mathrm{d}\vartheta$$

$$= \int (N_s \varepsilon_s + N_\vartheta \varepsilon_\vartheta + T_s \gamma_s + M_s \chi_s + M_\vartheta \chi_\vartheta)\, r \mathrm{d}\vartheta \mathrm{ds} \qquad (1.40)$$

Considering the static equations, we can rewrite the first equation of the principle of the virtual work in the following form:

$$\int_S \left[\left(-\frac{\mathrm{d}N_s}{\mathrm{ds}}-\frac{\sin\alpha}{r}N_s+\frac{\sin\alpha}{r}N_\vartheta-\frac{T_s}{R_1}\right)u+\left(\frac{N_s}{R_1}+\frac{N_\vartheta}{R_2}-\frac{\mathrm{d}T_s}{\mathrm{ds}}-\frac{\sin\alpha}{r}T_s\right)w+\left(T_s-\frac{\mathrm{d}M_s}{\mathrm{ds}}-\frac{\sin\alpha}{r}M_s+\frac{\sin\alpha}{r}M_\vartheta\right)\varphi_s\right]r\mathrm{d}\vartheta\mathrm{ds} \qquad (1.41)$$

By applying the Green's theorem to the derivate terms, we have that

$$-\int_S \frac{\mathrm{d}N_s}{\mathrm{d}s}u\,r\,\mathrm{d}\vartheta\,\mathrm{ds}=\int_S N_s\frac{\mathrm{d}(u\,r)}{\mathrm{d}s}\mathrm{d}\vartheta\,\mathrm{ds}-\oint_C N_s u\,r\,\mathrm{d}\vartheta=\int_S N_s\left(\frac{\mathrm{d}u}{\mathrm{d}s}+\frac{\sin\alpha}{r}u\right)r\,\mathrm{d}\vartheta\,\mathrm{ds}-\oint_C N_s u\,r\,\mathrm{d}\vartheta \qquad (1.42a)$$

$$-\int_S \frac{\mathrm{d}T_s}{\mathrm{d}s}w\,r\,\mathrm{d}\vartheta\,\mathrm{ds}=\int_S T_s\left(\frac{\mathrm{dw}}{\mathrm{ds}}+\frac{\sin\alpha}{r}w\right)r\,\mathrm{d}\vartheta\,\mathrm{ds}-\oint_C T_s w\,r\,\mathrm{d}\vartheta \qquad (1.42b)$$

$$-\int_S \frac{\mathrm{d}M_s}{\mathrm{d}s}\varphi_s\,r\,\mathrm{d}\vartheta\,\mathrm{ds}=\int_S M_s\left(\frac{\mathrm{d}\varphi_s}{\mathrm{ds}}+\frac{\sin\alpha}{r}\varphi_s\right)r\,\mathrm{d}\vartheta\,\mathrm{ds}-\oint_C M_s\varphi_s\,r\,\mathrm{d}\vartheta \qquad (1.42c)$$

By a substitution of the equations 1.42 in the previous integrals we observe that the integral terms along the contour C disappear. The equation 1.40 can be rewritten as

$$\int_S \left[N_s\left(\frac{\mathrm{d}u}{\mathrm{ds}}+\frac{w}{R_1}\right)+N_\vartheta\left(\frac{\sin\alpha}{r}u+\frac{w}{R_2}\right)+T_s\left(-\frac{u}{R_1}+\frac{\mathrm{d}w}{\mathrm{ds}}+\varphi_s\right)+M_s\left(\frac{\mathrm{d}\varphi_s}{\mathrm{ds}}\right)+M_\vartheta\left(\frac{\sin\alpha}{r}\varphi_s\right)\right]r\mathrm{d}\vartheta\mathrm{ds}=\int_S(N_s\varepsilon_s+N_\vartheta\varepsilon_\vartheta+T_s\gamma_s+M_s\chi_s+M_\vartheta\chi_\vartheta)r\,\mathrm{d}\vartheta\,\mathrm{ds} \qquad (1.43)$$

To respect this equation the two terms in the integral must be equal each other, and this happen if and only if

$$\varepsilon_s=\frac{\mathrm{d}u}{\mathrm{d}s}+\frac{w}{R_1} \qquad (1.44a)$$

$$\varepsilon_\vartheta=\frac{\sin\alpha}{r}u+\frac{w}{R_2} \qquad (1.44b)$$

$$\gamma_s = -\frac{u}{R_1} + \frac{\mathrm{d}w}{\mathrm{d}s} + \varphi_s \tag{1.44c}$$

$$\chi_s = \frac{\mathrm{d}\varphi_s}{\mathrm{d}s} \tag{1.44d}$$

$$\chi_\vartheta = \frac{\sin\alpha}{r}\varphi_s \tag{1.44e}$$

The equations 1.44 represents the kinematic equation and in a matrix form we have

$$\begin{bmatrix} \varepsilon_s \\ \varepsilon_\vartheta \\ \gamma_s \\ \chi_s \\ \chi_\vartheta \end{bmatrix} = \begin{bmatrix} \frac{\mathrm{d}}{\mathrm{d}s} & \frac{1}{R_1} & 0 \\ +\frac{\sin\alpha}{r} & \frac{1}{R_2} & 0 \\ -\frac{1}{R_1} & \frac{\mathrm{d}}{\mathrm{d}s} & +1 \\ 0 & 0 & \frac{\mathrm{d}}{\mathrm{d}s} \\ 0 & 0 & \frac{\sin\alpha}{r} \end{bmatrix} \begin{bmatrix} u \\ w \\ \varphi_s \end{bmatrix} \tag{1.45}$$

Observe that, in the symmetrically case we do not have the displacement *v* along the parallels, the rotation φ_ϑ about the meridians and the deformations $\gamma_{s\vartheta}$, γ_ϑ and $\chi_{s\vartheta}$ anymore.

So the foregoing demonstration, evidences that the static-kinematic duality is still valid for the shell of revolution, but we have to do a little trick: moving from the static equations to the kinematics' one, it is necessary to perform the following substitution:

$$\frac{d}{ds} + \frac{sen\ \alpha}{r} \rightarrow \frac{d}{ds}$$

Thus, is important to underline that the terms of the kinematic matrix operator (1.45), are correctly defined only referring to our approach of the shell problem. On the opposite side, considering the classical theory of Timoshenko or Novozhilov, the results of the analysis of the shell of revolution can be inaccurate, and obtain wrong results, especially when dealing with the shearing deformation; what is more is impossible to see the duality of the problem.

1.5 Static-geometric analogy

The static-geometric analogy is a Russian principle, defined for the first time by Lur'e Goldenveiser [Goldenveiser, 1961] and it is a simple analogy between the equations of the shell for the stretching (S) and bending surface (B). This concept was then reported in English by another important Russian author, C.R. Calladine, who is not mentioned in the Chapter of the German school, one of his most important books is the Theory of Shell Structure. In the appendix 6 of his book was presented the so called 'Static-geometric analogy'. For the name itself, it seems to be very similar to the static-kinematic duality, but now we will see that the two things are different.

First of all, the static-geometric analogy is limited to the theory of thin shell, instead the static-kinematic duality is valid for all the elements: the three dimensional bodies, beams, plates and shells.

To explain the analogy, let us report the equations for the S-surfaces and for the B-surfaces as follows:

$$\frac{N_x}{R_1} + \frac{N_y}{R_2} = p_S \qquad \text{(S1)} \qquad\qquad \frac{k_y}{R_1} + \frac{k_x}{R_2} = g_B \qquad \text{(B1)}$$

$$\left.\begin{aligned} &\frac{\partial N_x}{\partial x} + \frac{\partial N_{xy}}{\partial y} = 0 \\ &\frac{\partial N_y}{\partial y} + \frac{\partial N_{xy}}{\partial x} = 0 \end{aligned}\right\} \text{(S2)} \qquad\qquad \left.\begin{aligned} &\frac{\partial k_y}{\partial x} - \frac{\partial k_{xy}}{\partial y} = 0 \\ &\frac{\partial k_x}{\partial y} - \frac{\partial k_{xy}}{\partial x} = 0 \end{aligned}\right\} \text{(B2)}$$

$$\left.\begin{aligned} &N_x = \frac{\partial^2 \Phi}{\partial y^2} \\ &N_y = \frac{\partial^2 \Phi}{\partial x^2} \\ &N_{xy} = \frac{\partial^2 \Phi}{\partial x \partial y} \end{aligned}\right\} \text{(S3)} \qquad\qquad \left.\begin{aligned} &k_x = -\frac{\partial^2 w}{\partial x^2} \\ &k_{xy} = -\frac{\partial^2 w}{\partial x \partial y} \\ &k_y = -\frac{\partial^2 w}{\partial y^2} \end{aligned}\right\} \text{(B3)}$$

$$\frac{\partial^2 \varepsilon_y}{\partial x^2} - \frac{\partial^2 \gamma_{xy}}{\partial x \partial y} + \frac{\partial^2 \varepsilon_x}{\partial y^2} = g_S \qquad \text{(S4)}$$

$$\frac{\partial^2 M_x}{\partial x^2} - \frac{2\partial^2 M_{xy}}{\partial x \partial y} + \frac{\partial^2 M_y}{\partial y^2} = -p_B \qquad \text{(B4)}$$

$$\left.\begin{aligned} \varepsilon_x &= \left(N_x - \nu N_y\right)/Et \\ \varepsilon_y &= (N_y - \nu N_x)/Et \\ \gamma_{xy} &= 2(1+\nu)N_{xy}/Et \end{aligned}\right\} \qquad \text{(S5)}$$

$$\left.\begin{aligned} M_y &= D\left(k_y + \nu k_x\right) \\ M_x &= D\left(k_x + k_y\right) \\ M_{xy} &= D(1-\nu)k_{xy} \end{aligned}\right\} \qquad \text{(B5)}$$

$$\Gamma^2 \phi = p_S \qquad \text{(S6)}$$

$$\Gamma^2 \mathrm{w} = g_B \qquad \text{(B6)}$$

$$-\left(\frac{1}{Et}\right) \nabla^4 \phi = g_S \qquad \text{(S7)}$$

$$D \nabla^4 w = p_B \qquad \text{(B7)}$$

The equations S1, S2, S3, S4 and S5 are the static equations, the S6 is the Poissont's equation and S7 is formally identical to the Airy's equation. For the Bending side there are the B1, B2 and B3, that can be called Geometric equations of the curvature, the B4 is an equation of equilibrium, equations B5 are the constitutive equations, B6 is the compatibility equation and finally we have the Sophie-Germann's equation (B7).

The analogies consist of:

$N_x \leftrightarrow k_y \qquad N_y \leftrightarrow k_x \qquad N_{xy} \leftrightarrow -k_{xy}$

$\varepsilon_x \leftrightarrow M_y \qquad \varepsilon_y \leftrightarrow M_x \qquad \gamma_{xy} \leftrightarrow -2M_{xy}$

$\phi \leftrightarrow -w \qquad g_S \leftrightarrow p_B \qquad p_S \leftrightarrow g_B$

Let us now explain the derivation of this analogies, considering three different groups

1. (S2), (S3) ↔ (B2), (B3)
2. (S1) ↔ (B1)
3. (S4) ↔ (B4)

Once these three will be explained, the other ones will be clearly.

For the first group the demonstration is clear, because the relations are the same, if the signs are not considered; the forces N correspond to the curvatures changes k, and the Airy function ϕ corresponds to the displacements w .

For the second analogy let us consider the Figure 1.15.

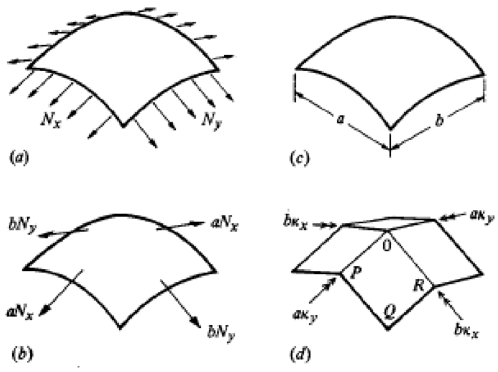

Figure 1.15

By imposing the equilibrium of the forces normal to the xy plane in the Fig 1.15a, the equation S1 is obtained. For the B1 is considered the figure c, simplified in a square version by the figure d. In the 1.15d there is a polygonalised shell, in which an increasing of the hinge angles ak_y and bk_x is applied; the aim is to calculate the angular defect. To calculate it, we consider the four vectors showed in the figure d and then sum the components in the direction normal to the plane xy. Thus, the change of the angular defect is:

$$ab\left(\frac{k_x}{R_2}+\frac{k_y}{R_2}\right)$$

To explicate the last group, which is an analogy between the equilibrium equations, let us consider the Figure 1.16.

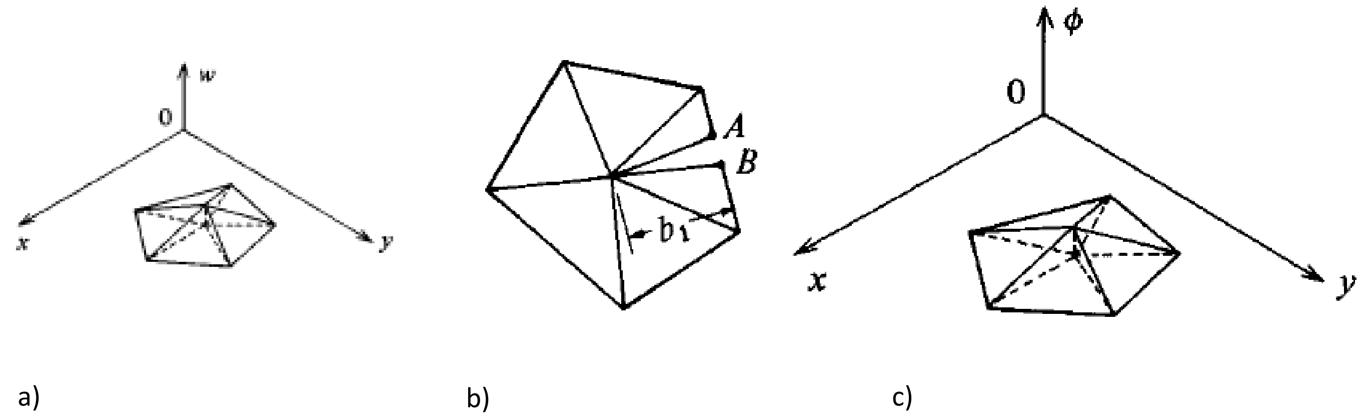

Figure 1.16

The equation (B4) can be derived by considering a flat plate, as shown in the Figure 1.16a and to this plate is applied a load p_B constant over the area. Let us consider a virtual displacement w defined by the quantity Δ. If Δ is known, it is easy to calculate ϑ_i, the rotation of each hinge of the plate.

So, considering that A is the base area of the plate, l_i is the extension of the geometric hinge i and M_i is the bending moment about the i-hinge, and applying the virtual work we obtain the following expression:

$$\frac{1}{3} p_S A\Delta = \sum_i M_i l_i \vartheta_i \qquad (1.46)$$

From the equation 1.46, it is possible to derivate the (B4) if we consider a square base of side 2h and consider the limit for $h \rightarrow 0$.

For the equation of the stretching (S4) we consider the figure 1.16 c, in which we have the same flat plate of the figure a) but now we take into account the Airy function ϕ and "..the pyramidal function ϕ corresponds to a self-equilibrating set of radial compressions and circumferential tensions lying along the plane projection of the edges of the triangles meeting at the vertex." [Calladine, 1983]

To evaluate the change of the angular defect, *v,* we apply again the principle of the virtual work:

$$\frac{1}{3} g_B A\Delta = \sum_i \varepsilon_i l_i \vartheta_i \qquad (1.47)$$

Where: ε_i is the tensile strain along line i

$\frac{1}{3} g_B A b_1$ is the change in the Gaussian curvature

$\Delta = b_1 \vartheta_i$

The equation 1.47 is formally identical to the 1.46, so it is demonstrated that B4 is equal to the S4.

In conclusion, we have demonstrated the static-geometric analogy, which is really different from the static-kinematic duality and is also less intuitive and less useful.

2. FUNICULARITY

The static problem of elastic domes is governed by two parameters: the shallowness ratio and the thickness of the dome. When the thickness of the dome tends to zero, the funicularity emerges and prevails, independently of the shallowness ratio or the shape of the dome; on the other hand, when the thickness is finite, it is possible to define an optimal shape that minimizes the flexural regime, if compared to the membrane one.

If we consider a shell with a negligible flexural stiffness due to a small thickness, it will be subjected only to compressive and tensile forces contained in their tangent planes. Thus, we will have simplified kinematic and static equations, because there will only be forces along the meridians and the parallels, N_S and N_ϑ, as well as the displacements along the meridians and those normal to the middle surface, *u* and *w,* respectively:

$$\begin{bmatrix} \left(\frac{\mathrm{d}}{\mathrm{d}s} + \frac{\sin\alpha}{r}\right) & -\frac{\sin\alpha}{r} \\ -\frac{1}{R_1} & -\frac{1}{R_2} \end{bmatrix} \begin{bmatrix} N_s \\ N_\vartheta \end{bmatrix} + \begin{bmatrix} p_s \\ q \end{bmatrix} = \begin{bmatrix} 0 \\ 0 \end{bmatrix} \tag{2.1a}$$

$$\begin{bmatrix} \varepsilon_s \\ \varepsilon_\vartheta \end{bmatrix} = \begin{bmatrix} \frac{\mathrm{d}}{\mathrm{d}s} & -\frac{1}{R_1} \\ \frac{\sin\alpha}{r} & \frac{1}{R_2} \end{bmatrix} \begin{bmatrix} u \\ w \end{bmatrix} \tag{2.1b}$$

The first static equation represents the equilibrium to translation along the meridian, whereas the second one represents the equilibrium to translation along the normal.

So, it is possible to say that moving from shell to membrane, so tending the flexural stiffness to zero, the elastic problem shifts from internally twice hyperstatic to isostatic. If we have a small thickness, the funicular regime prevails and, independently from the shallowness ratio or the shape, the thin dome sustains only compressive or tensile forces contained in its tangent plane. On the opposite hand, when the thickness is finite, the elastic problem is governed by both: the dome thickness and its shallowness ratio and it is possible to define an optimal shape that minimize the flexural regime, if compared to the membrane's one.

Many authors have studied the problem of the shell of revolution in a funicular regime, trying to find a simple way to analyse this problem and to solve this type of structures.

In the following paragraphs, we will see the studies of three different authors and their proposal.

2.1 O'Dwyer

Dermot O'Dwyer, in the paper "Funicular analysis of masonry vaults", describes a new technique for the limit state analysis of arcuate masonry vaults. The technique consists in modelling the principal stresses in a masonry vault as a discrete network of forces. This network of forces has to belong to the masonry vaults and to be in equilibrium with the applied loads. The network gives the opportunity to calculate the geometric factor of safety, if we have a set of known loads, but also the collapse load factor for a given pattern of imposed loading.

In particular, O'Dwyer uses the force network model to evaluate the collapse load factor of a masonry vault with an imposed point load.

2.1.1 Arch analysis

The shape of an arch defines his stability. In fact, the strength of a masonry arch, is a function of the arch's shape and thickness. The failure of an arch is always an instability failure.

If we take into account an example of an arch made by steel voussoirs, it will fail under the pressure of a finger. This is due to the fact that the strength of the voussoirs does not influence the load that determinate the failure, although it is defined in function of the arch's form and of where the load is applied.

In the structural analysis the dependence of the arch's strength upon its shape is an advantage, because we can study bigger structures only by scaling up a structure and keeping the same proportions. Obviously, this is not true anymore when we deal with structures in which the strength depends on the material's behaviour.

The state of stress of an arch can be represented by a line of thrust, considering the resultant forces of the stresses in any voussoirs and defining a funicular polygon. As said Robert Hooke in 1676, "the ideal shape for an arch is that of funicular polygon"

According to O'Dwyer, the geometric factor of safety is the relationship between the thickness of an arch ring and the thickness of the thinnest arch which can contain the line of thrust.
An arch is always stable when the line of thrust, defined by the sum of all the loading applied, is contained in the arch ring.
The determination of the line of thrust is a problem of third degree; for all the arches there are different possible lines of thrust and the true one can be identified only by knowing the horizontal force at the end-constraints and the position of the line at least at two points.
In his studies, Heyman supposed that a masonry has no tensile strength, but an infinite compressive strength and the failure due to sliding between voussoirs, is prevented by the relative friction.
According to Heyman's safe theorem, the structure is safe for any system of force that is contained in the structure and, it is in equilibrium with the external loads.
With a mechanism analysis we can define an upper bound on the arch's collapse load. The collapse mechanism for an arch will be formed if we have the born of four hinges, which in turn will transform the bar into a four bar mechanism, which will be formed if the entity of the applied load is sufficient to cause a negative potential energy.
With the modern software is simple to calculate the loads that determinate the mechanism.

2.1.2 Shell analysis

The mechanism method is quite useful for two-dimensional structures, but become more inaccurate when it is necessary to study a three-dimensional structure and to find the surface of thrust.

Indeed, to correctly applying the mechanism analysis, it is necessary to know the critical failure mechanism, that is difficult to be identified, especially if the structure or the loading are not symmetrical. These limits preclude a large use of the mechanism method.

Another type of analyses that can be adopted, is the membrane's one, in which is considered that the middle surface of the vault is the surface of thrust. However, this analysis can show errors in presence of discontinuous structures or load pattern.

Lame, Heyman and Poleni introduce a new type of technique: the slicing technique. The structure is divided in sections, the analyst should identify the best pattern of cuts; in this case the stability of the structure is ensured by imposing the equilibrium of all the sections, but this type of analysis is inaccurate because do not take into account the favourable contribution of the upper portion of the dome that is in compression.

So, we can say that none of the previous method is a general method.

2.1.3 O'Dwyer's method

O'Dwyer performed an analysis of a masonry vault and considered the surface of thrust. The surface of thrust is a force network model that describes the state of stresses in the shell.

The force network model consists of nodes, which represent the points of the surface of thrust, and of network of forces, which links the nodes, that are the forces applied to the shell element. An example of the surface of thrust is represented in the Figure 2.1.

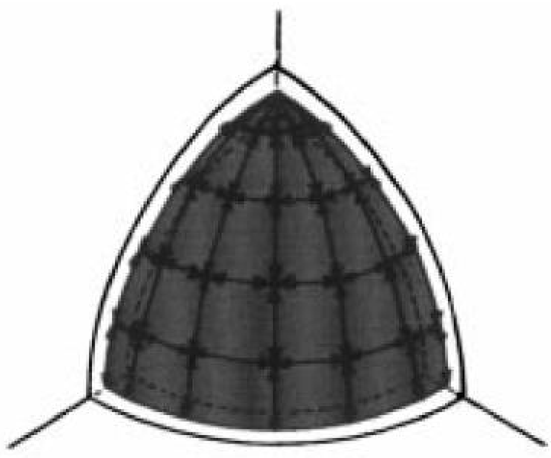

Figure 2.1

The accuracy of this method is function of the network's mesh density. The distributed loads can be described by discretizing them into discrete loads. It is simple to represents holes, because it can be done only by deleting all the network that passes through them. In general, we can say that:

- it is possible to have only compressive forces in the surface, because we are under the hypothesis that the masonry has no tensile strength;
- It is necessary to ensure the equilibrium, at each node, between the forces network and loads applied to that node;
- All the nodes of the surface have to stay between the upper and lower-bound of the masonry.

O'Dwyer, established that the procedure through which it is possible to determinate the force network model, can be described by seven steps. Moreover, thanks to this process is possible also to determinate the collapse load factor λ, for a given pattern of imposed loads. These steps will be described below.

2.1.3.1 Identify the principal load paths

This step consists in evaluating all the possible paths by which the shell element sustains the applied loads and transfers them to the foundation. According to the hypothesis of no tensile strength, all the forces have to be compression forces. There is not only one path, and all the possible ones must be identified.

However, in the book *"Limit state analysis of masonry vaults",* written by O'Dwyer itself, there are reported some experimental techniques for identifying all the ways through which the shells support their loads.

Let us consider a groined vault and identify two of all the possible paths. (Figure 2.2).

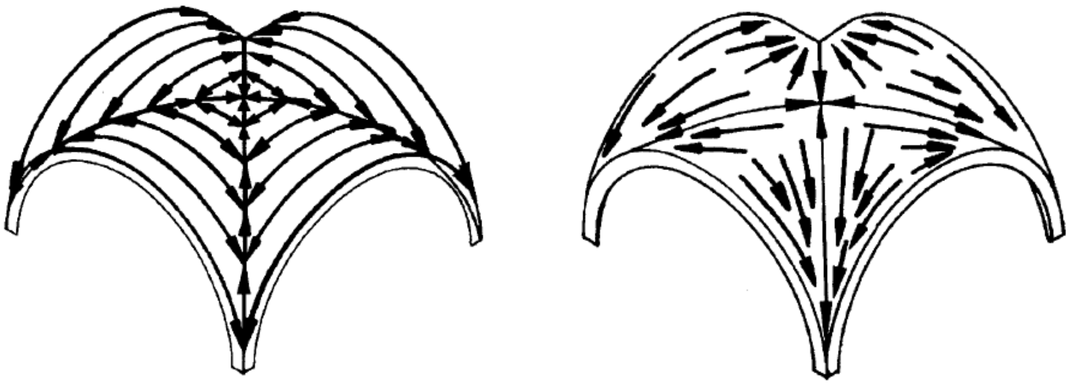

Figure 2.2

2.1.3.2 Select a mesh pattern and density

The chosen mesh pattern must represent the principal compressive forces of the shell element and in order to have sufficient accurate results, the density has to be quite enough, but the mesh cannot be too denser, otherwise the analysis could become more time-consuming.

Considering the groined vault of the Figure 2.2, it is possible to identify, for example, the mesh pattern of the Figure 2.3, which is suitable for both of the force paths of the Figure 2.2. Any pattern is represented in two-dimensions, by defining the coordinates *x* and *y* of all the nodes and their connectivity.

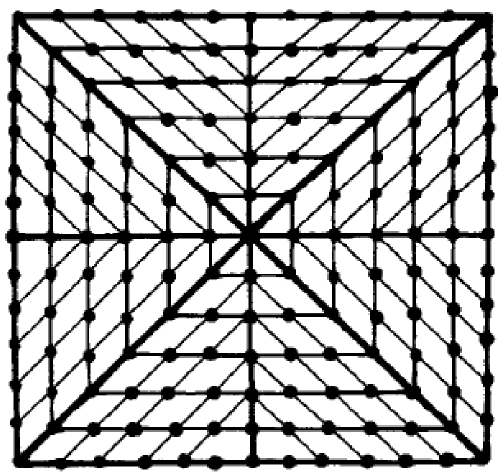

Figure 2.3

2.1.3.3 *Discretize the load.*

All the loads applied in the nodes are divided in D_i, which are the dead loads, and L_i, which are the imposed loads. These two are summarised as point loads.

Then, the example provided by O'Dwyer, shows the discretization of the load, in the case in which the purpose of the analysis is to calculate the collapse load factor λ, for a set of given loads. However, if we want to evaluate the geometric factor of safety, the discretization will be different.

2.1.3.4 *Identify the constraints on the node heights*

It is necessary to identify the coordinate *z* of each node of the network. The height is not known a priori, but we know that all the nodes must be contained in the thickness of the shell element.

So it is imposed the following inequality:

$$Z_{Ii} < z_i < Z_{Ei} \qquad \forall z_i \tag{2.1}$$

Where *i* is the generic node, *z* is the height, Z_{Ii} is the height of the upper bound of the shell and Z_{Ei} is the height of the lower bound of the shell.

2.1.3.5 *Define the vertical equilibrium constraints*

In order to determinate the surface of thrust, it is necessary to formulate the vertical equilibrium, i.e. imposing that, at each node, the equilibrium between the forces of the network and the imposed loads must be ensured.

Let us take into account the node *i,j* of the Figure 2.4, in which the force $W_{i,j}$ is expressed as follows:

$$W_{i,j} = D_{i,j} + \lambda L_{i,j} \tag{2.2}$$

The equilibrium should be written in function of unknowns z_i and of *Hi,* which are the horizontal components of the forces of the network.

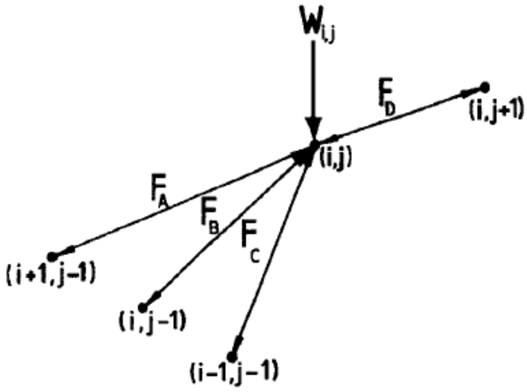

Figure 2.4

Thus, imposing the equilibrium, there will be the following equation:

$$W_{i,j} = \frac{z_{i,j} - z_{i+1,j-1}}{\sqrt{(x_{i,j}-x_{i+1,j-1})^2+(y_{i,j}-y_{i+1,j-1})^2}} H_A + \frac{z_{i,j} - z_{i,j-1}}{\sqrt{(x_{i,j}-x_{i,j-1})^2+(y_{i,j}-y_{i,j-1})^2}} H_B +$$

$$\frac{z_{i,j} - z_{i-1,j-1}}{\sqrt{(x_{i,j}-x_{i-1,j-1})^2+(y_{i,j}-y_{i-1,j-1})^2}} H_C + \frac{z_{i,j} - z_{i,j+1}}{\sqrt{(x_{i,j}-x_{i,j+1})^2+(y_{i,j}-y_{i,j+1})^2}} H_D \qquad (2.3)$$

Where *H* are the horizontal components of the forces *F* represented in the Figure 2.5.

To simplify the problem, it is also possible to consider a simple arch, in which the force network coincides with the force polygon. In this case, the equilibrium equation is written as follows:

$$H\left(\frac{z_i - z_{i-1}}{x_i - x_{i-1}}\right) + H\left(\frac{z_i - z_{i+1}}{x_{i+1} - x_i}\right) = W_i \qquad (2.4)$$

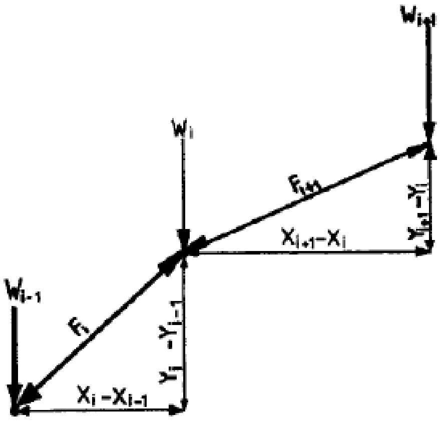

Figure 2.5

2.1.3.6 *Linearize the equilibrium constraints*

The problem, as presented before, is a nonlinear problem, because we need to find the maximum factor *λ*, in function of the unknowns z_i and H_i. It is a well-known fact that non-linear problems are difficult to be solved, so we need to linearize the problem. This is possible, by assuming certain values for the horizontal components *H*.

Considering again the Figure 2.5, it is possible to rewrite the equation (2.4) as follows:

$$\left(\frac{H}{x_i - x_{i-1}} + \frac{H}{x_{i+1} - x_i}\right) z_i - \left(\frac{H}{x_i - x_{i-1}}\right) z_{i-1} - \left(\frac{H}{x_{i+1} - x_i}\right) z_i = W_i \tag{2.5}$$

where *x* components are assumed. Then, considering a generic value for *H* and, that W_i can be written as the sum of the dead load D_i and the imposed load L_i, multiplied for λ, we have:

$$C_1 z_{i-1} + C_2 z_i + C_3 z_{i+1} - \lambda L_i = D_i \tag{2.6}$$

where *C* are assigned constants.

So, now we have to solve the foregoing linear problem: maximizing the collapse load factor λ in function of the two imposed constraints. The height of the nodes should be between the upper and the lower-bound of the vault, and the vertical equilibrium has to be ensured for each node.

This problem can be easily solved by programming algorithms, which can define the optimum shape of the force network, for any possible imposed value of the forces *H.*

2.1.3.7 *Repeat the linear optimization problem to define the true value of the forces H*

Until now, the horizontal forces *H*, are assumed as known values. In order to find the optimum value of horizontal forces, it can be used an optimization algorithms, the so called "hill climbing". "*This gradient based algorithms use the results from the previous iterations to select the values for the assumed* *horizontal forces, H_i, in the next iteration. Each successive linear programming solution generates an acceptable safe solution. Successive solutions should converge to the global optimum*" [O'Dwyer, 1999]

An example of the surface of thrust, modelled as a force network, can be seen in the Figure 2.6, where it is represented the optimum shape of the net for a masonry dome loaded by a point load.

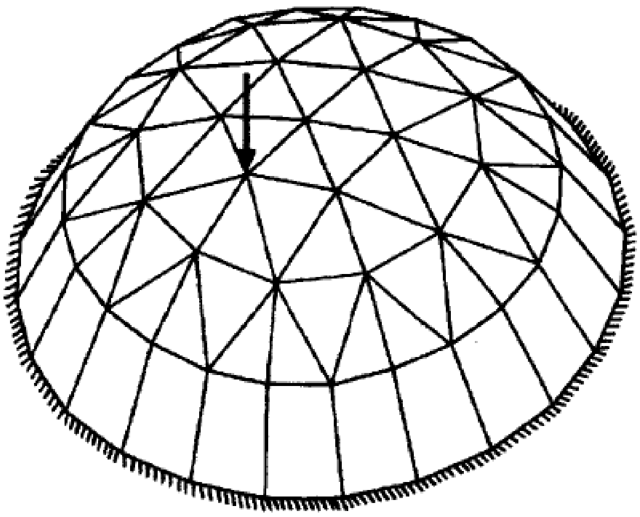

Figure 2.6

If the purpose of the analysis is to calculate the geometric factor of safety, it is necessary to perform some changes. First of all, the geometric factor of safety is defined by the ratio *D/d,* where *D* is the thickness of the real arch and *d* is the thickness of the thinnest arch that can sustain the applied loads. In this case, the equation (2.6) of equilibrium does not change, whereas for the other equation (2.1), we have to impose:

$$Z_{Ii} + (Z_{Ei} - Z_{Ii})\beta \leq z_i \leq Z_{Ei} - (Z_{Ei} - Z_{Ii})\beta \tag{2.7}$$

Where: $\frac{D}{d} = \frac{1}{1-2\beta}$

Now, the aim of the analysis is to maximize *β,* that means maximizing the geometric factor of safety. The method provided by O'Dwyer, allows the user to evaluating the collapse load factor for a defined load or the geometric factor of safety with known applied loads.

The most significant drawback of this method consists in the fact that, to implement the analysis, it is necessary to suppose a force distribution, thing that is quite easy for simple structures, but becomes very difficult when we deal with complex elements. So, the solution obtained will be always function of the user's choices about the mesh adopted.

2.2 Block and Ochsendorf

O'Dwyer's idea was then taken up by John A. Ochsendorf and his student Philippe Block, from MIT in Boston. They designed a new type of analysis, *Thrust Network Analysis (TNA),* which is based on the concept of the reciprocal figure, developed by Maxwell. A thrust network is characterized by n_n nodes and n_b branches, which link two different nodes; it describes the set of internal forces that balances the applied loads.

The TNA proposed by Block, is based on the same assumption made by O'Dwyer, so the branches of the network can be only compressive forces and the equilibrium of the vertical forces at each node, has to be guaranteed, and all nodes of the network must lie in the thickness of the shell element; moreover, this analysis is possible only in the condition in which all the forces, are vertical forces.

They started from the concept of Maxwell's reciprocal figures (Figure 2.7), according to which: "*Two plane figures are reciprocal when they consist of an equal number of lines, so that corresponding lines in the two figures are parallel, and corresponding lines which converge to a point in one figure form a closed polygon in the other";* thus, there will be two figures, the primal grid Γ, which is the 2D projection of the thrust network *G,* and the dual grid Γ*, which are reciprocal, regardless from the size of the dual grid, represented by the scale factor ζ.

The equilibrium of a node in Γ is represented by a closed polygon in Γ* and vice versa. Through the Maxwell's definition, it is not always true that the forces are only of compression, so William added another assumption: the closed polygon in the figures must be clockwise.

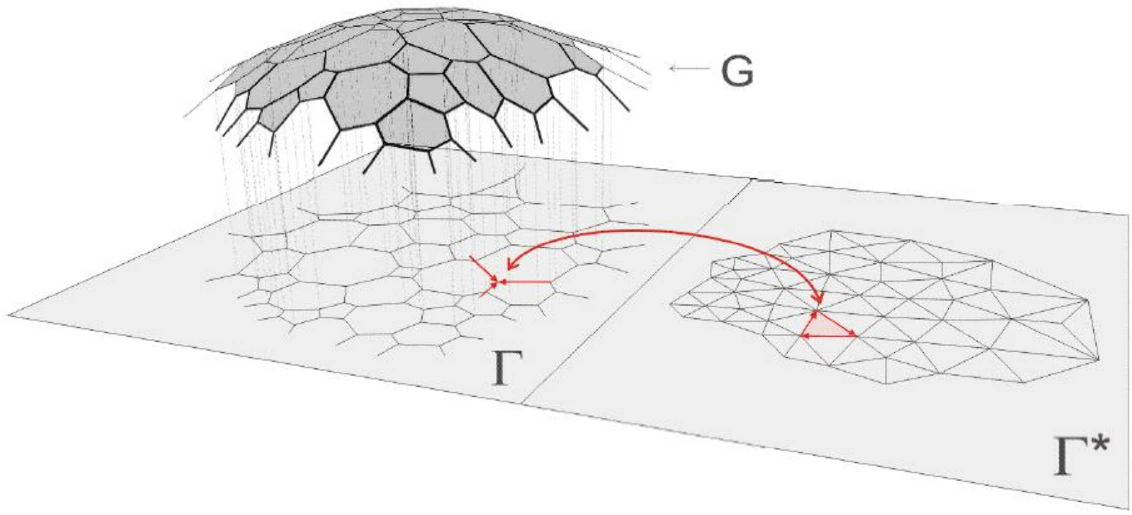

Figure 2.7

2.2.1 Main steps of the method

The method provided by Block consists in eight steps, that will be summarized as follows:

1. First of all, it is necessary to define a possible load path, i.e. defining a possible primal grid Γ, that is the projection of the unknown thrust network G.
2. Then, it is imposed a constraint on the nodal height and, all the nodes of the final solution G, must have a height z, included between z^{LB} and z^{UB} . This means that all the nodes must lie into the thickness of the vault.
3. All the loads have to be discretized and there will be a vertical load p, applied in all the nodes of G (Figure 2.8c). The force p includes both self-weight and external load applied.
4. The equilibrium of the nodes has to be ensured, so it is written an equation of equilibrium between the branches of the node in the primal grid and the applied loads in the node. This equation is expressed in function of the branch lengths, the nodal heights z and the horizontal components of the forces acting in the surface of thrust.
5. Considering the definition of the reciprocal figure, the dual grid Γ* is generated. If we multiply the length of the branches of Γ*, by ζ (that is an unknown), it is possible to obtain a possible final solution of *G.*

6. As in O'Dwyer's method, in this case the constraint of equilibrium, which is non-linear, will be linearized, but by expressing the equilibrium in function of the z of the nodes and ζ, which are the unknowns of the problem.
7. Now the unknowns can be determined by using a one-step linear optimization. Then, since ζ will be known, the horizontal components of G can be determined, by multiplying the length of the branches of Γ* by ζ.
8. Not always the dual grid generated in the step 5, gives a possible solution of *G*. In this case, the dual grid will be modified and all the steps are repeated. The last two points are repeated until a good solution is obtained.

From now on, we will see how the procedure for evaluating the thrust network model was implemented, focusing on some steps described in the following paragraph by a mathematical point of view.

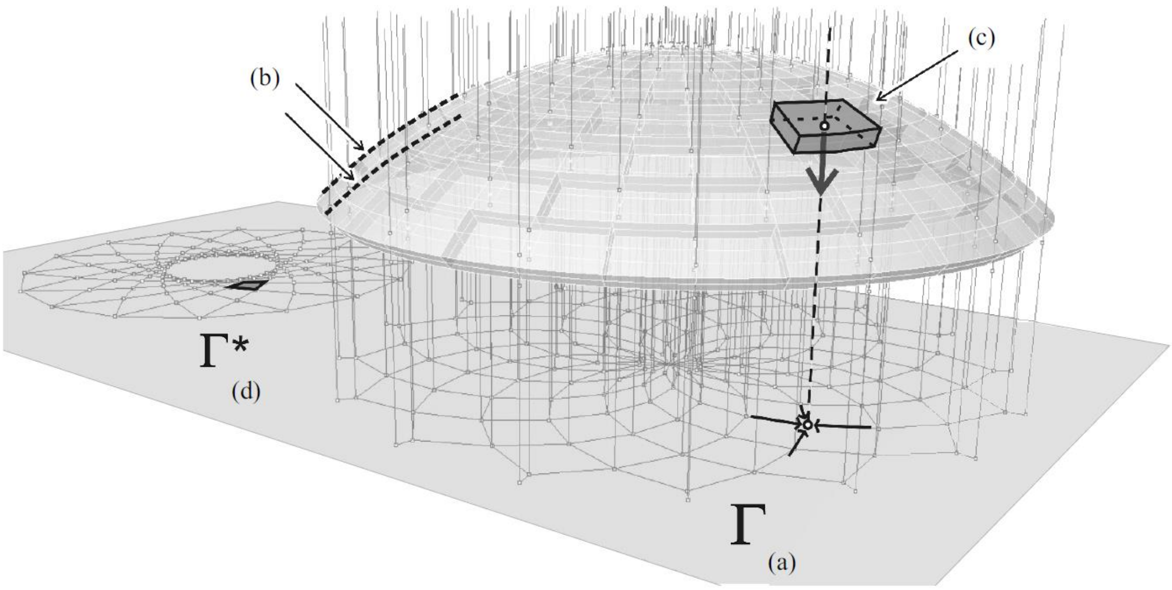

Figure 2.8

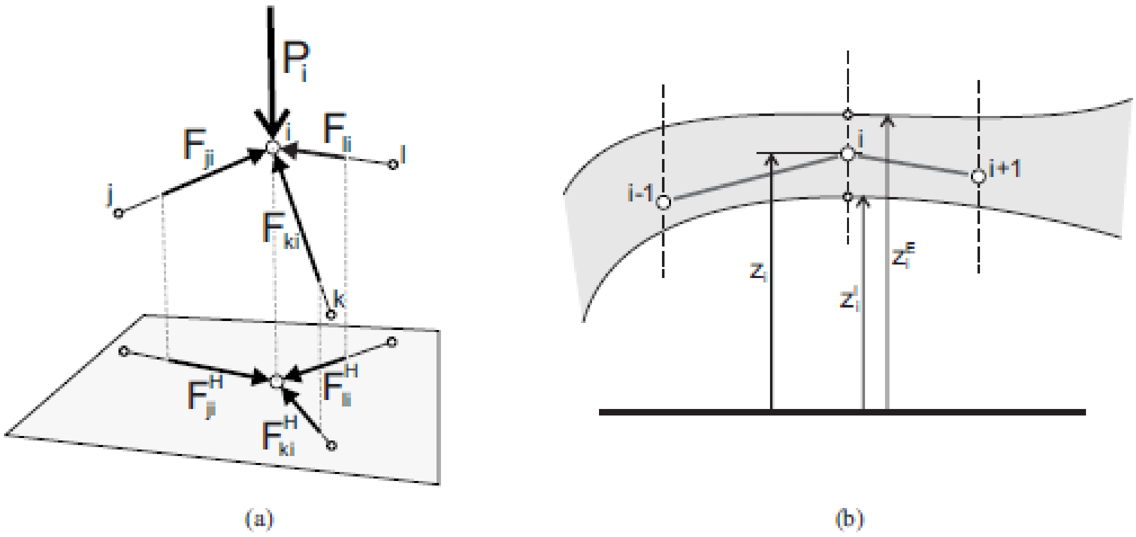

Figure 2.9

2.2.2 Constraints' equations

The vertical equilibrium of all the nodes of the network, as established in the point 4 of the previous paragraph, has to be ensured. Let us distinguish the internal nodes, called *i*, from the external one, *b*, and considering a generic node i represented in the Figure 2.9a. The equation of the vertical equilibrium is:

$$F_{ji}^{V} + F_{ki}^{V} + F_{li}^{V} = P_i \tag{2.8}$$

where with the apex V is indicated the vertical component of the branches forces.

It is possible to write n_i equations as in (2.8), for all the *i* nodes of the primal grid.

The equation (2.8) can be rewritten in function of the horizontal components of the forces F^H, and of the coordinates *x, y* and *z* of the surface of thrust G.

$$F_{ji}^{H} \cdot \frac{(z_i - z_j)}{\sqrt{(x_i - x_j)^2 + (y_i - y_j)^2}} + F_{ki}^{H} \cdot \frac{(z_i - z_k)}{\sqrt{(x_i - x_k)^2 + (y_i - y_k)^2}} + F_{li}^{H} \cdot \frac{(z_i - z_l)}{\sqrt{(x_i - x_l)^2 + (y_i - y_l)^2}} = P_i \tag{2.9}$$

Considering that the length of the branches in Γ can be expressed as follows

$$L_{ji}^{H} = \sqrt{(x_i - x_j)^2 + (y_i - y_j)^2} \tag{2.10}$$

the equation (2.9) can be rewritten as:

$$F_{ji}^{H} \cdot \frac{(z_i - z_j)}{\sqrt{L_{ji}^{H}}} + F_{ki}^{H} \cdot \frac{(z_i - z_k)}{\sqrt{L_{ki}^{H}}} + F_{li}^{H} \cdot \frac{(z_i - z_l)}{\sqrt{L_{li}^{H}}} = P_i \tag{2.11}$$

The equations (2.11) written for all the internal nodes have two unknowns, the height z_i and the horizontal components of the branches F^H, so the problem is non-linear.

In addition to the equilibrium's conditions, another type of constraint has to be imposed: all the nodes of G must be included between the intrados and extrados of the shell. So:

$$z_i^I \leq z_i \leq z_i^E \tag{2.12}$$

where,

$$z_i^E = z_i^{UB} \tag{2.13a}$$

$$z_i^I = z_i^{LB} \tag{2.13b}$$

Thus, there are $n_i + 2n$ constraints, n_i equations of equilibrium for each node, and $2n$ inequations of the node's heights.

2.2.3 Linearization of constraints

The primal and dual grid are reciprocal, so for the definition of reciprocal figures, the branch forces of Γ can be expressed as:

$$F_{ji}^{H} = \zeta \cdot L_{ji}^{H*} \tag{2.14}$$

and the branch lengths of the dual grid are:

$$L_{ji}^{H*} = \sqrt{\left(x_i^* - x_j^*\right)^2 + \left(y_i^* - y_j^*\right)^2} \tag{2.15}$$

By substituting the (2.14) in the (2.11), and multiplying both member by *r,* which is the inverse of the unknown ζ, we obtain:

$$\left(\frac{L_{ji}^{H*}}{L_{ji}^{H}} + \frac{L_{ki}^{H*}}{L_{ki}^{H}} + \frac{L_{li}^{H*}}{L_{li}^{H}}\right) \cdot z_i - \frac{L_{ji}^{H*}}{L_{ji}^{H}} \cdot z_j - \frac{L_{ki}^{H*}}{L_{ki}^{H}} \cdot z_k - \frac{L_{li}^{H*}}{L_{ki}^{H}} \cdot z_l - P_i \cdot r = 0 \tag{2.16}$$

In the equation (2.16) the branch lengths of the primal and dual grid are known, so the problem is linear, in the only unknown *z*.

2.2.4 Computational set-up

In order to describe the problem in a matrix form, let us consider the branch-node matrix ***C,*** which describes the nodes of the network and their linking. To create the matrix ***C***, it is necessary to numerate the nodes and the branches, going from the internal to the external ones. The (*n* x1) coordinates vectors of the final solution *G* are:

$$\boldsymbol{x} = \begin{bmatrix} \boldsymbol{x}_i \\ \boldsymbol{x}_b \end{bmatrix} \quad , \quad \boldsymbol{y} = \begin{bmatrix} \boldsymbol{y}_i \\ \boldsymbol{y}_b \end{bmatrix} \quad , \quad \boldsymbol{z} = \begin{bmatrix} \boldsymbol{z}_i \\ \boldsymbol{z}_b \end{bmatrix} \tag{2.17}$$

where *i* stay for internal nodes, and *b* for boundary nodes.

If we deal with a primal grid with *m* branches and *n* nodes, ***C*** will have dimensions *m* x *n,* with the branches described in the rows and the nodes described in the column. The matrix ***C*** is set as:

$$\boldsymbol{C}(i,j)=\begin{cases}1 & if\ node\ j\ is\ the\ head-node\ of\ branch\ i\\ -1 & if\ node\ j\ is\ the\ tail-node\ of\ branch\ i\\ 0 & otherwis\end{cases} \tag{2.18}$$

The branch-matrix $\boldsymbol{C}$ can be also written as:

$$\boldsymbol{C}=\left[\begin{array}{c|c} \boldsymbol{C}_i & \boldsymbol{C}_b \end{array}\right] \tag{2.19}$$

Where $\boldsymbol{C}_i$ is referred to the internal nodes, and $\boldsymbol{C}_b$ is referred to boundary nodes.

In the same way it is also possible to define the branch-node matrix $\boldsymbol{C}^*$ of the dual grid (when we deal with the dual grid the nomenclature has always a *); Γ* has n^* nodes, that correspond to the number of faces present in Γ.

Knowing the coordinates x, y and z, as expressed in (2.17), and the matrix $\boldsymbol{C}$, it is possible to evaluate $\boldsymbol{u}$, $\boldsymbol{v}$, $\boldsymbol{w}$, that are the branch coordinate vectors of Γ

$$\boldsymbol{u}=\ \boldsymbol{Cx}=\ \boldsymbol{C_i x_i}+\boldsymbol{C_b x_b} \tag{2.20a}$$

$$\boldsymbol{v}=\ \boldsymbol{Cy}=\ \boldsymbol{C_i y_i}+\boldsymbol{C_b y_b} \tag{2.20b}$$

$$\boldsymbol{w}=\ \boldsymbol{Cz}=\ \boldsymbol{C_i z_i}+\boldsymbol{C_b z_b} \tag{2.20c}$$

In the same way, for the dual grid Γ*, there will be $\boldsymbol{u}^*$ and $\boldsymbol{v}^*$ ($\boldsymbol{z}^*$=0, because the dual grid has only two dimensions):

$$\boldsymbol{u}^*=\boldsymbol{C}^*\boldsymbol{x}^* \tag{2.21a}$$

$$\boldsymbol{v}^*=\boldsymbol{C}^*\boldsymbol{y}^* \tag{2.21b}$$

Let us consider now $\boldsymbol{U}$, $\boldsymbol{V}$, $\boldsymbol{W}$, $\boldsymbol{U}^*$ and $\boldsymbol{V}^*$, which are the diagonalized square matrices of the respectively vectors, so the diagonalized length of Γ and Γ* are:

$$\boldsymbol{L_H} = \sqrt{\boldsymbol{U^tU} + \boldsymbol{V^tV}} \tag{2.22a}$$

$$\boldsymbol{L_H^*} = \sqrt{\boldsymbol{U^{*t}U^*} + \boldsymbol{V^{*t}V^*}} \tag{2.22b}$$

Thus, considering ***p*** as the vectors of the forces that load all the nodes, ***s*** as the vector which includes the branch forces, and ***L*** as the vector of the branch lengths, the equilibrium equations can be expressed as:

$$\boldsymbol{C_i^tUL^{-1}s} = \boldsymbol{p_x} \tag{2.23a}$$

$$\boldsymbol{C_i^tVL^{-1}s} = \boldsymbol{p_y} \tag{2.23b}$$

$$\boldsymbol{C_i^tWL^{-1}s} = \boldsymbol{p_z} \tag{2.23c}$$

Then, considering that there are only vertical loads and that

$$\boldsymbol{q} = \boldsymbol{L^{-1}s} = \boldsymbol{L_H^{-1}s_H} \tag{2.24}$$

By substituting the (2.24) in the (2.23c)

$$\boldsymbol{C_i^tWq} = \boldsymbol{p_z} \tag{2.25}$$

And assuming that ***Wq*** = ***Qw,*** we will have

$$\boldsymbol{C_i^tQCz} = \boldsymbol{p_z} \tag{2.26}$$

The horizontal components $\boldsymbol{s_H}$ of the branch forces are

$$\boldsymbol{s_H} = \boldsymbol{L_H^*\zeta} \tag{2.27}$$

with $\boldsymbol{\zeta}$ the branch scale vector, with dimensions (*m* x 1).

Substituting the (2.27) in the (2.26) there will be:

$$\boldsymbol{q} = \boldsymbol{L_H^{-1}L_H^*\zeta} \tag{2.28}$$

Substituting now the final definition of the force densities ***q,*** in the equation (2.26) and, dividing by *r,* we have

$$\boldsymbol{C_i^t}(\boldsymbol{L_H^{-1}L_H^*})\boldsymbol{C_z} - \boldsymbol{p_zr} = \boldsymbol{0} \tag{2.29}$$

2.2.5 Solving procedure

In the equation (2.29) we can differentiate the boundary nodes from the internal ones, so:

$$\boldsymbol{C_i^t}(\boldsymbol{L_H^{-1}L_H^*})\boldsymbol{C_i z_i} + \boldsymbol{C_i^t}(\boldsymbol{L_H^{-1}L_H^*})\boldsymbol{C_b z_b} - \boldsymbol{p_z} = \boldsymbol{0} \tag{2.30}$$

The problem can be simplified by considering the constraint matrixes $\boldsymbol{D_i}$ and $\boldsymbol{D_b}$, of dimensions (n_i x n_i) and (n_i x n_b),

$$\boldsymbol{D_i} = \boldsymbol{C_i^t}(\boldsymbol{L_H^{-1}L_H^*})\boldsymbol{C_i} \tag{2.31a}$$

$$\boldsymbol{D_i} = \boldsymbol{C_i^t}(\boldsymbol{L_H^{-1}L_H^*})\boldsymbol{C_b} \tag{2.31b}$$

By substituting the last two equations in the (2.30), there will be:

$$\boldsymbol{D_i z_i} - \boldsymbol{D_b z_b} - \boldsymbol{p_z r} = \boldsymbol{0} \tag{2.32}$$

Supposing that, r is known, therefore the scale factor is known, and the z_b are known, the heights of the internal nodes are easy to be evaluated through the equation (2.32), so the final solution G is determined. However, in this way, the second set of constraints, which is the constraint on the height of the nodes, it is not considered.

Considering the equation (2.12), the problem can be expressed as a linear optimization problem:

$$\min_{\boldsymbol{x}} \boldsymbol{c}^{\mathbf{t}}\boldsymbol{x} \quad \text{such that} \quad \begin{cases} \boldsymbol{Ax} \le \boldsymbol{b} \\ \boldsymbol{A}_{eq}\boldsymbol{x} = \boldsymbol{b}_{eq} \\ \boldsymbol{lb} \le \boldsymbol{x} \le \boldsymbol{ub} \end{cases} \tag{2.33}$$

"*.. where **c** is the objective (or cost) function vector, **x** are the variables, **A** and $\boldsymbol{A_{eq}}$ are the inequalities and equalities constraint matrices with **b** and $\boldsymbol{b_{eq}}$ the corresponding right hand sides, and **lb** and **ub** the lower and upper bounds on the value of the variables.*" [Block, 2007]

The vector $\boldsymbol{x}$ can be defined as:

$$\boldsymbol{x} = \begin{bmatrix} z \\ \hline r \end{bmatrix} \tag{2.34}$$

And considering the definition of ***c***, the cost function is written as:

$$\boldsymbol{c}^{\mathbf{t}}\boldsymbol{x} = \left[\begin{array}{c|c} \mathbf{0} & \pm 1 \end{array}\right] \cdot \left[\begin{array}{c} \boldsymbol{z} \\ \hline r \end{array}\right] = \pm r \tag{2.35}$$

To obtain the upper solution, contained in the thickness, *r* has to be minimized and the cost function will be positive. On the opposite hand, to obtain the lower solution, *r* has to be maximized and $\boldsymbol{c}^t\boldsymbol{x}$ will be negative.

Then it is possible to consider the following expressions for equalities and inequalities:

$$\boldsymbol{A} = [\ \ ] \quad , \quad \boldsymbol{b} = [\ \ ] \tag{2.36a}$$

$$\boldsymbol{A}_{eq} = \left[\begin{array}{c|c} \boldsymbol{D} & \boldsymbol{p}_z \end{array}\right] \quad , \quad \boldsymbol{b}_{eq} = \left[\begin{array}{c} \mathbf{0} \end{array}\right] \tag{2.36b}$$

The matrixes of inequality are empty because there are not these kinds of constraints.

Considering that, to obtain only compressive forces, ζ must be higher than 0, we can use the following expressions for the vectors ***lb*** and ***ub***.

$$\boldsymbol{lb} = \left[\begin{array}{c} \boldsymbol{z}^{\mathbf{LB}} \\ \hline 0 \end{array}\right] \quad , \quad \boldsymbol{ub} = \left[\begin{array}{c} \boldsymbol{z}^{\mathbf{UB}} \\ \hline +\infty \end{array}\right] \tag{2.37}$$

Finally, the linear optimization problem that should be resolved, can be expressed as:

$$\min_{\boldsymbol{z},r} \pm r \quad \text{such that} \quad \begin{cases} \boldsymbol{D}\boldsymbol{z} - \boldsymbol{p}_z r = \mathbf{0} \\ \boldsymbol{z}^{\mathbf{LB}} \leq \boldsymbol{z} \leq \boldsymbol{z}^{\mathbf{UB}} \\ 0 \leq r \leq +\infty \end{cases} \tag{2.38}$$

So, from the previous equation we identify *z* and *r,* and the scale factor ζ. Knowing this, from the (2.27) it is possible to identify the horizontal components of *G*, $\boldsymbol{s}_H$, and the axial forces of *G,* by:

$$s = Lq = LL_H^{-1}L_H^*\zeta \qquad (2.39)$$

An overview of the Thrust Network analysis proposed by Block and Ochsendorf is reported in the Figure 2.10.

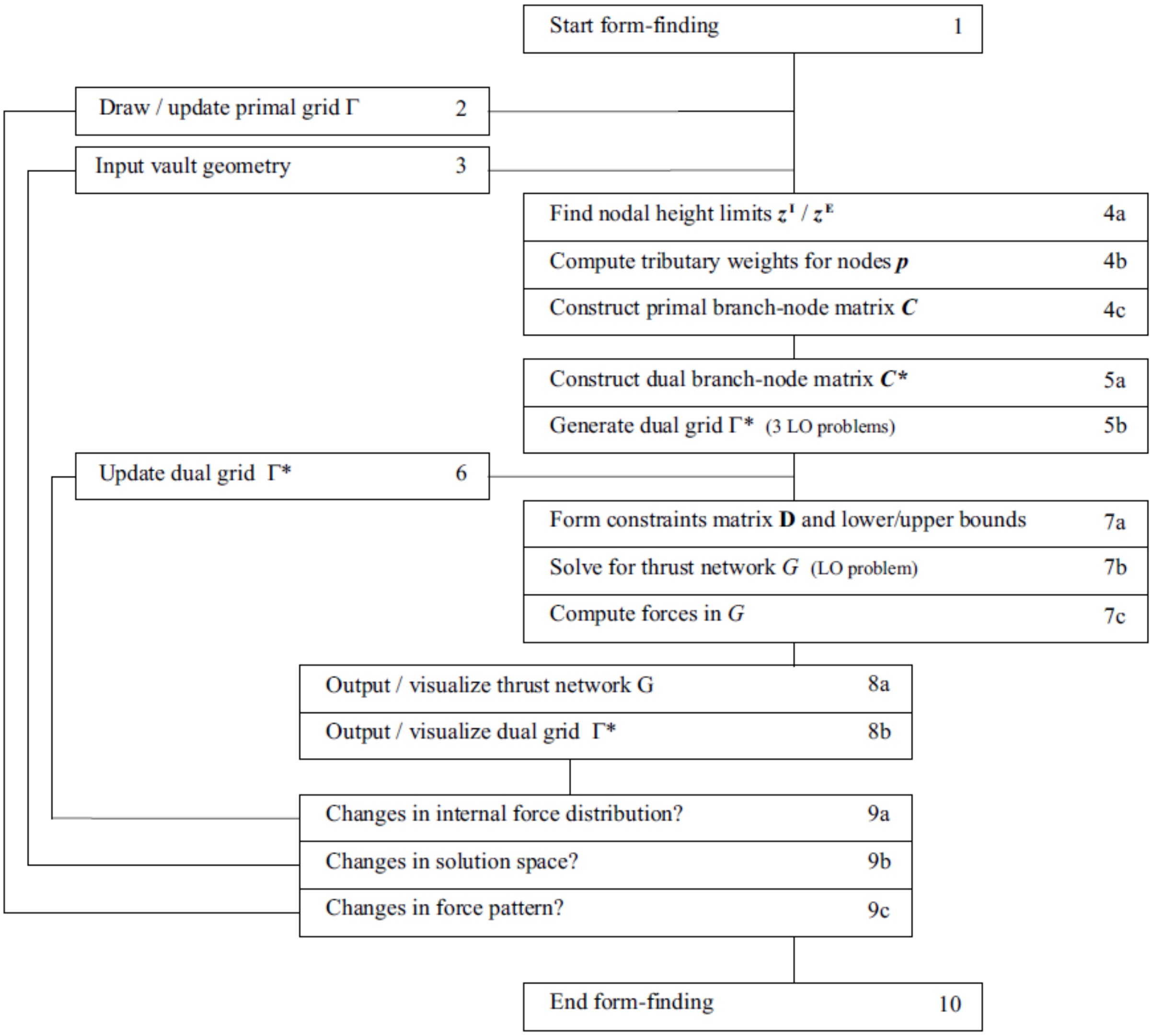

Figure 2.10

2.3 Marmo and Rosati

Francesco Marmo and Luciano Rosati, from Federico II University in Naples, propose a new methodology for the analysis of masonry structures, based on Block's studies. They took up the Thrust Network model, with a special interest in boost the field of application to seismic area. Thus, the analysis made by these two considers not only vertical applied loads, but also horizontal ones and, in addition, they want to simplify the process of creating the forces network, so in the formulation of the analysis, the dual grid Γ* is not used anymore, but it is considered only the primal one is considered. In this way, the creation of the TN becomes less immediate, but the number of variables included in the linear optimization are considerably reduced.

2.3.1 Thrust Network Analysis

In this paragraph, a summary of the Thrust Network Analysis of Block, taken up by Marmo, will be made, in order to understand, in a better way, the changes made in its formulation.

By definition, the Thrust Network is characterized by N_n nodes and N_b branches. Nodes can be divided in internal nodes (N_i), external nodes (N_r) that are the nodes of the constraints, and edge node (N_e). In the same way it is possible to divide the branches. The division is very clear from the Figure 2.11.

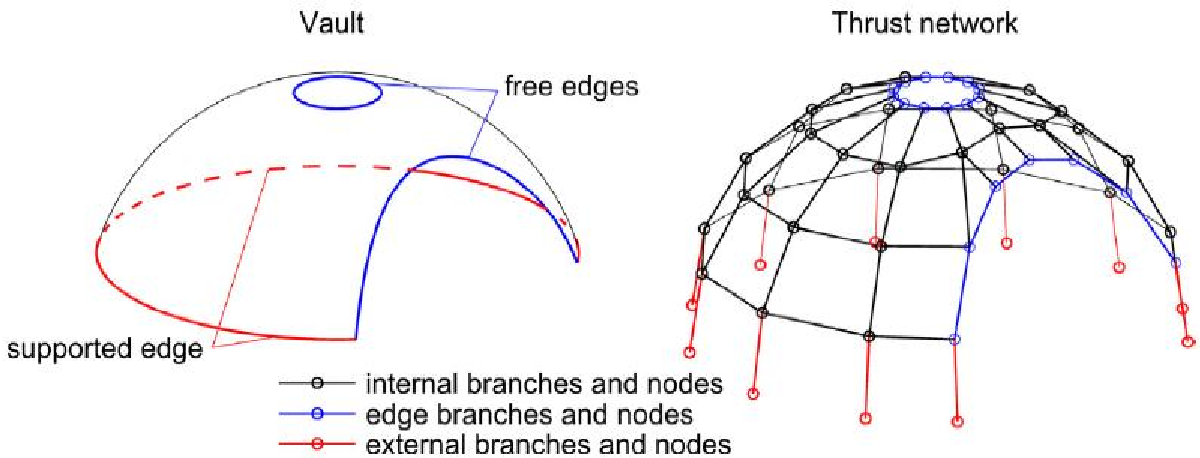

Figure 2.11

Each node is identified by its coordinates x_n, y_n, z_n, and they are loaded by external forces $f^{(n)} = \left(f_x^{(n)},\ f_y^{(n)}, f_z^{(n)}\right)$ and by the branches, which represent the internal forces. Whereas branches are identified by the two nodes that they link and by the thrust force $t^{(b)} = \left(t_x^{(b)},\ t_y^{(b)}, t_z^{(b)}\right)$.

To determinate the TN, the conditions of equilibrium of the horizontal and vertical loads, are now imposed:

$$\sum_{b\in B_n} t_x^{(b)} + f_x^{(n)} = 0 \tag{2.40a}$$

$$\sum_{b\in B_n} t_y^{(b)} + f_y^{(n)} = 0 \tag{2.40b}$$

$$\sum_{b\in B_n} t_z^{(b)} + f_z^{(n)} = 0 \tag{2.40c}$$

where b and n are, respectively, the generic branch and node, B_n includes all the branches that connect the node n. Obviously the (2.40a) and (2.40b) represent the horizontal equilibrium, instead the (2.40c) is referred to the vertical equilibrium.

The equations (2.40) can be simplified by expressing the thrust force t in function of t_h,which is the norm of the horizontal projection of the thrust in b, and l_h,, which is its length.

$$\sum_{b\in B_n} \frac{x_n - x_m^{(b)}}{l_h^{(b)}} t_h^{(b)} + f_x^{(n)} = 0 \tag{2.41a}$$

$$\sum_{b\in B_n} \frac{y_n - y_m^{(b)}}{l_h^{(b)}} t_h^{(b)} + f_y^{(n)} = 0 \tag{2.41b}$$

$$\sum_{b\in B_n} \frac{z_n - z_m^{(b)}}{l_h^{(b)}} t_h^{(b)} + f_z^{(n)} = 0 \tag{2.41c}$$

Where n and $m^{(b)}$ are the two generic nodes linked by b.

Then, considering that

$$t_h^{(b)} = \zeta \hat{t}_h^{(b)} = \frac{1}{r} \hat{t}_h^{(b)} \tag{2.42}$$

where, $\hat{t}_h^{(b)}$is the reference thrust value.

Thus, substituting the (2.42) in the (2.41) we have:

$$\sum_{b \in B_n} \left[\frac{\hat{t}_h^{(b)}}{l_h^{(b)}} x_n - \frac{\hat{t}_h^{(b)}}{l_h^{(b)}} x_m^{(b)} \right] + f_x^{(n)} r = 0 \quad (2.43a)$$

$$\sum_{b \in B_n} \left[\frac{\hat{t}_h^{(b)}}{l_h^{(b)}} y_n - \frac{\hat{t}_h^{(b)}}{l_h^{(b)}} y_m^{(b)} \right] + f_y^{(n)} r = 0 \quad (2.43b)$$

$$\sum_{b \in B_n} \left[\frac{\hat{t}_h^{(b)}}{l_h^{(b)}} z_n - \frac{\hat{t}_h^{(b)}}{l_h^{(b)}} z_m^{(b)} \right] + f_z^{(n)} r = 0 \quad (2.43c)$$

The ratio $\frac{\hat{t}_h^{(b)}}{l_h^{(b)}}$ indicates the reference thrust densities.

From the equation (2.42c) it is possible to obtain the height of the *n* node, z_n.

2.3.2 Amendments to Block's TNA

Essentially, the formulation of the thrust network made by Marmo differs from the Block's one, for three main things:

- Marmo wants to include horizontal loads in the analysis, in such a way that the method is applicable also in seismic areas
- The dual grid is abandoned, so the problem of optimization became more straightforward
- The analysis can be used also for domes with free edges.

So, for all the possible cases that we can have, we will see the different approaches proposed by Marmo.

2.3.2.1 TNA for vaults without edge nodes and loaded by vertical loads

First of all, it is possible to determinate, with a linear optimization process, and using the equilibrium equations, the horizontal components of the branch thrusts.

We are under the hypothesis of no horizontal loads, and so, the equations (2.43) can be written in the following matrix form:

$$\begin{cases} \boldsymbol{C_i}\boldsymbol{\hat{t}_h} = \boldsymbol{0_i} \\ \boldsymbol{S_i}\boldsymbol{\hat{t}_h} = \boldsymbol{0_i} \end{cases} \tag{2.44}$$

Where $\mathbf{C}_i$ and $\mathbf{S}_i$ are the matrixes of the cosine directors of the horizontal projections of the branches. It is possible to write $2N_i$ equations of equilibrium, the unknowns are N_b-3, so the system of equations (2.44) is undetermined.

In order to evaluate the horizontal projections of the branches $\hat{t}_h^{(b)}$, the following process of linear optimization is set:

$$\min_{\hat{\hat{t}}_h}(\boldsymbol{i_b} \cdot \boldsymbol{\hat{t}_h}) \text{ such that} \begin{cases} \begin{bmatrix} \boldsymbol{C}_i \\ \boldsymbol{S}_i \end{bmatrix} \boldsymbol{\hat{t}_h} = \boldsymbol{0}_{2i} \\ \boldsymbol{\hat{t}_h} \geq \boldsymbol{\hat{t}_{h,min}} \end{cases} \tag{2.45}$$

where $\mathbf{i}_b$ = (1,1..,1) is set in such a way that the products gives the set of all the horizontal projections $\boldsymbol{\hat{t}_h}$.

So, from the (2.45), it is possible to deduce that the thrust has to be higher than a minimum value, in this way the trivial solution is deleted. In this formulation the minimum value is assumed to be different for every branch, whereas in the original formulation of TNA it is the same for all the branches and is set equal to *d,* an assigned scalar parameter.

Furthermore, another difference stays in the formulation of the matrices **C** and **S**, because for Block, these are evaluated by numbering all the nodes, from the internal to the external ones, and accordingly to this numeration the branches are oriented, going from the lower to the higher. This hypothesis is now abandoned and **C** and **S** are evaluated by assemblage. The generic columns $\mathbf{C}^{(b)}$ and $\mathbf{S}^{(b)}$ are determined by considering the contribution of the branch *b* in the following way:

$$\boldsymbol{C}^{(b)} = \frac{1}{l_h^{(b)}} \begin{bmatrix} x_n - x_m^{(b)} \\ x_m^{(b)} - x_n \end{bmatrix} \tag{2.46a}$$

$$\boldsymbol{S}^{(b)} = \frac{1}{l_h^{(b)}} \begin{bmatrix} y_n - y_m^{(b)} \\ y_m^{(b)} - y_n \end{bmatrix} \tag{2.46a}$$

Then, to evaluate the height of each node, it is imposed another problem of linear optimization, but, this time, the procedure of Marmo is equal to the original one. The problem of optimization can be written in the following way

$$\min_{\mathbf{z},r} \pm r \text{ such that } \begin{cases} \begin{bmatrix} \mathbf{D}_i & \mathbf{f}_{z,i} \end{bmatrix} \begin{bmatrix} \mathbf{z} \\ r \end{bmatrix} = \mathbf{0}_i \\ \begin{bmatrix} \mathbf{z}_{min} \\ 0 \end{bmatrix} \leq \begin{bmatrix} \mathbf{z} \\ r \end{bmatrix} \leq \begin{bmatrix} \mathbf{z}_{max} \\ +\infty \end{bmatrix} \end{cases} \tag{2.47}$$

Where **D** are evaluated by assembling the thrust densities.

So, we impose the vertical equilibrium of the forces and force the z_i to be included between the thickness of the vaults. Minimizing or maximizing the scale factor ζ, and applying a linear optimization, the nodal heights are established.

2.3.2.2 TNA for vaults with edge nodes and loaded by vertical loads

If in the thrust network there are edge nodes, their horizontal coordinates are unknown and have to be determined. Block consider this problem only in the case in which the distribution of thrusts is constant. Considering that Marmo want to include the case of vaults loaded by horizontal loads, in which the distribution of thrusts is surely not constant, he decided to develop a solution procedure for network with edge nodes in a general case.

Originally the horizontal coordinates of the edge nodes are supposed coincident with the free edge of the dome, so it is possible to apply the equation (2.45) and evaluate the branch thrust densities. Once these are assigned, to determinate the real position of the edge and internal nodes, the Force Density Method (FDM) is used. The FDM consists of imposing $2(N_i + N_e)$ equations of the horizontal equilibrium:

$$\mathbf{D}_{i+e}\mathbf{x} = \mathbf{0}_{i+e} \tag{2.48a}$$

$$\mathbf{D}_{i+e}\mathbf{y} = \mathbf{0}_{i+e} \tag{2.48b}$$

Where **D** are evaluated by assembling the thrust densities of the network branches and the subscript $i + e$ represents the internal and edge nodes, **x** and **y** are the vectors of the horizontal coordinates of the nodes. We are in the case of no horizontal loads, so the vector of the external forces is **0**.

The matrix $\mathbf{D}_{i+e}$ and the coordinates vectors can be rewritten separating the internal and edge nodes from the external ones. Thus, the equations (2.48) can be expressed as:

$$\mathbf{D}_{i+e,i+e}\mathbf{x}_{i+e} + \mathbf{D}_{i+e,r}\mathbf{x}_r \; = \; \mathbf{0}_{i+e} \tag{2.49a}$$

$$\mathbf{D}_{i+e,i+e}\mathbf{y}_{i+e} + \mathbf{D}_{i+e,r}y_r \; = \; \mathbf{0}_{i+e} \tag{2.49a}$$

Finally, from the (2.49) it is possible to evaluate the coordinates of all the edge and internal nodes. Now, again, the procedure of linear optimization, which aims to calculate the z_i of all the nodes is the same of Block's procedure.

2.3.2.3 TNA for vaults with edge nodes and loaded by vertical and horizontal loads

Marmo and Rosati are particularly interested in considering the presence of the horizontal loads, in order to extend this analysis to seismic zones. In the original formulation of TNA was only mentioned the case of horizontal loaded structures and Block said that the creation of the dual grid becomes more difficult. In this new propose of the TNA the dual grid is not considered anymore, so there is not this type of problem.

If the vault is loaded by horizontal load, the equation (2.44) becomes

$$\begin{cases} \mathbf{C}_i\mathbf{t}_h + \mathbf{f}_{x,i}r = \mathbf{0}_i \\ \boldsymbol{S}_i\mathbf{t}_h + \mathbf{f}_{y,i}r = \mathbf{0}_i \end{cases} \tag{2.50}$$

The equation (2.50) with the (2.47) forms a system of non-linear equations.

The problem can be solved by considering the following linear optimization problem:

$$\min_{\hat{\mathbf{t}}_h}(\mathbf{i}_b \cdot \hat{\mathbf{t}}_h) \text{ such that } \begin{cases} \begin{bmatrix} \mathbf{C}_i \\ \mathbf{S}_i \end{bmatrix} \hat{\mathbf{t}}_\mathrm{h} = -\begin{bmatrix} \mathbf{f}_{x,i} & r \\ \mathbf{f}_{y,i} & r \end{bmatrix} \\ \hat{\mathbf{t}}_h \geq \hat{\mathbf{t}}_{h,min} \end{cases} \tag{2.51}$$

From the (2.51) we derive the thrusts $\hat{\mathbf{t}}_h^{(j)}$ that can be employed to determinate the horizontal coordinates through a develop of equations (2.49):

$$\mathbf{x}_{i+e} = -\left[\mathbf{D}_{i+ei+e}^{(j)}\right]^{-1}\left[\mathbf{D}_{i+er}^{(j)}\mathbf{x}_r + \mathbf{f}_{x,i+e}r^{(j)}\right] \tag{2.52a}$$

$$\mathbf{y}_{i+e} = -\left[\mathbf{D}_{i+ei+e}^{(j)}\right]^{-1}\left[\mathbf{D}_{i+er}^{(j)}\mathbf{y}_r + \mathbf{f}_{y,i+e}r^{(j)}\right] \tag{2.52b}$$

Then, the $\hat{\mathbf{t}}_h^{(j)}$ are used in the equation (2.47) and so a new value for *r* is obtained. This *r* is used in the (2.51), and this process is repeated in an iterative way until the two consecutive *r* obtained are more or less equal.

The process now illustrated is in presence of edge nodes. If there are not present the analysis can be simplified and the generic thrust $\hat{\mathbf{t}}_h^{(j)}$ can be evaluated as:

$$\hat{\mathbf{t}}_h^{(j)} = \hat{\mathbf{t}}_h^{(0)} + \frac{r^{(j)}}{r^{(1)}}\left[\hat{\mathbf{t}}_h^{(1)} - \hat{\mathbf{t}}_h^{(0)}\right] \quad if \quad r^{(j)} \geq r^{(1)} \tag{2.53}$$

Where $r^{(j)}$ is the generic scale factor, $\hat{\mathbf{t}}_h^{(0)}$ and $\hat{\mathbf{t}}_h^{(1)}$ are obtained by (2.51), considering $r=r^{(0)} = 0$ and $r=r^{(1)} = r_1$, with r_1 an assigned positive scalar.

3. PARAMETRIC ANALYSIS

The abovementioned approaches are quite complex and tricky, employing a large number of equations to be solved. Therefore, the aim of the present thesis is to analyse the behaviour of thin or shallow shells in order to find a simple way for defining quantitatively the concept of Funicularity.

Our studies have been implemented by "SAP2000" FEM software, in which we have created different shell elements using the shell template (Figure 3.1), with the shell type "Parabolic Dome" (Figure 3.2).

First, for its design it is necessary to define the so-called "Parabolic Dome Dimensions", which are:

- Start X, that is the dimension of the hole in the upper part of the dome, if it is present (in our cases we will consider only continuous domes, so there will be always Start X=0);
- End X, which is the Radius;
- Start Angle, Tz1;
- End Angle, Tz2;
- Constant, C, this is defined by the following formula

$$C \cdot z = x^2$$

  Where *z* is the height of the dome and *x* is the radius (so through C it is possible to define, indirectly, the height of the dome);

- Number of angular divisions
- Number of divisions along the axes Z, that is the vertical axes.

All these parameters are specified by the Figure 3.2.

In the proposal solving procedure the number of divisions in angular direction is set as 15, whereas the number of divisions along Z is 10. This remains invariant for each model.

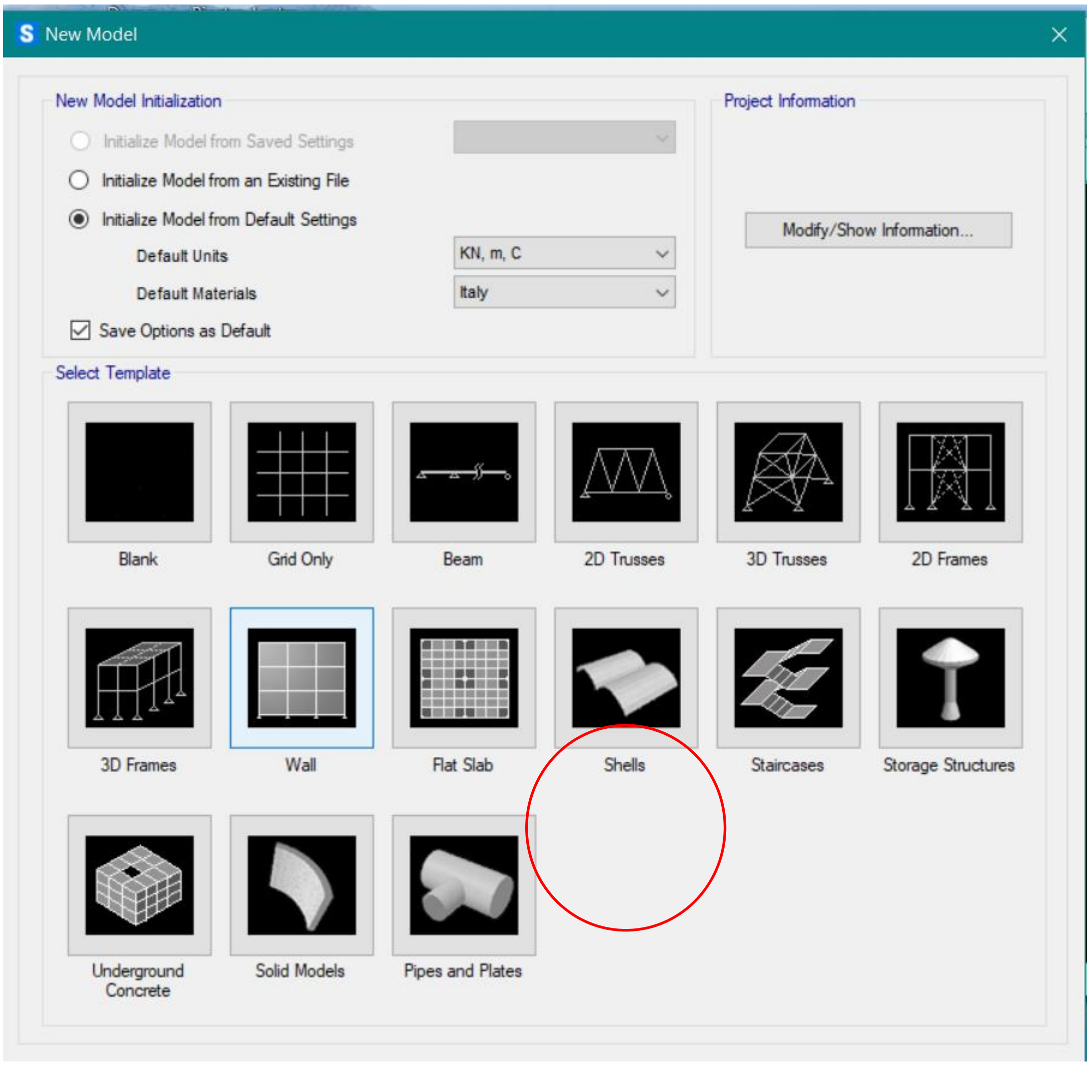

Figure 3.1

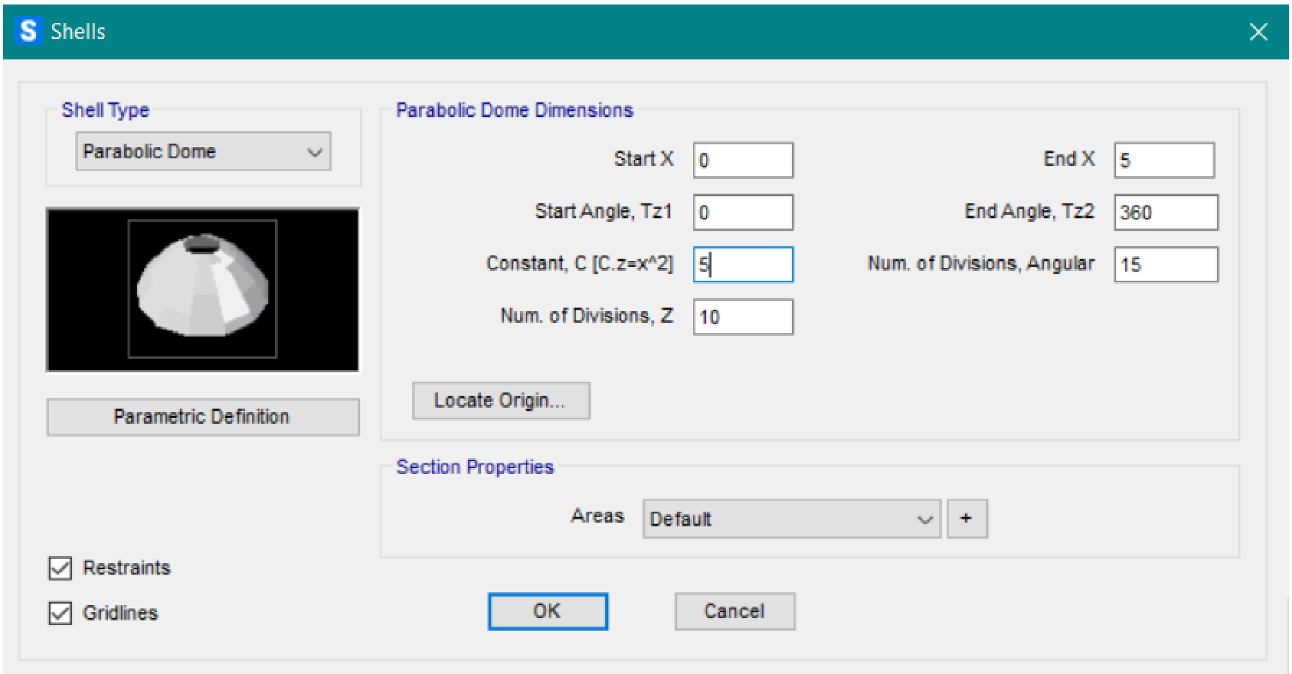

Figure 3.2

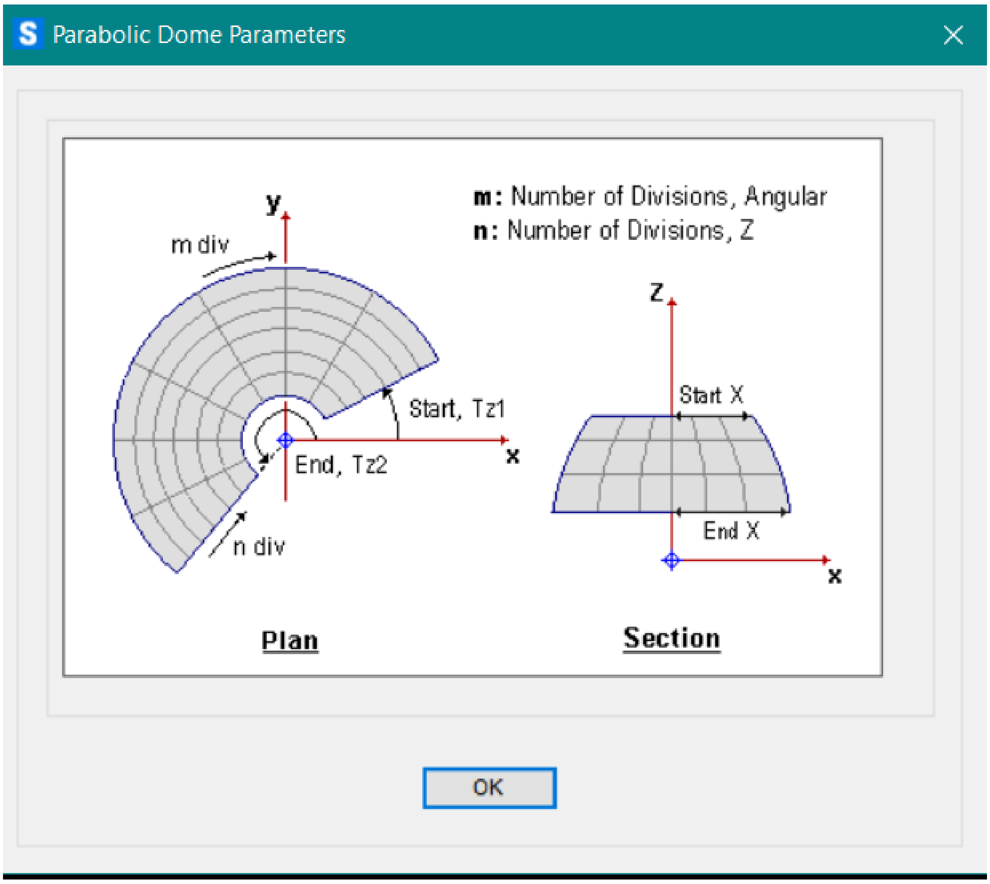

Figure 3.3

Then in SAP we must define the area sections and we have decided to adopt thick shell, characterized by the material Concrete C28/35 with E=32308000 kN/m² and ν=0.2 (Figure 3.4).

It has been then decided to perform a *parametric analysis*, in which we always set the same radius R=5 m but variate the relative thickness (t/2R) and the relative height (H/R), in the following way:

$$H/R \rightarrow \frac{5}{5}, \frac{4}{5}, \frac{3}{5}, \frac{2}{5}, \frac{1}{5}$$

$$t/2R \rightarrow \frac{1}{15}, \frac{1}{25}, \frac{1}{40}, \frac{1}{70}, \frac{1}{100}, \frac{1}{200}, \frac{1}{500}$$

so, for the relative thickness we adopted a logarithmic scale, until 1/100, and then added thinner shells to evaluate their behaviour. In the end 35 finite element models have been obtained, by the combination of these two parameters.

The five models with different shallowness are represented from the Figure 3.5 to the Figure 3.9.

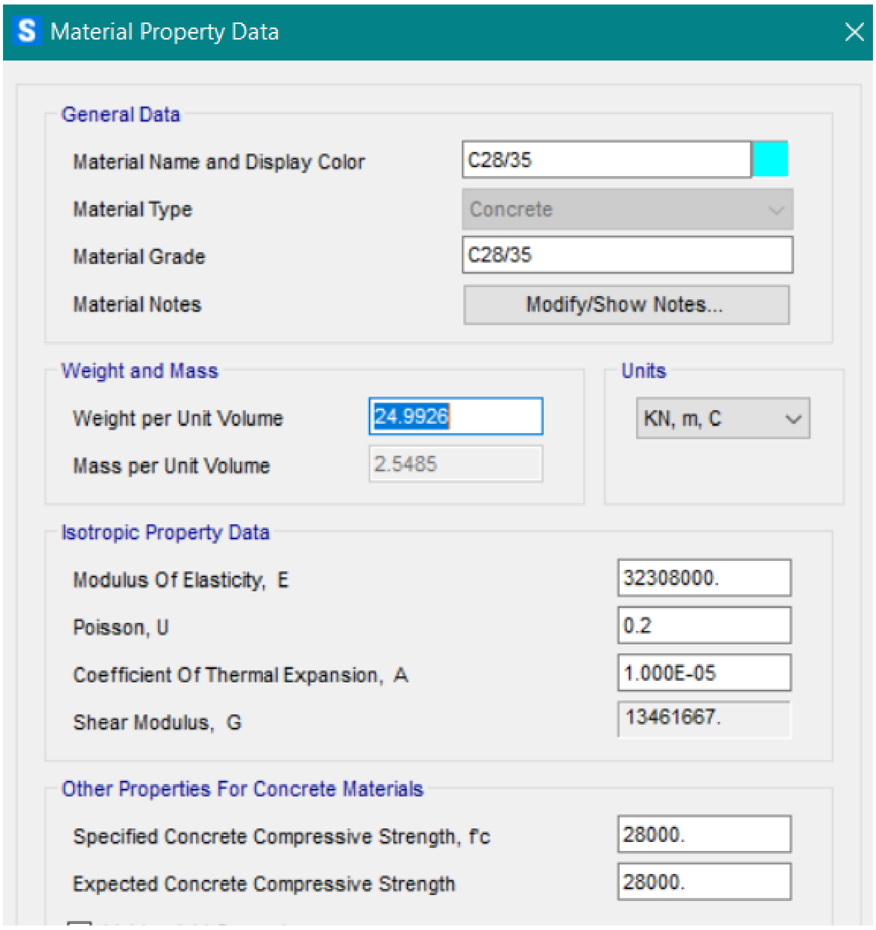
Material Property Data
General Data
Material Name and Display Color
C28/35
Material Type
Concrete
Material Grade
C28/35
Material Notes
Modify/Show Notes...
Weight and Mass
Weight per Unit Volume
24.9926
Mass per Unit Volume
2.5485
Units
KN, m, C
Isotropic Property Data
Modulus Of Elasticity, E
32308000.
Poisson, U
0.2
Coefficient Of Thermal Expansion, A
1.000E-05
Shear Modulus, G
13461667.
Other Properties For Concrete Materials
Specified Concrete Compressive Strength, f'c
28000.
Expected Concrete Compressive Strength
28000.

Figure 3.4

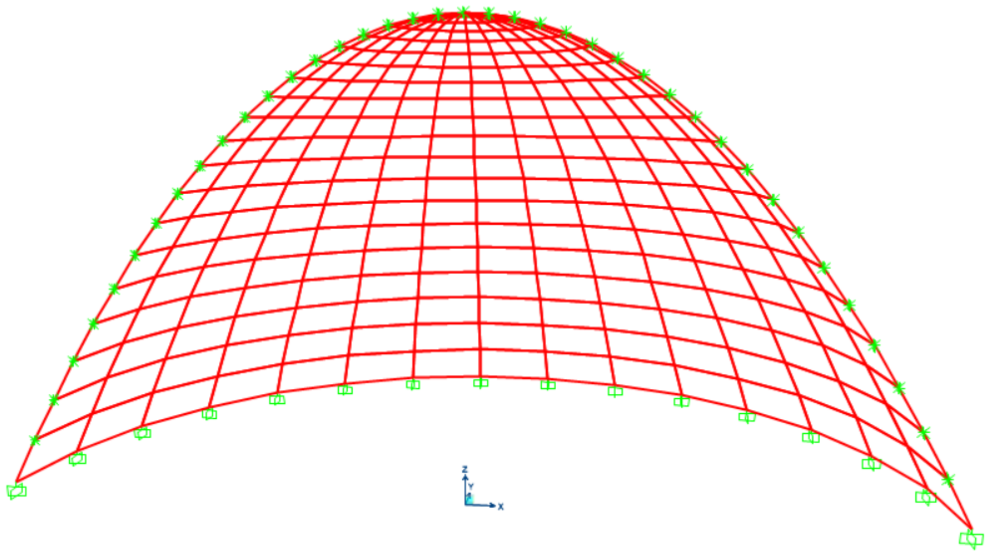

Figure 3.5a – Dome with H/R= 5/5

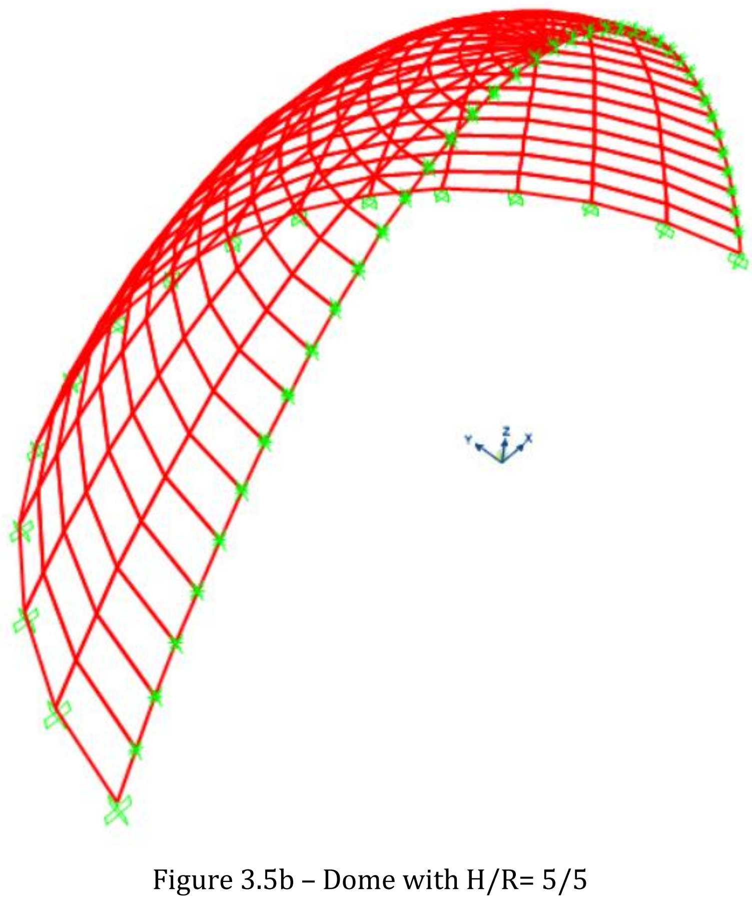

Figure 3.5b – Dome with H/R= 5/5

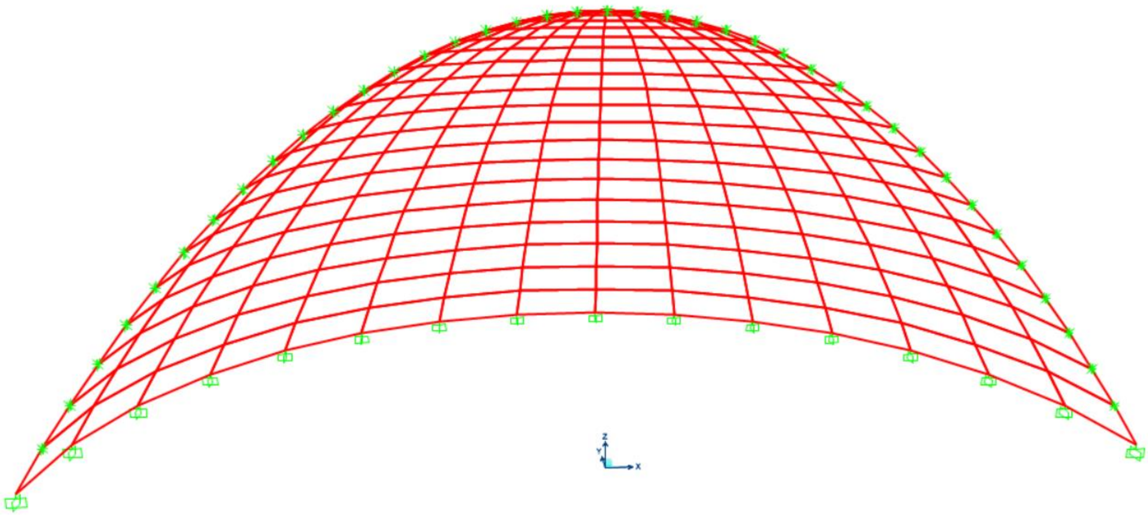

Figure 3.6a – Dome with H/R= 4/5

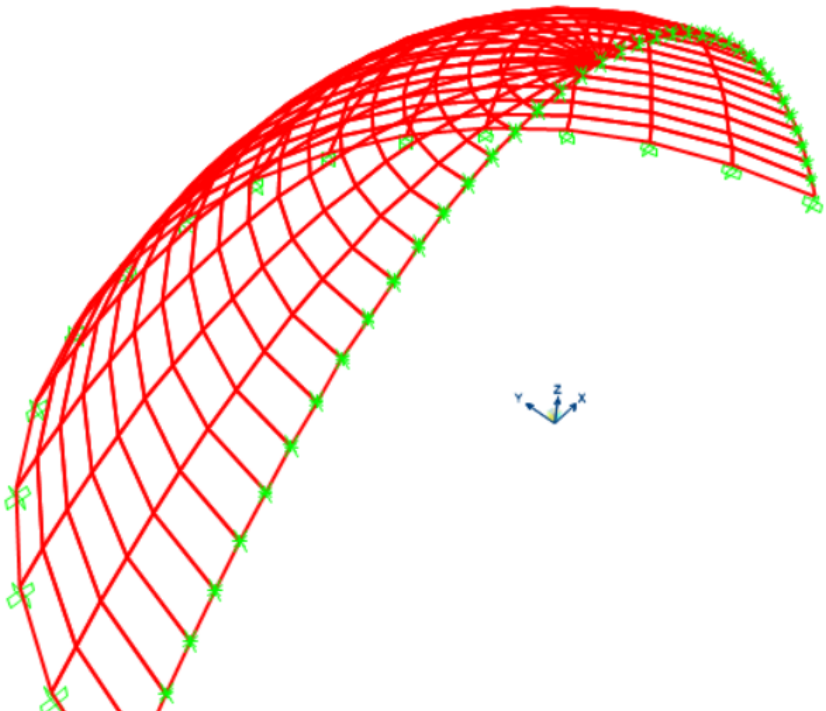

Figure 3.6b – Dome with H/R= 4/5

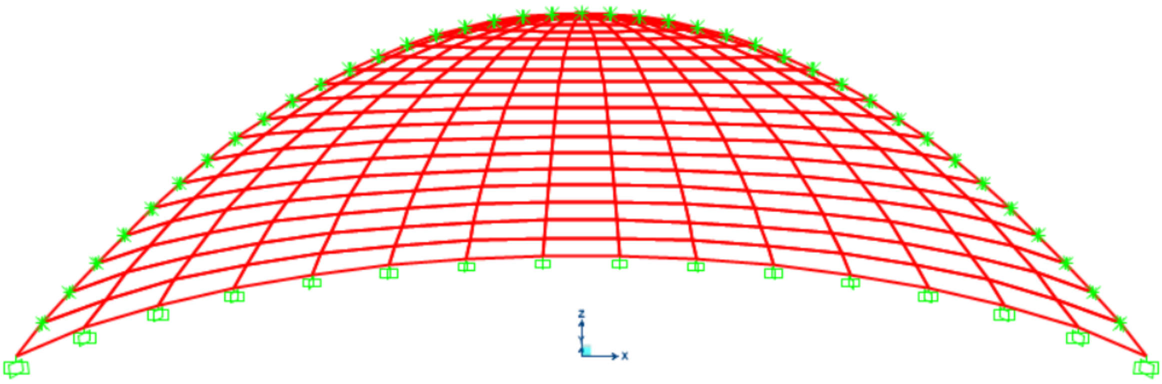

Figure 3.7a – Dome with H/R= 3/5

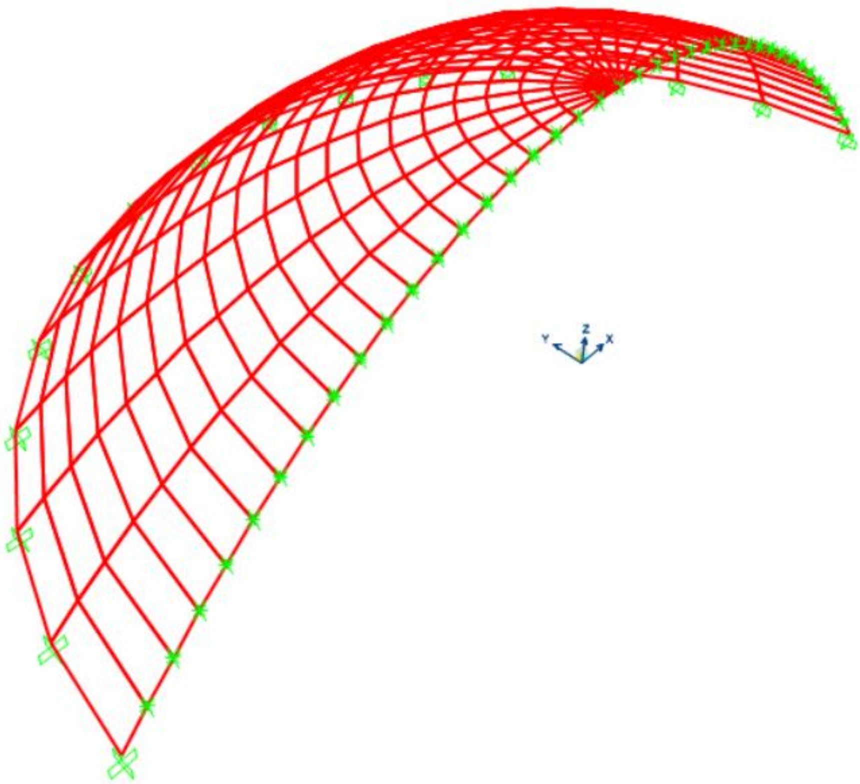

Figure 3.7b – Dome with H/R= 3/5

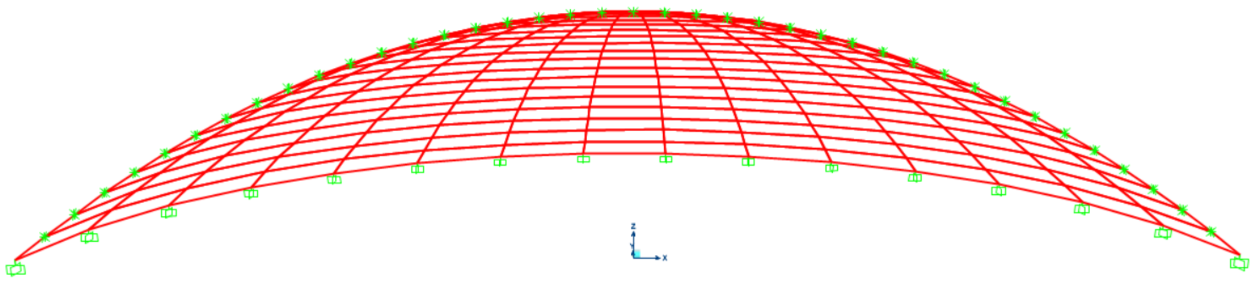

Figure 3.8a – Dome with H/R= 2/5

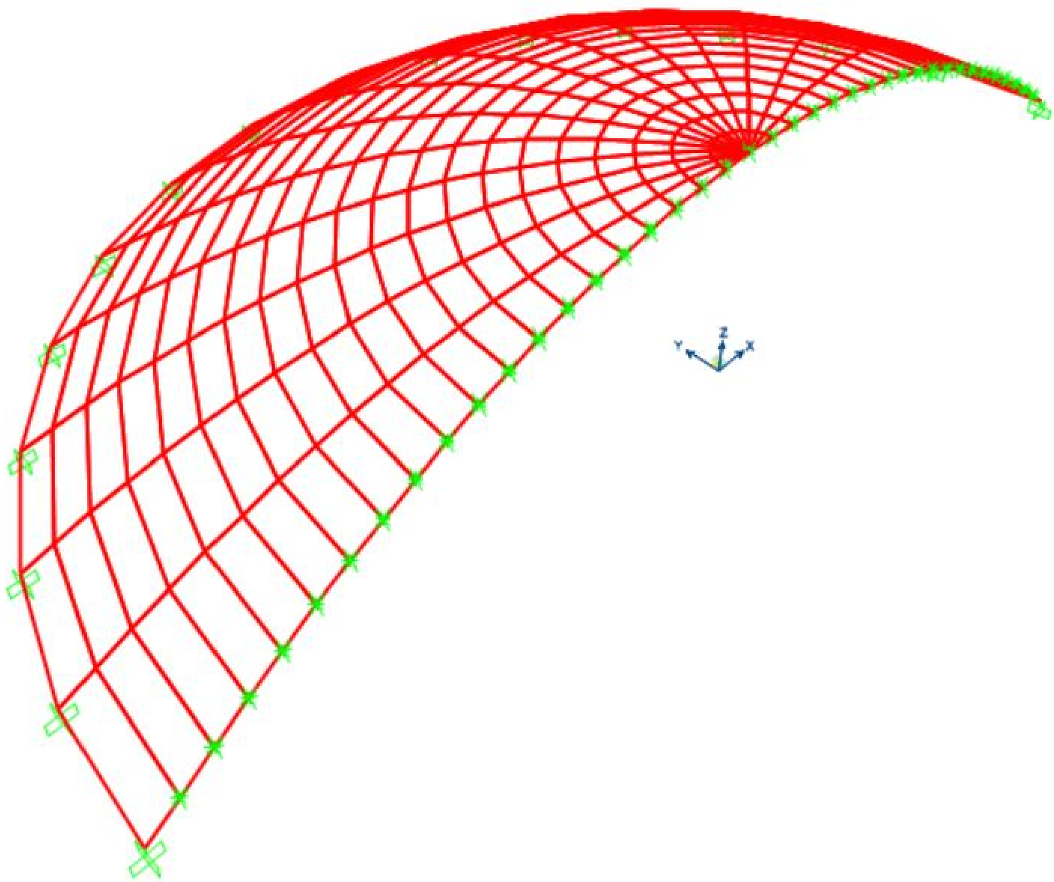

Figure 3.8b – Dome with H/R= 2/5

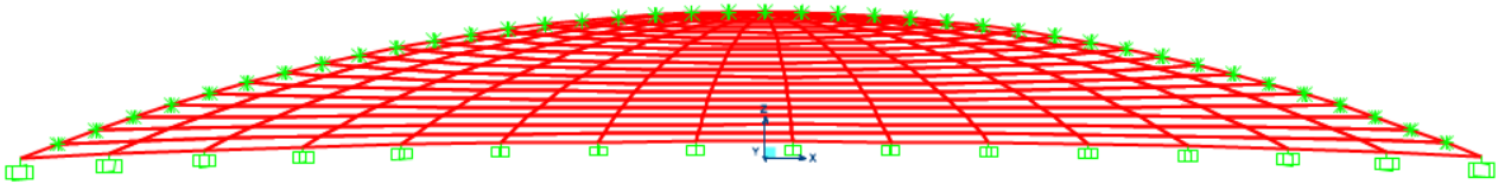

Figure 3.9a – Dome with H/R= 1/5

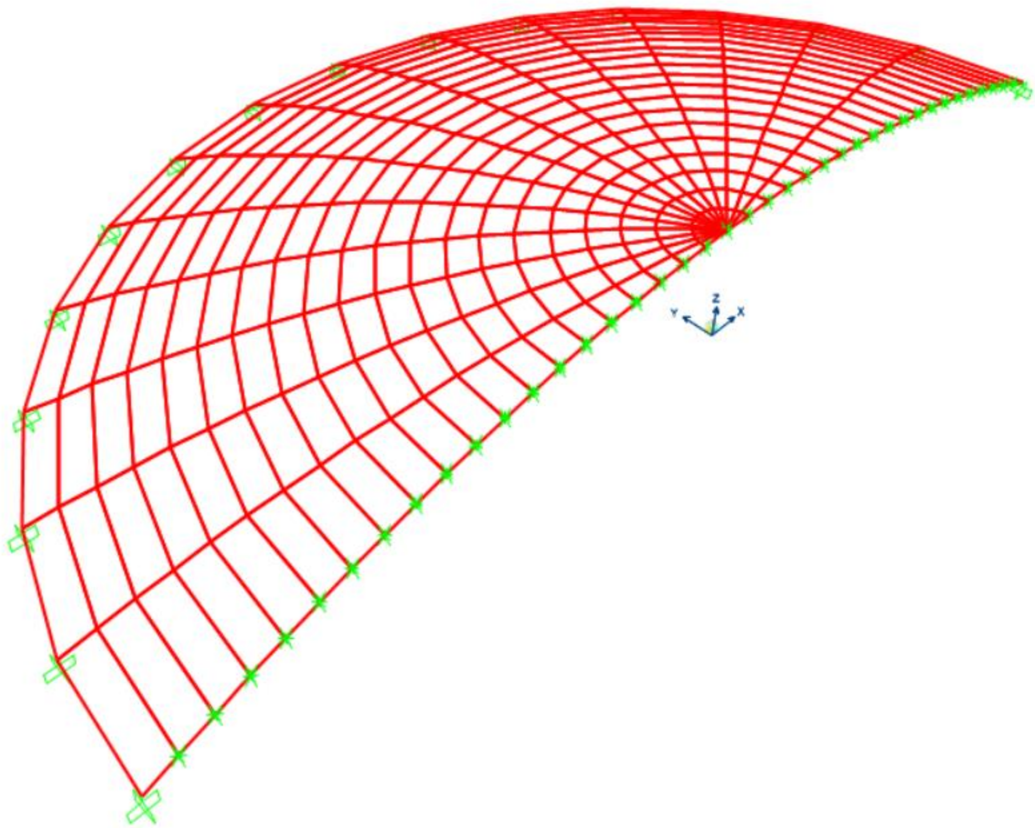

Figure 3.9b – Dome with H/R= 1/5

Once models have been obtained, we have to define a method which allow us to identify the surface of thrust; in this case of study, we have axial-symmetric geometry and so we have studied the problem in two dimensions, searching for a line of thrust, and the surface of thrust can be obtained only by rotating of 360 degrees the line of thrust.

From the SAP models, in which the shell elements are loaded by only dead loads, we have extrapolated the reactions of the joints who belong to a generic half of arch (21 nodes).

Thus, for each node, we have obtained M_x, M_y, N_x and N_y from which it is possible to derivate the eccentricities along the horizontal axis in the following way

$$e_x = \frac{M_x}{N_x}$$

$$e_y = \frac{M_y}{N_y}$$

Then, the line of thrust is determined by considering the average of the eccentricities along the X and Y directions:

$$e_{av} = \frac{e_x + e_y}{2}$$

So, for each one of the 35 models, once the eccentricities of the 21 nodes are obtained, these were copied in a .txt file.

Then a simple code wrote in Matlab has been used, from which we have obtained the lines of thrust, given by the succession of the eccentricities.

Finally, we have five diagrams, which differs by H/R and, on each diagram, there are 8 lines: one is the medium line of the shell elements and the other seven are the lines of thrust, obtained for different relative thickness. For every diagram it is reported a zoom on the boundary constraint region of the dome, in order to observe, with particular attention, the behaviour in this zone.

The final diagrams are represented in the following

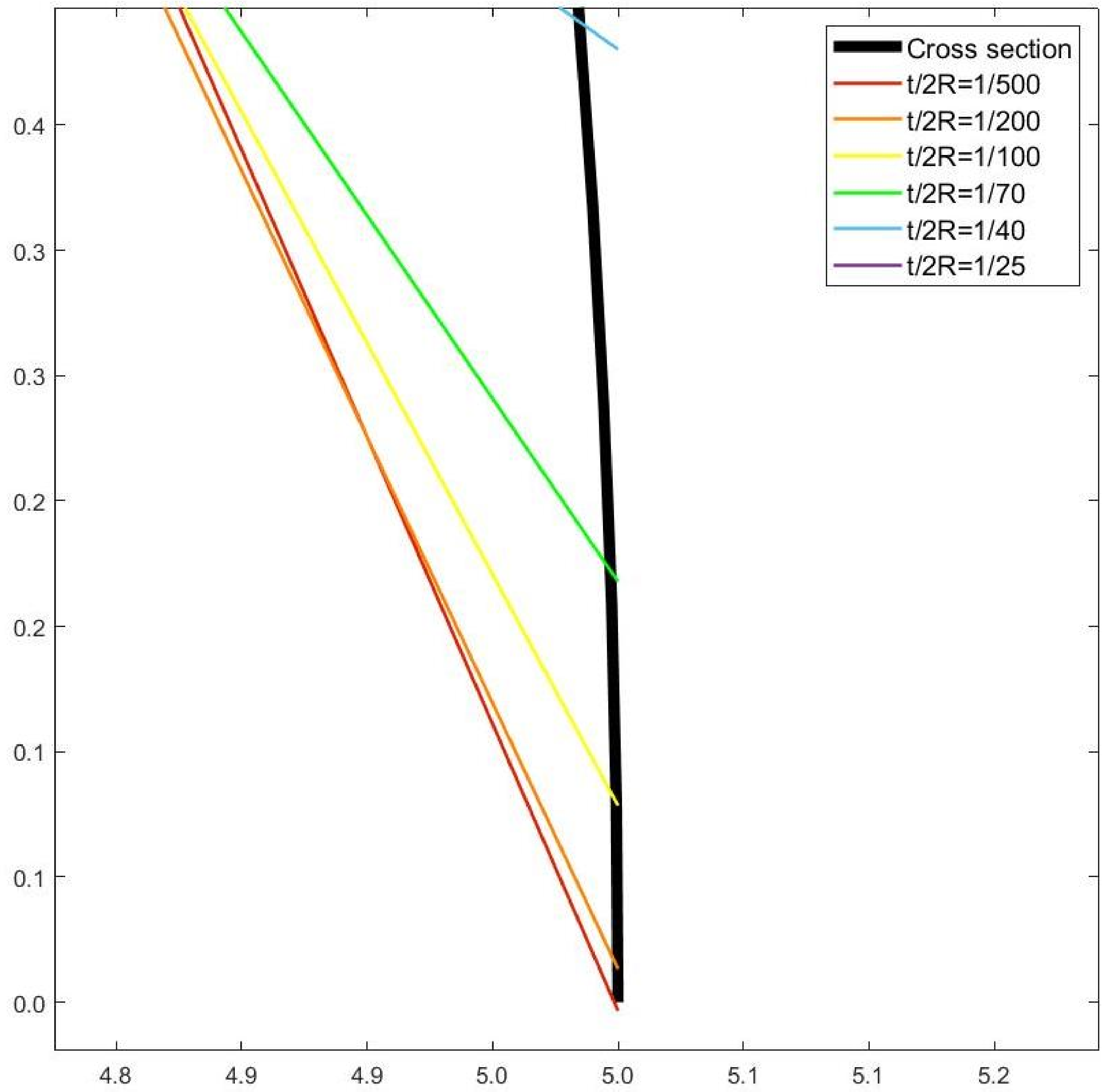
Cross section
t/2R=1/500
t/2R=1/200
t/2R=1/100
t/2R=1/70
t/2R=1/40
t/2R=1/25
0.4
0.3
0.3
0.2
0.2
0.1
0.1
0.0
4.8
4.9
4.9
5.0
5.0
5.1
5.1
5.2

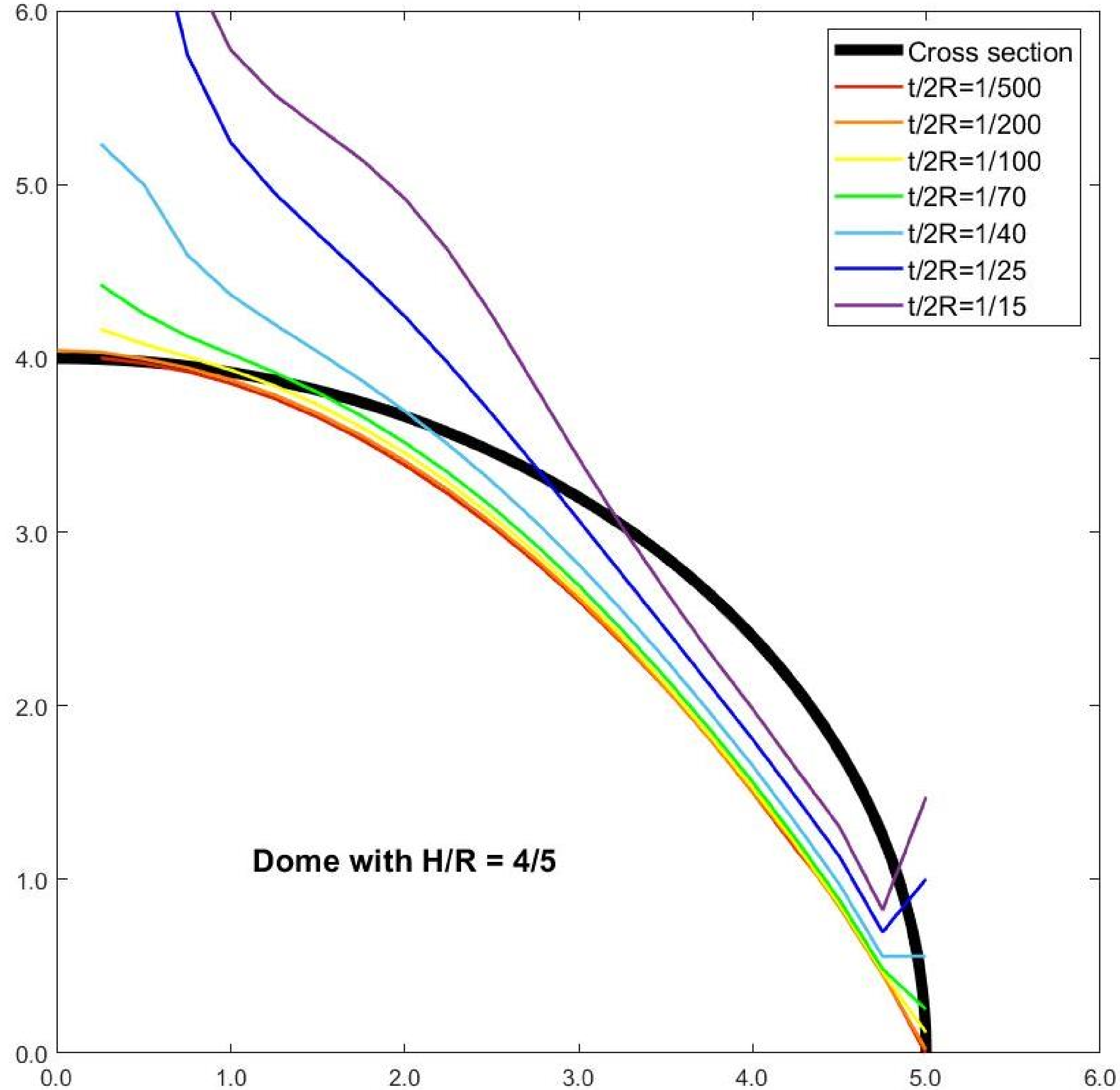
Cross section
t/2R=1/500
t/2R=1/200
t/2R=1/100
t/2R=1/70
t/2R=1/40
t/2R=1/25
t/2R=1/15
Dome with H/R = 4/5
0.0
1.0
2.0
3.0
4.0
5.0
6.0

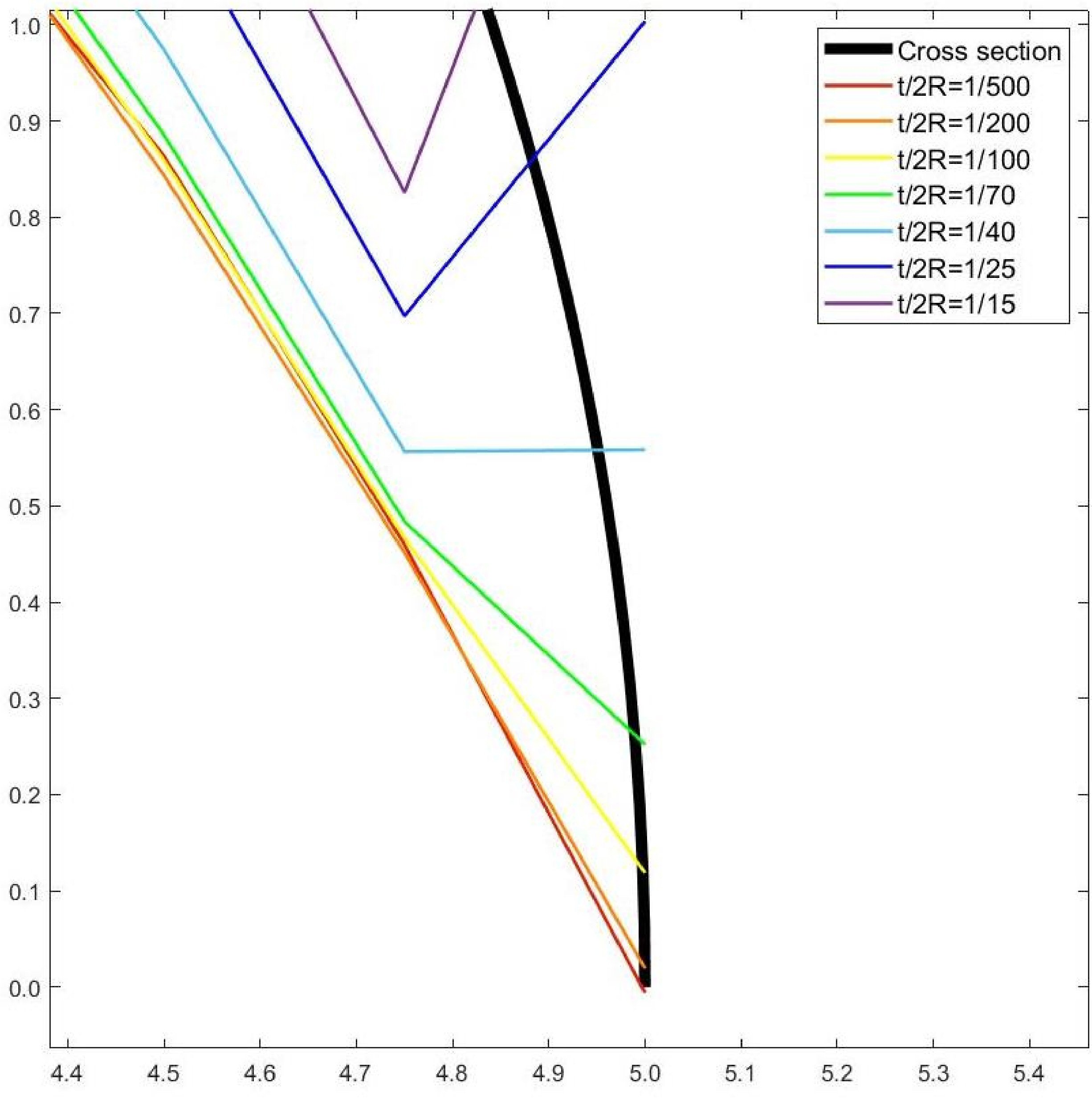
Cross section
t/2R=1/500
t/2R=1/200
t/2R=1/100
t/2R=1/70
t/2R=1/40
t/2R=1/25
t/2R=1/15
1.0
0.9
0.8
0.7
0.6
0.5
0.4
0.3
0.2
0.1
0.0
4.4
4.5
4.6
4.7
4.8
4.9
5.0
5.1
5.2
5.3
5.4

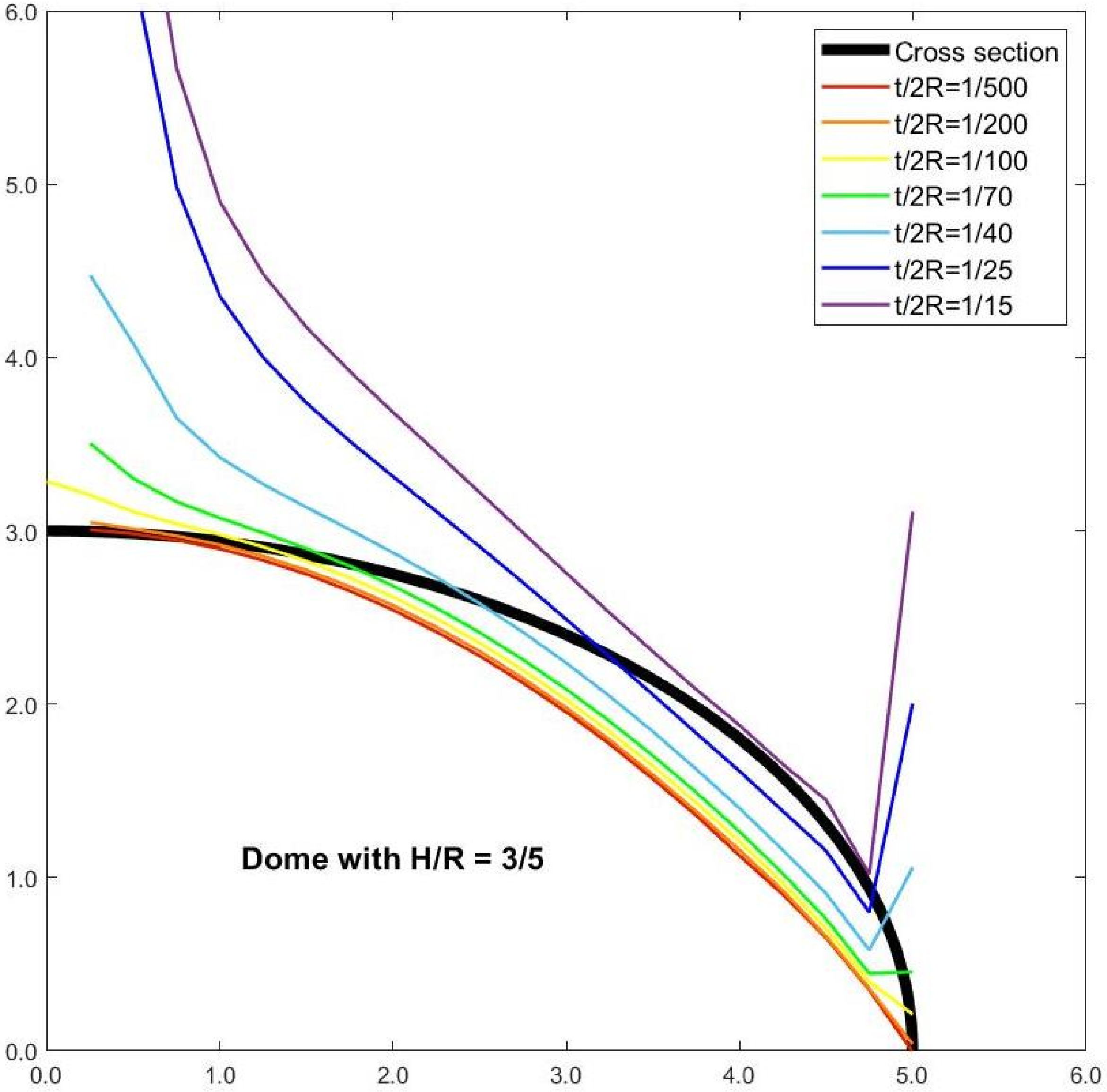
Cross section
t/2R=1/500
t/2R=1/200
t/2R=1/100
t/2R=1/70
t/2R=1/40
t/2R=1/25
t/2R=1/15
Dome with H/R = 3/5
0.0
1.0
2.0
3.0
4.0
5.0
6.0

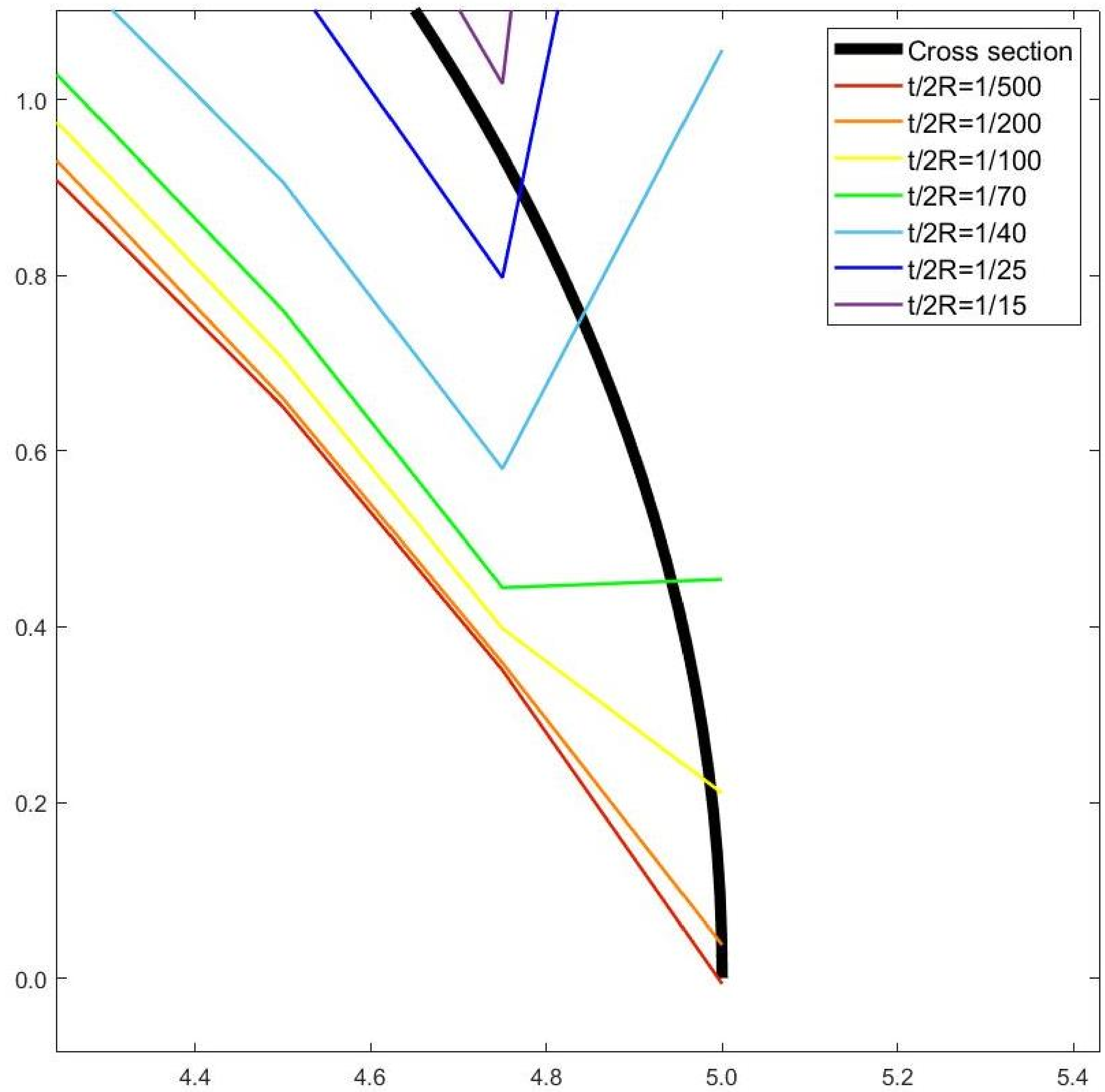
Cross section
t/2R=1/500
t/2R=1/200
t/2R=1/100
t/2R=1/70
t/2R=1/40
t/2R=1/25
t/2R=1/15
1.0
0.8
0.6
0.4
0.2
0.0
4.4
4.6
4.8
5.0
5.2
5.4

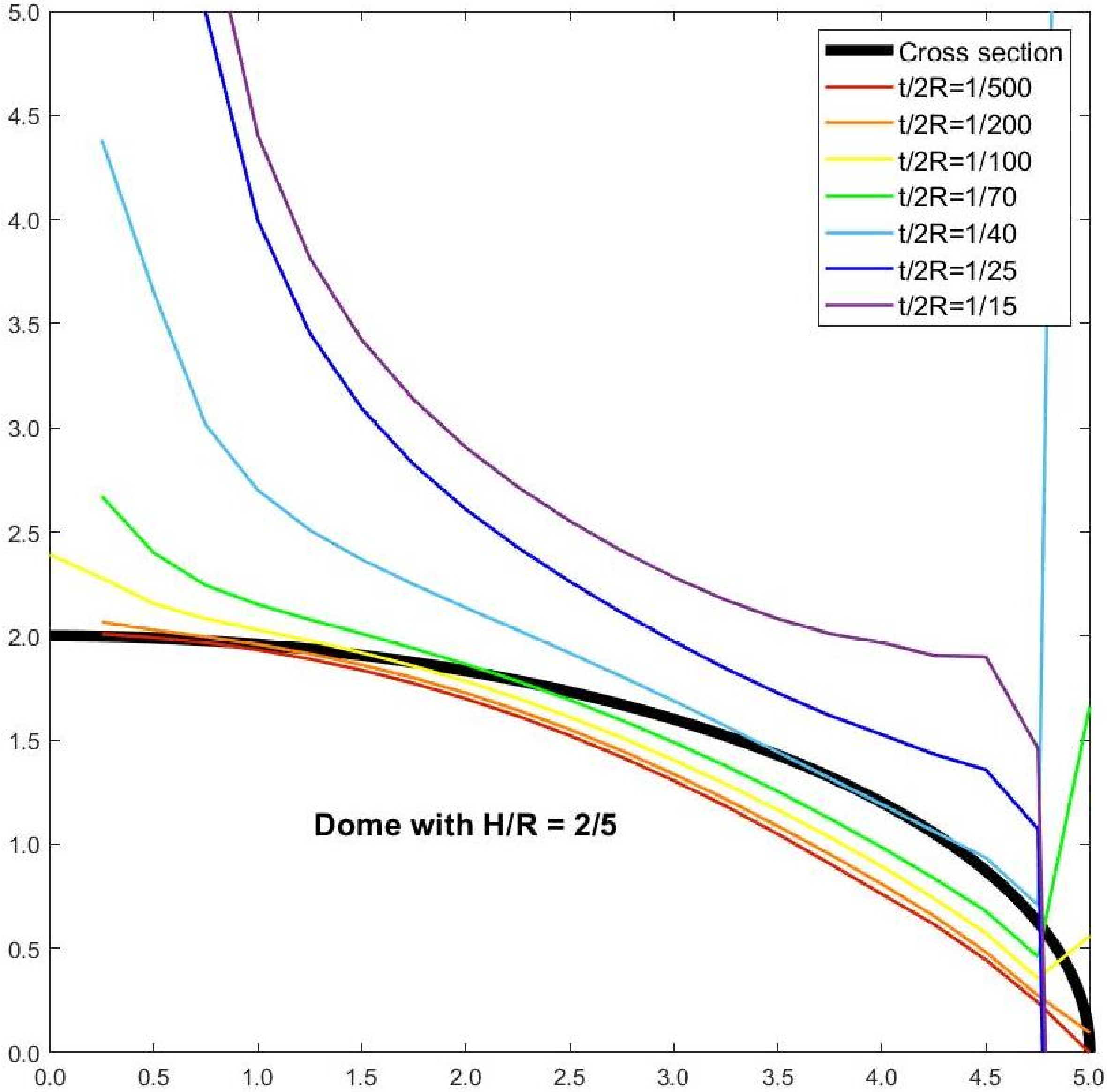

Cross section
t/2R=1/500
t/2R=1/200
t/2R=1/100
t/2R=1/70
t/2R=1/40
t/2R=1/25
t/2R=1/15
Dome with H/R = 2/5
0.0
0.5
1.0
1.5
2.0
2.5
3.0
3.5
4.0
4.5
5.0

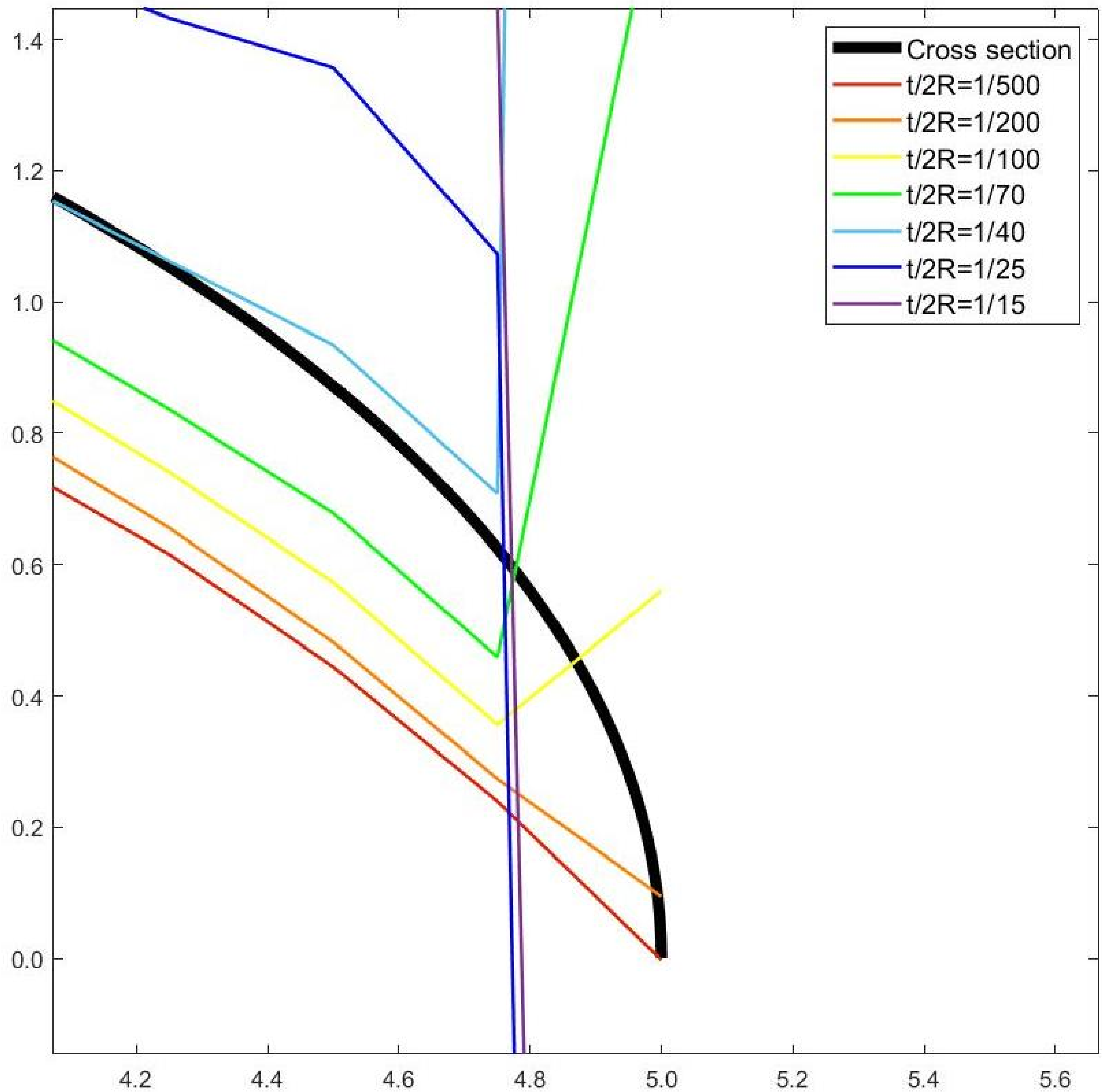
Cross section
t/2R=1/500
t/2R=1/200
t/2R=1/100
t/2R=1/70
t/2R=1/40
t/2R=1/25
t/2R=1/15
1.4
1.2
1.0
0.8
0.6
0.4
0.2
0.0
4.2
4.4
4.6
4.8
5.0
5.2
5.4
5.6

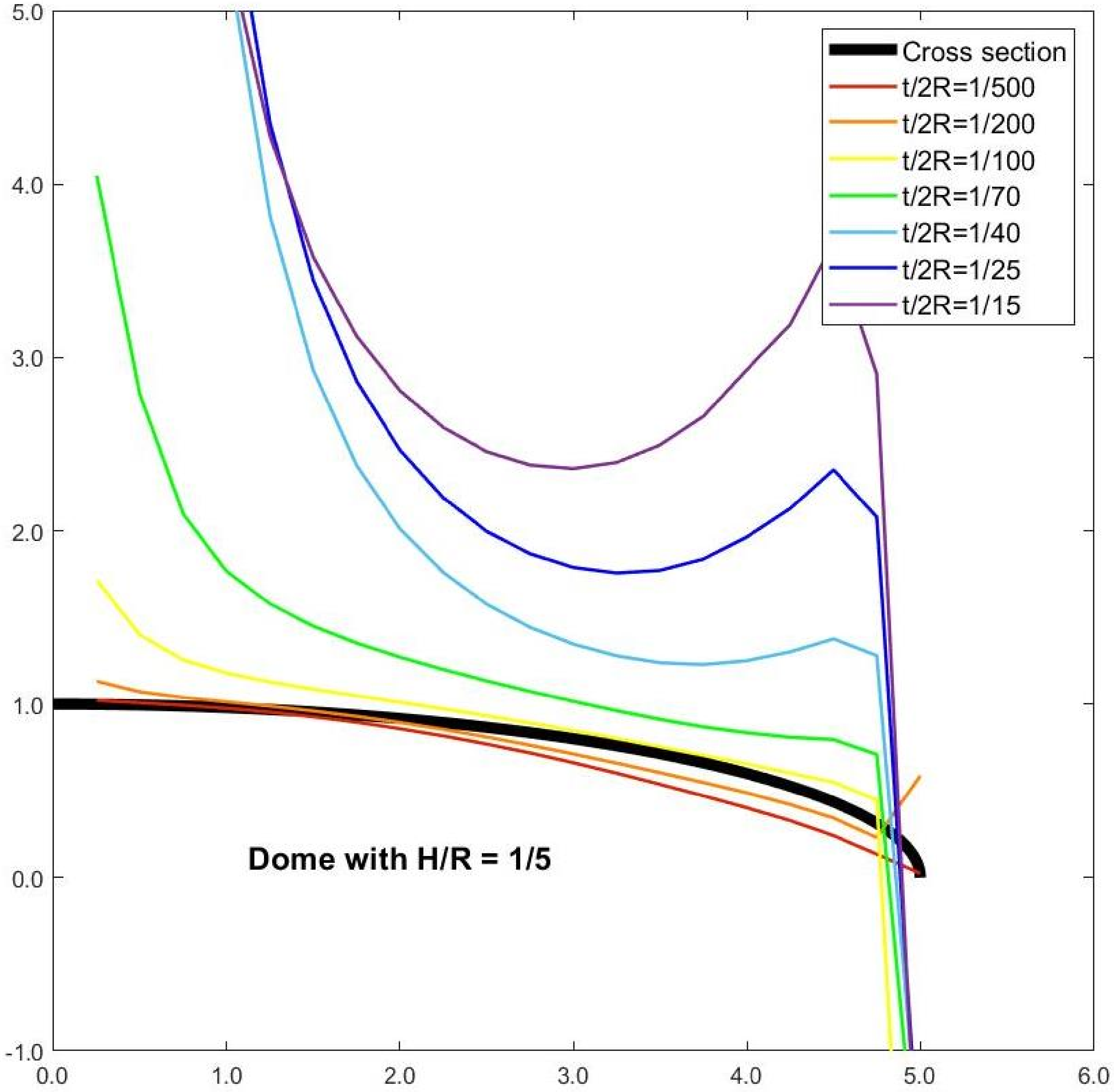

Cross section
t/2R=1/500
t/2R=1/200
t/2R=1/100
t/2R=1/70
t/2R=1/40
t/2R=1/25
t/2R=1/15
Dome with H/R = 1/5
5.0
4.0
3.0
2.0
1.0
0.0
-1.0
0.0
1.0
2.0
3.0
4.0
5.0
6.0

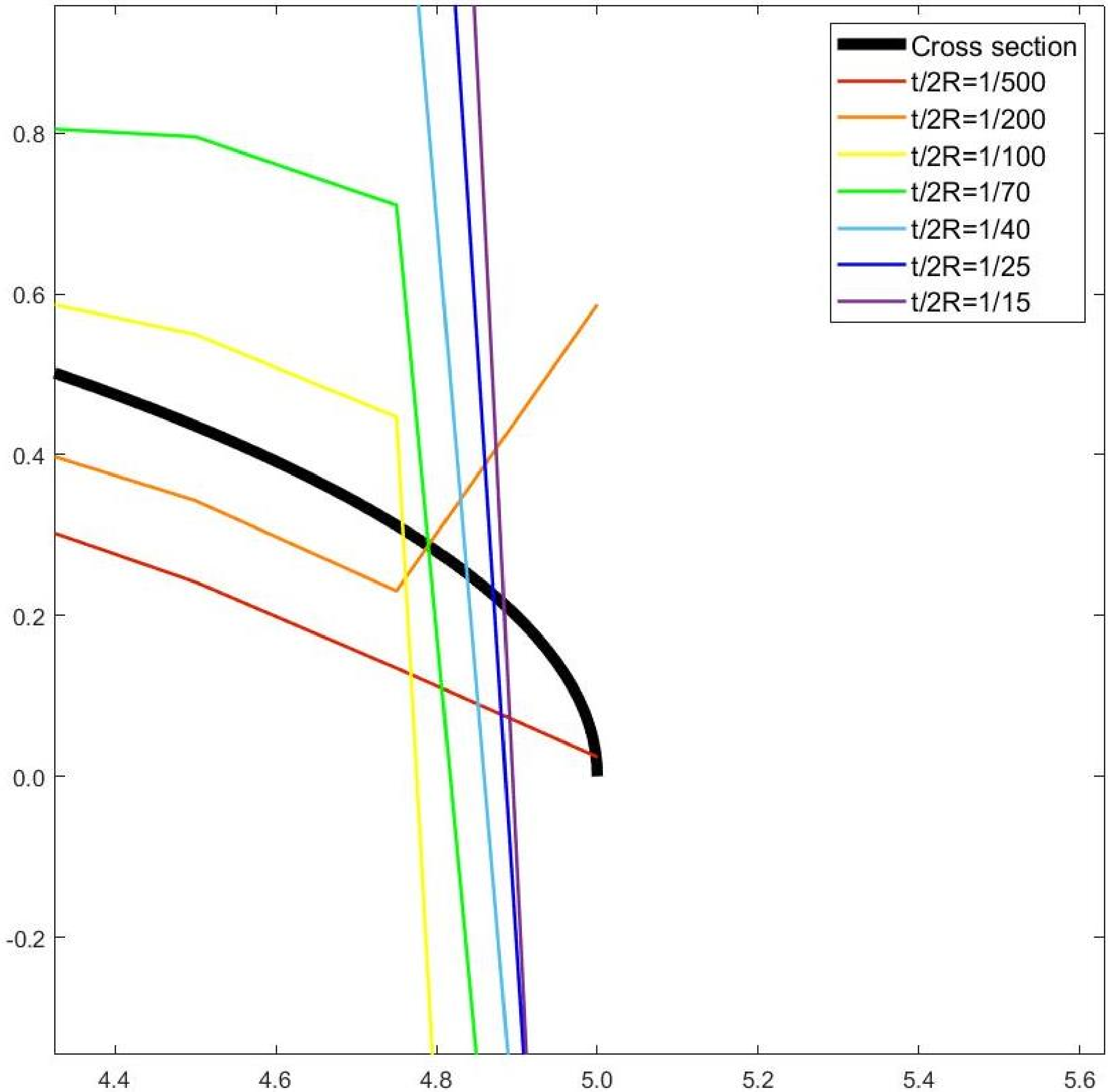
Cross section
t/2R=1/500
t/2R=1/200
t/2R=1/100
t/2R=1/70
t/2R=1/40
t/2R=1/25
t/2R=1/15
0.8
0.6
0.4
0.2
0.0
-0.2
4.4
4.6
4.8
5.0
5.2
5.4
5.6

Moreover, the surface of thrust has been evaluated also for the eccentricities along the local axes x, and the local axes y. In the following are represented the graphs obtained by the analysis.

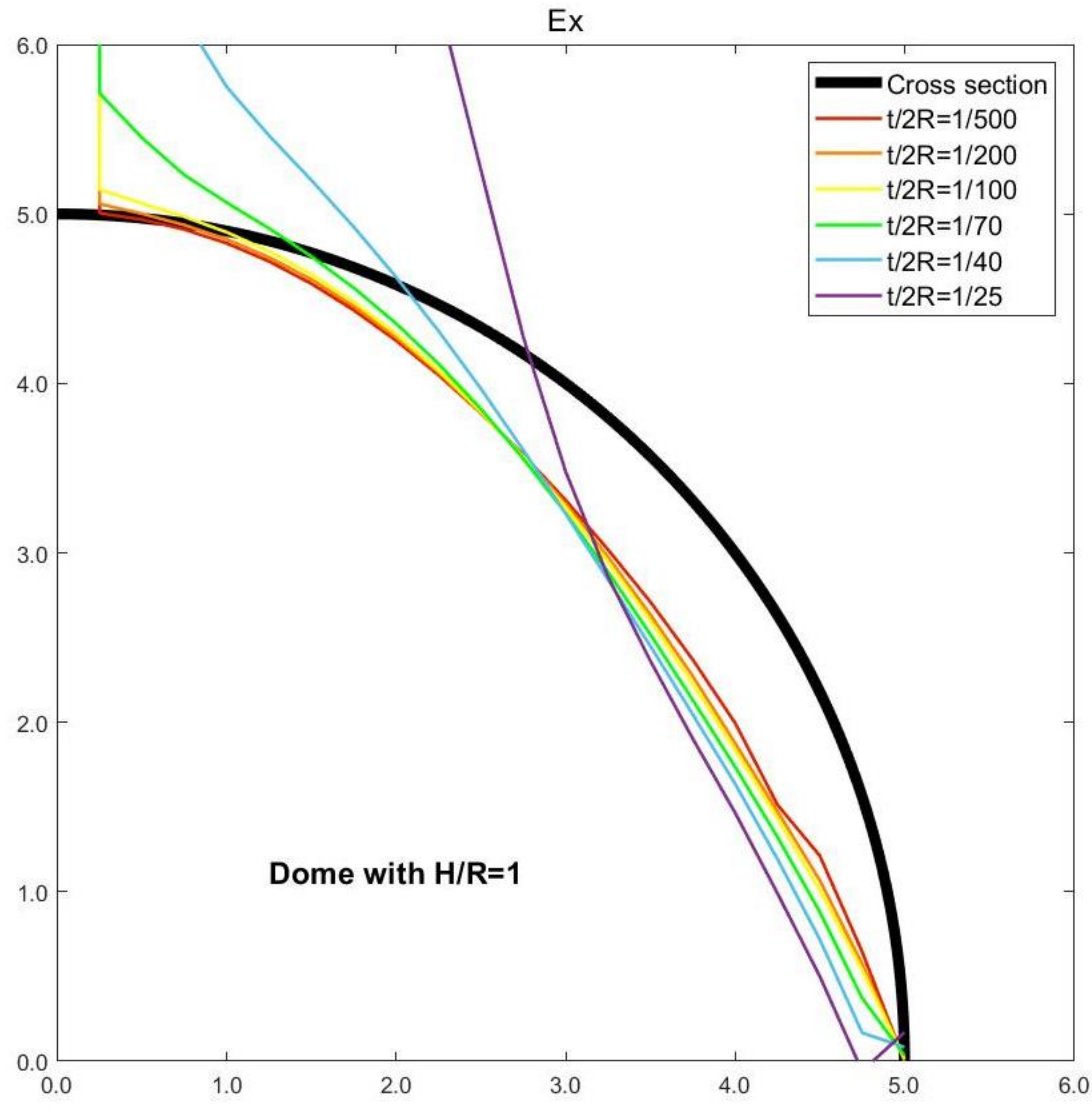

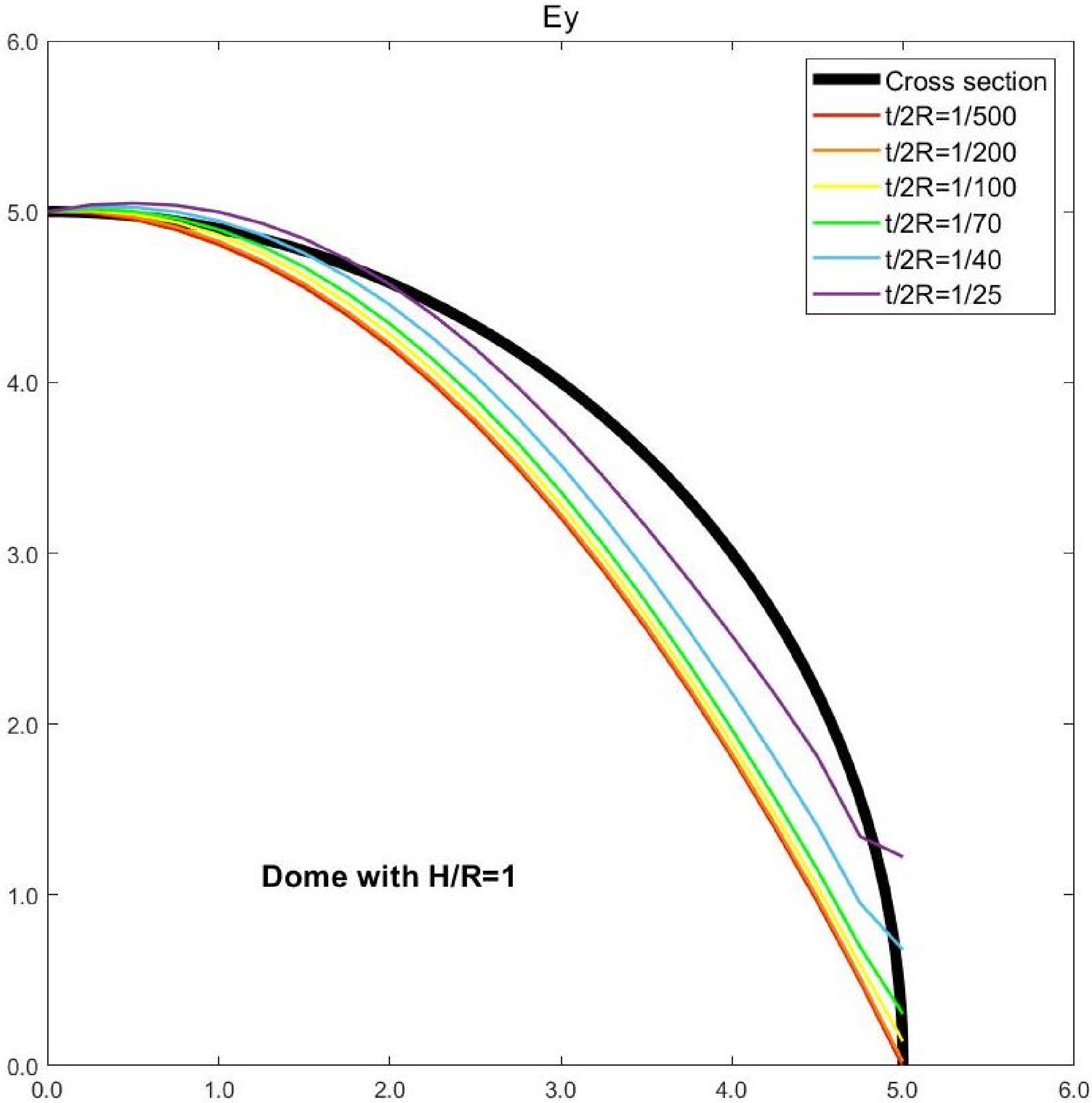

Ey
Cross section
t/2R=1/500
t/2R=1/200
t/2R=1/100
t/2R=1/70
t/2R=1/40
t/2R=1/25
Dome with H/R=1
6.0
5.0
4.0
3.0
2.0
1.0
0.0
0.0
1.0
2.0
3.0
4.0
5.0
6.0

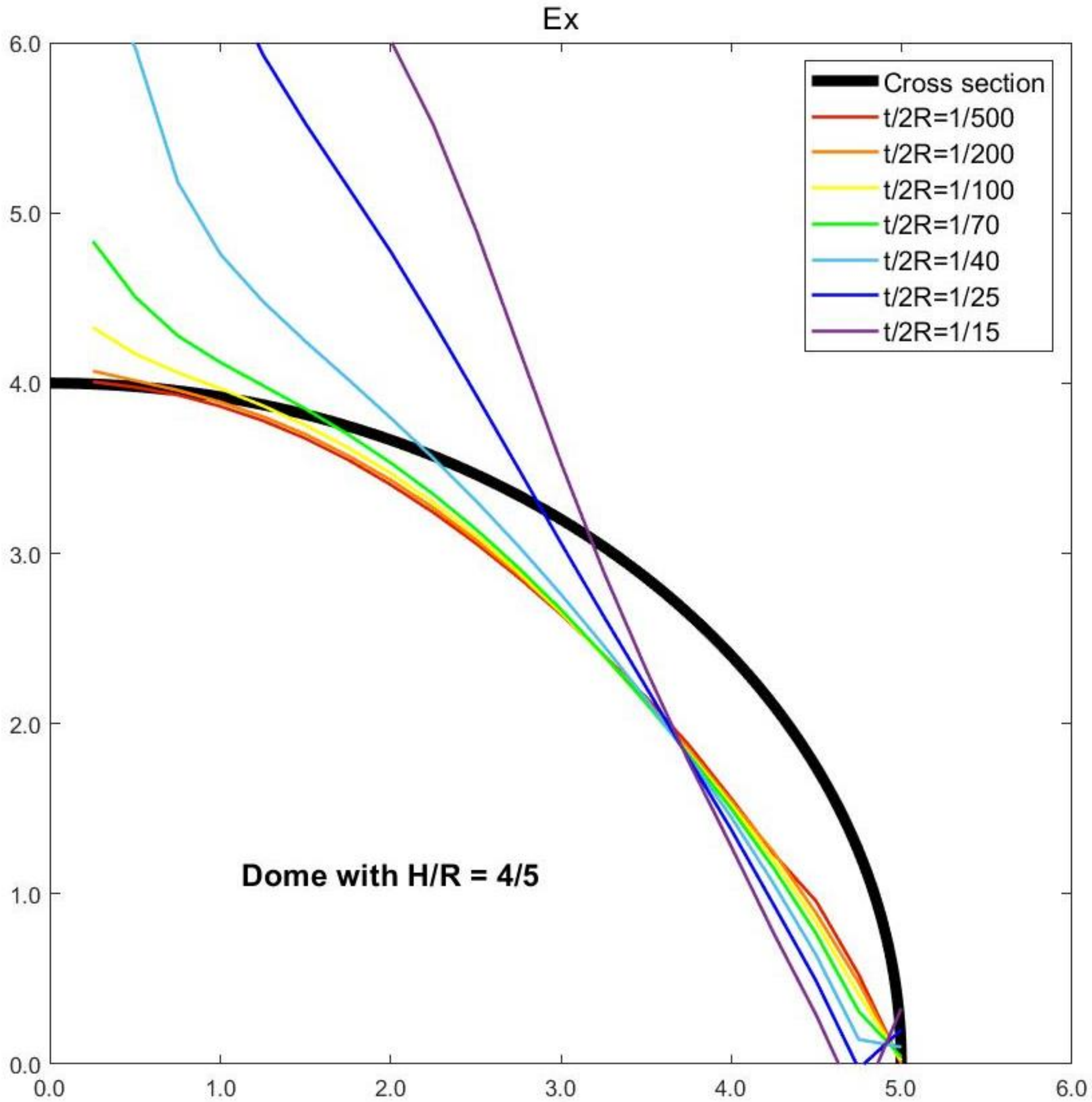

Ex
Cross section
t/2R=1/500
t/2R=1/200
t/2R=1/100
t/2R=1/70
t/2R=1/40
t/2R=1/25
t/2R=1/15
Dome with H/R = 4/5
0.0
1.0
2.0
3.0
4.0
5.0
6.0

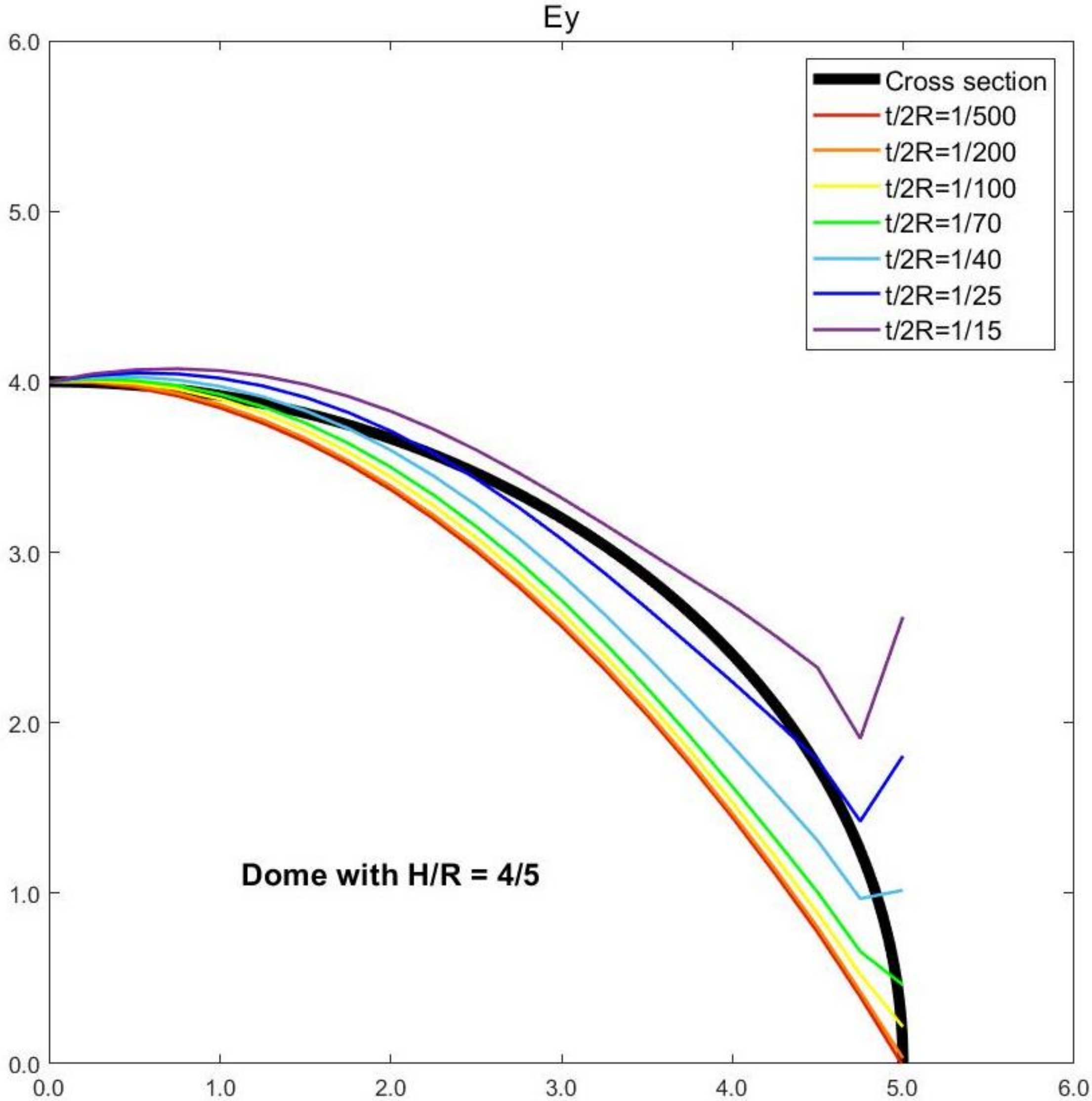

Ey
Cross section
t/2R=1/500
t/2R=1/200
t/2R=1/100
t/2R=1/70
t/2R=1/40
t/2R=1/25
t/2R=1/15
Dome with H/R = 4/5
6.0
5.0
4.0
3.0
2.0
1.0
0.0
0.0
1.0
2.0
3.0
4.0
5.0
6.0

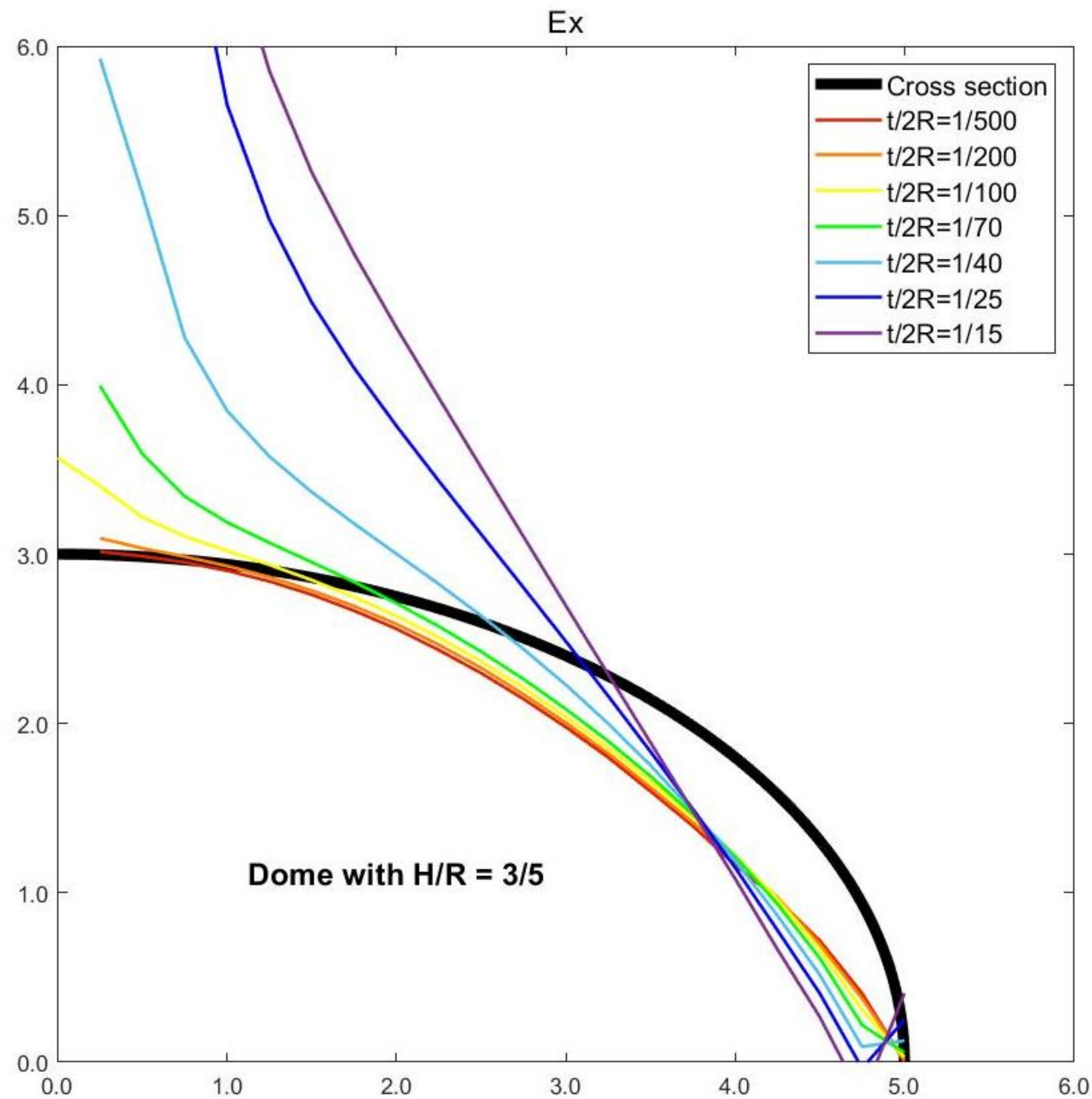

Ex
Cross section
t/2R=1/500
t/2R=1/200
t/2R=1/100
t/2R=1/70
t/2R=1/40
t/2R=1/25
t/2R=1/15
Dome with H/R = 3/5
0.0
1.0
2.0
3.0
4.0
5.0
6.0

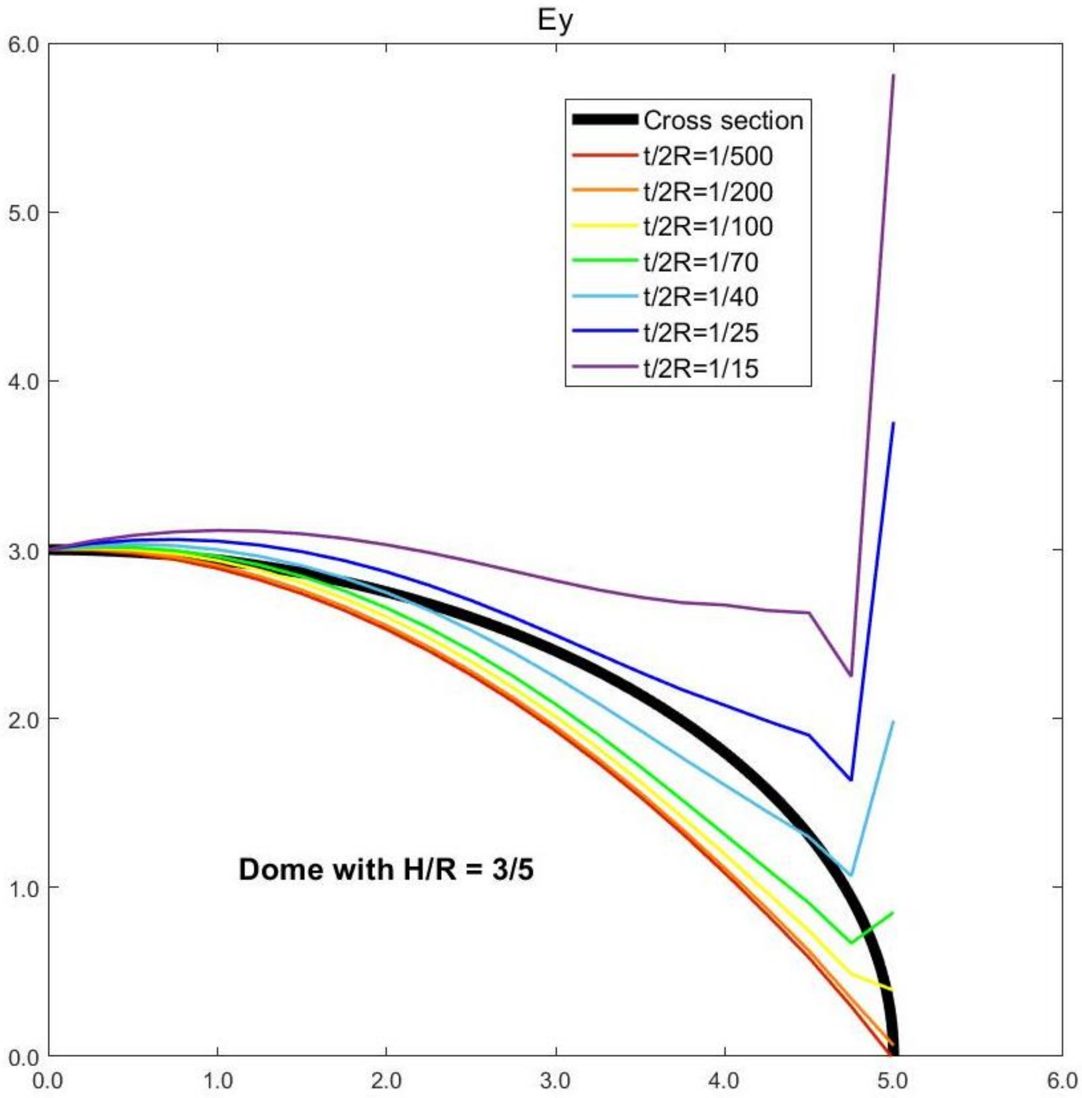

Ey
Cross section
t/2R=1/500
t/2R=1/200
t/2R=1/100
t/2R=1/70
t/2R=1/40
t/2R=1/25
t/2R=1/15
Dome with H/R = 3/5
6.0
5.0
4.0
3.0
2.0
1.0
0.0
0.0
1.0
2.0
3.0
4.0
5.0
6.0

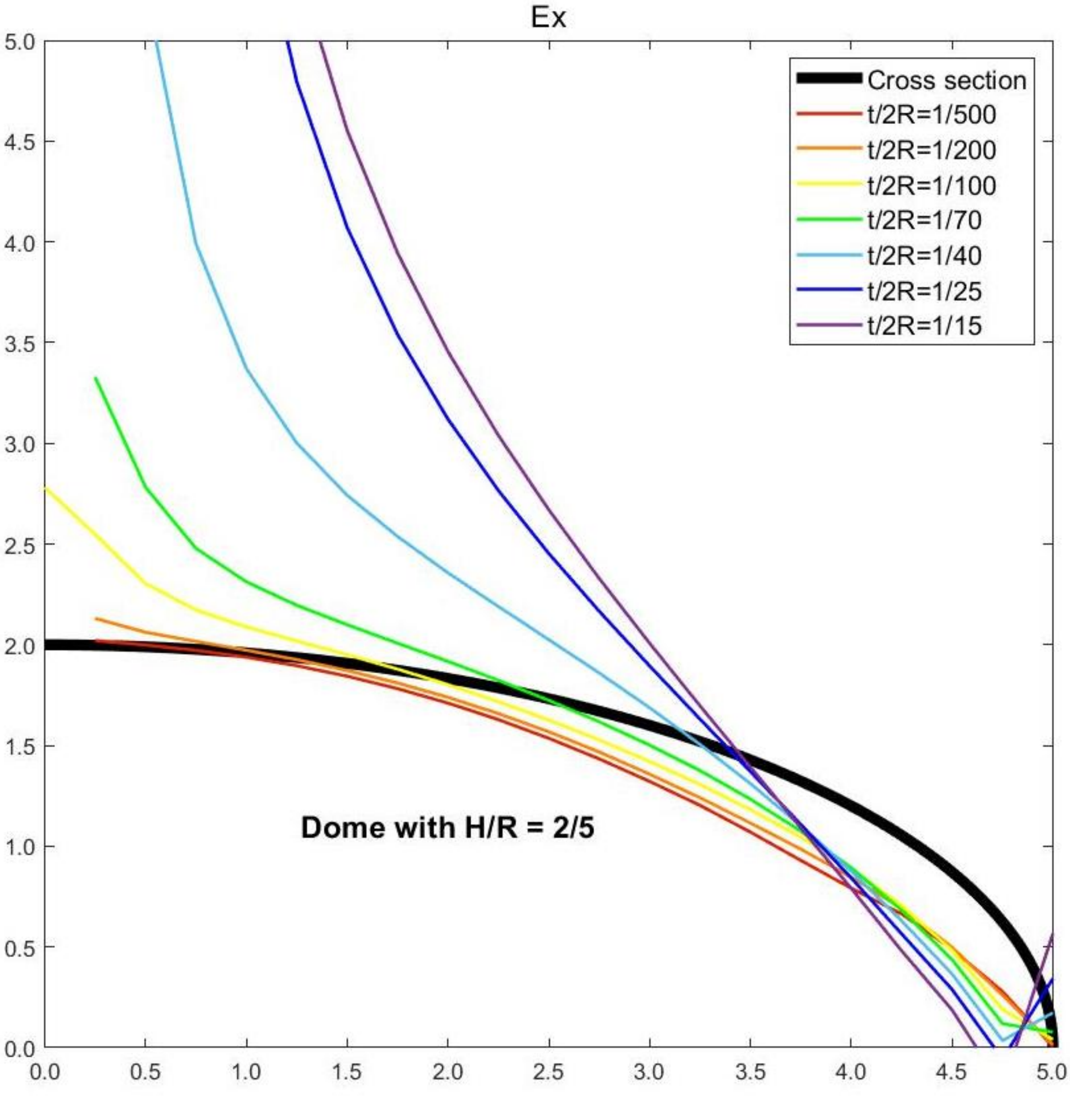
Ex
Cross section
t/2R=1/500
t/2R=1/200
t/2R=1/100
t/2R=1/70
t/2R=1/40
t/2R=1/25
t/2R=1/15
Dome with H/R = 2/5
5.0
4.5
4.0
3.5
3.0
2.5
2.0
1.5
1.0
0.5
0.0
0.0 0.5 1.0 1.5 2.0 2.5 3.0 3.5 4.0 4.5 5.0

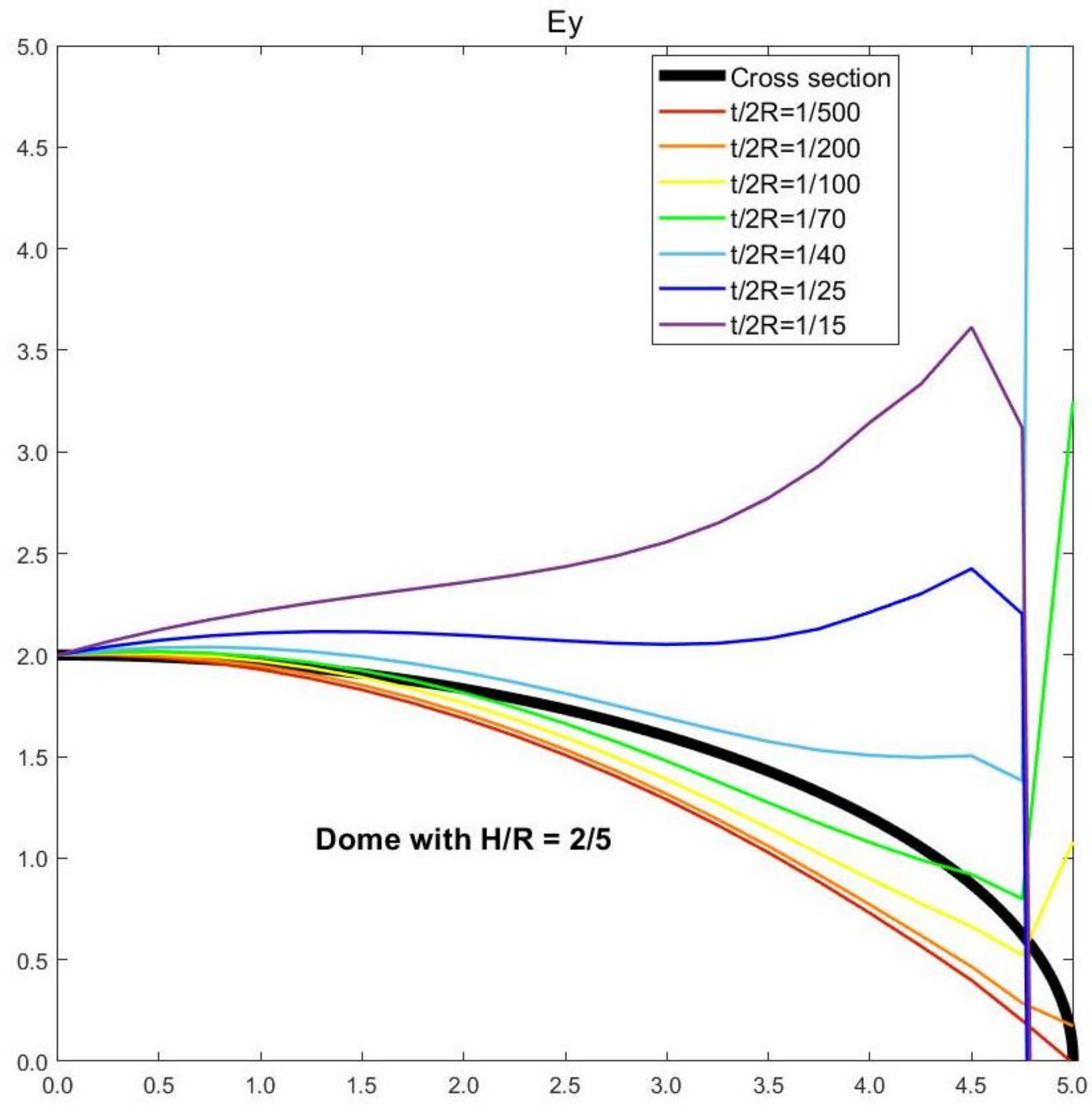
Ey
Cross section
t/2R=1/500
t/2R=1/200
t/2R=1/100
t/2R=1/70
t/2R=1/40
t/2R=1/25
t/2R=1/15
Dome with H/R = 2/5
0.0
0.5
1.0
1.5
2.0
2.5
3.0
3.5
4.0
4.5
5.0

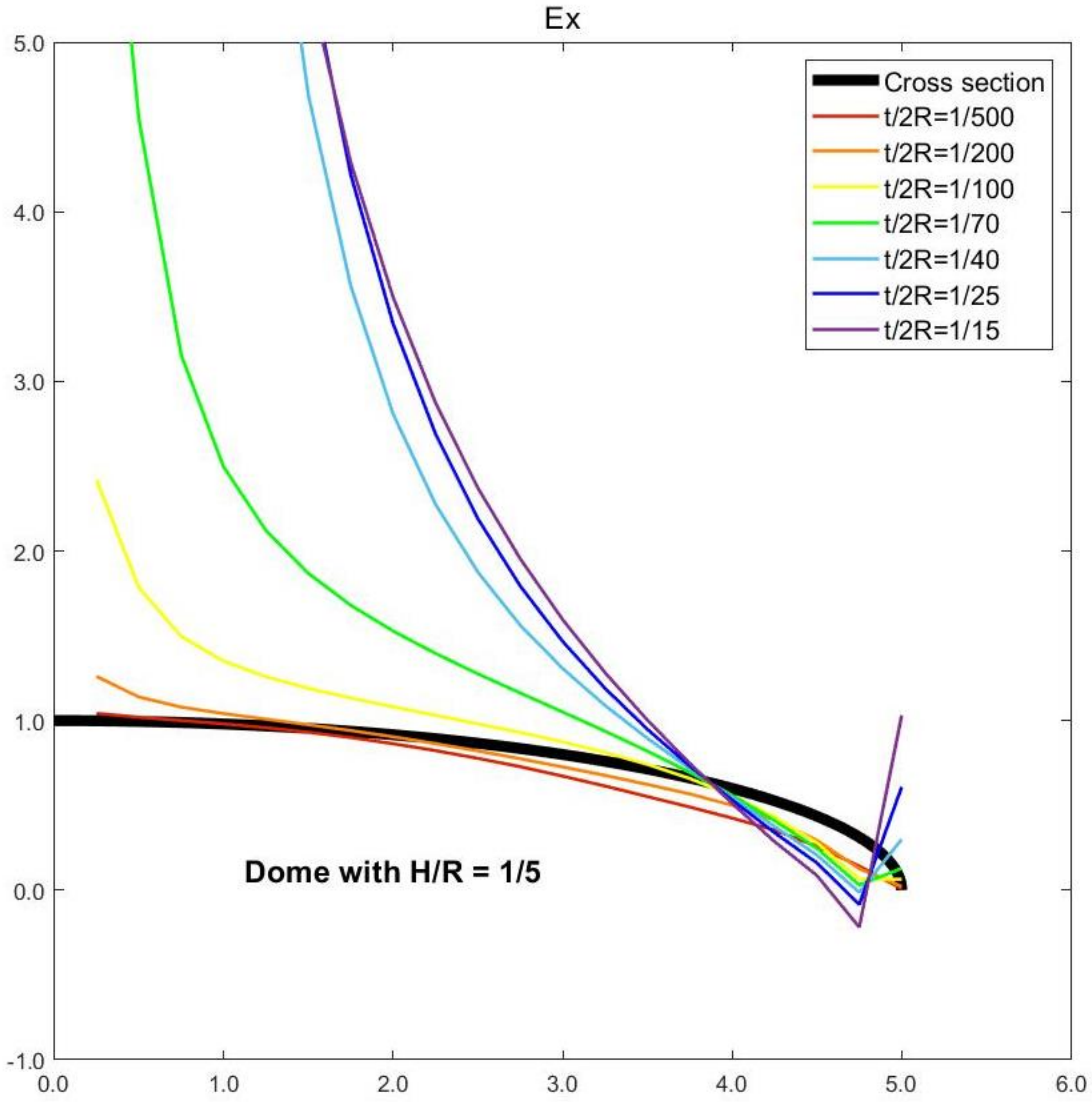
Ex
Cross section
t/2R=1/500
t/2R=1/200
t/2R=1/100
t/2R=1/70
t/2R=1/40
t/2R=1/25
t/2R=1/15
Dome with H/R = 1/5
5.0
4.0
3.0
2.0
1.0
0.0
-1.0
0.0
1.0
2.0
3.0
4.0
5.0
6.0

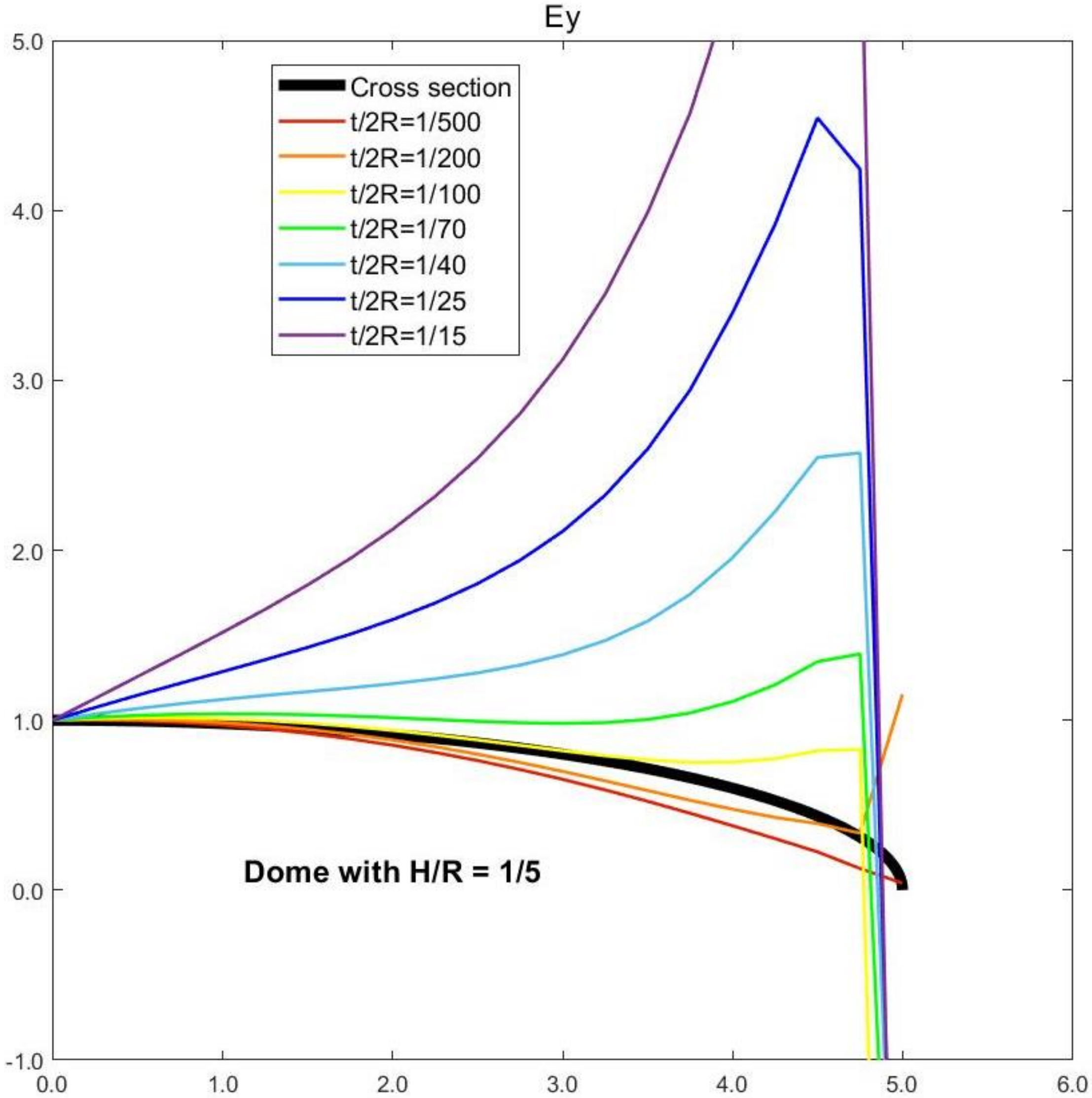
Ey
Cross section
t/2R=1/500
t/2R=1/200
t/2R=1/100
t/2R=1/70
t/2R=1/40
t/2R=1/25
t/2R=1/15
Dome with H/R = 1/5
5.0
4.0
3.0
2.0
1.0
0.0
-1.0
0.0
1.0
2.0
3.0
4.0
5.0
6.0

Finally, it is evident from the graphs that, the eccentricities along x are high at the top of the shell elements and very low in the boundary constraint region, on the other hand, the eccentricities along the y axes are very low on the top of the element and high in the constraint region.

4. CONCLUSIONS

This dissertation is divided in three main parts.

The first chapter is about the theory of shell structures, going from the plate elements to the shell of revolution and finally to the thin shells and membranes. Then, there is an analysis of the theory of shell structures proposed by both the German and Russian schools. In the final part of the first chapter the static kinematic duality is mentioned, comparing it with the static-geometric analogy proposed by Calladine, a Russian engineer. The latter, proved to be of less practical use.

In the second part there is an analysis of the fundamental of funicularity, in order to find a simple way for defining quantitatively the concept of Funicularity. So, there is an excursus of the authors who take into account this concept. The first mention in the scientific literature about the condition of Funicularity was due to Dermot O'Dwyer, who, starting from the analysis of arches, suggested a method to find the surface of thrust. Then, the method proposed by Block and Ochsendorf is explained. They designed a new methodology to evaluate the surface of thrust called Thrust Network Analysis. This one, was then taken up by Marmo and Rosati, who simplified the TNA deleting some geometric hypothesis and expanded the field of application of the analysis to the seismic area, also including the shell elements loaded by horizontal loads.

The abovementioned approaches are quite complex; therefore, in the third part of this thesis it is described in detail the approaches used to identify a simple and effective way to evaluate the surface of thrust. This approach consists in defining the eccentricities of the points of the shell structure along the local axis x and y, and then considering the average of these ones.

From the analysis of the obtained surfaces of thrust, it is possible to observe that the effect of Funicularity, is obtained for small thicknesses. Moreover, by decreasing the shell relative thickness, the surface of thrust tends to overlap with the geometrical axis of the structure, particularly in the boundary constraint region. Finally, it is evident that, for each shallowness ratio, the bending moment acting at the shell supports tends to vanish.

In our cases of study, we considered only shell elements characterized by an axial-symmetric geometry, a possible future development could be to consider the generic shell element and define the surface of thrust, with the same procedure, but with a more generic approach, taking into account from the beginning three dimensions.

REFERENCES

Aron, H. (1874) *Das Gleichgewicht und die Bewegung einer unendlich dünnen, beliebig gekrümmten elastischen Schale*, Journal für die Reine und Angewandte Mathematik 78, 136–174.

Block, P. and Ochsendorf, J. (2007) *Thrust network analysis: a new methodology for threedimensional equilibrium*, J Int Assoc Shell Spatial Struct, 48:167–73.

By EdieT - Own work, CC BY-SA 4.0, https://commons.wikimedia.org/w/index.php?curid=46741439 (Figure of Zeiss dome in Jena).

Calladine, C.R. (1983) *Theory of shell structure*, Appendix 6 The 'static-geometric analogy', Cambridge University Press.

Carpinteri, A. and Accornero, F. (2020) *Funicularity in elastic domes: Coupled effects of shape and thickness,* Curved and Layered Structures, vol. 8, no. 1, 2021, pp. 181-187.

Carpinteri, A., Accornero, F. (2019) *Static–kinematic duality in the shells of revolution: Historical aspects and present developments*, Arch Appl Mech 89, 2313–2320.

Carpinteri, A. (2017) *Static-kinematic duality in beams, plates, shells and its central role in the finite element method*. Curved Layer. Struct. 4, 38–51.

Carpinteri, A. (1992) *Scienza delle Costruzioni*, Vol. 1 and 2, Pitagora, Bologna.

Cauchy, A. (1828): *Sur l'équilibre et le movement d'une lame solide, Exercices de Mathématique*, p. 3 .

Crisfield, M.A. and Packham, A.J. (1987) *A mechanism program for computing the strength of masonry arch bridges*, Transport and Road Research Laboratory, Department of Transport, Research Report 124.

Dischinger, F. (1928) *Die Schalenbauweise Zeiss-Dywidag unter besonderer Berücksichtigung von Kühlturmbauten*, Dyckerhoff & Widmann, Wiesbaden.

Dischinger, F. (1928) *Schalen und Rippenkuppeln*, In: Handbuch für Eisenbetonbau, pp. 151–371. Wilhelm Ernst & Sohn, Berlin.

Donnell, L.H. (1933) *Stability of thin-walled tubes under torsion*, NACA Report No. 479, Washington.

Elias, Z.M. (1967) *On the Duality Between the Problems of Stretching and of Bending of Plates,* National Aeronautics and Space Administration.

Foppl, A. (1892) *Das Fachwerk im Raume.* Leipzig: B. G. Teubner.

Fraternali, F., Angelillo, M. and Fortunato, A. (2002). *A lumped stress method for plane elastic problems and the discrete-continuum approximation,* International Journal of Solids and Structures 39.

Fraternali, F. and Rocchetta, G. (2002). *Shape optimization of masonry vaults,* In Proceedings of the Second International Conference on Advances in Structural Engineering and Mechanics, ASEM'02, Busan, Korea.

Grigolyuk, È.I. and Pelekh, B.L. (1972) *Static-geometric analogy and complex transformation in the theory of three-layered shells with light fillers,* in Doklady Akademii Nauk (Vol. 207, No. 3, pp. 563-565), Russian Academy of Sciences.

Grigolyuk, É.I. and Pelekh, B.L. (1973*) Static-Geometric Analogy and Complex Transformation in the Theory of Three-Layered Shells with Light Fillers*, in *Soviet Physics Doklady* (Vol. 17, p. 1108).

Grigorenko, Y. M., & Mukoed, A. P. (1986) *Application of the static-geometric analogy to the derivation of boundary conditions in the improved theory of shells*, Soviet Applied Mechanics, *22*(11), 1068-1073.

Heyman, J. (1977) *Equilibrium of shell structures*, Oxford:Oxford University Press.

Heyman, J. (1982) *The masonry arch,* Chichester: EllisHorwood.

Heyman, J. (1988) *Poleni's problem*, In: Proceedings of ICE,Part 1, 84. p. 737±59.

Hung, N. D. (1971) *Duality in the analysis of shells by the finite element method,* International Journal of Solids and Structures 7, no. 3: 281-299.

Kirchoff, G.R. (1850) *Über das Gleichgewicht und die Bewegung einer elastichen Schleibe*, Journal für die Reine und Angewandte Mathematik , 51–88.

Kleiber, M. and Wozniak, C. (1971) *On equations of the linear theory of elastic lattice shells* (Elastic lattice shells linear theory, deriving stress functions and equations from static- geometric analogy), Academie polonaise des sciences, Bulletin, Serie des sciences techniques, 19(3), 97.

Kurrer, K.E. (2002) *Geschichte der Baustatik*, Ernst & Sohn, Berlin.

Kurrer, K.E. (2008) *The History of the Theory of Structures. From Arch Analysis to Computational Mechanics*, Ernst & Sohn, Berlin.

Lamé, G. and Clapeyron, B.P.E. (1883) *Mémoire sur l'équilibre intérieur des corps solides homogènes*, Mémoires de l'Académie Royal des Sciences de l'Institut de France, 4.

Lun, E.I. and Pelekh,B.L (1970) *Static-geometric analogy and the method of complex transformation in a Timoshenko type linear theory of elastic shells* (Novozhilov complex transformation method extended to Timoshenko theory of elastic shells constructed with allowance for transverse shear deformation), In AKADEMIIA NAUK SSSR, DOKLADY, vol. 192, p. 1239.

Lun, E.I. and Pelekh, B. (1969) *A static-geometric analogy and the complex equations of a Timoshenko-type shell theory* (Static-geometric analogy of Kirchhoff-Love shell theory applied to Timoshenko complex equations allowing for transverse shear deformation), MEKHANIKA POLIMEROV, 5, pp.942-945.

Lurie, A. I. (1961) *On the static-geometric analogy of the theory of shells*, Muschilishvili Anniversary Volume .

Lur'e, A. I. (1961) *O statiko-geometricheskoy analogii teorii obolochek [On the shells theory static-geometric analogy]* Problemy mekhaniki sploshnoy sredy [Continuum mechanics prob-lems], Moscow, Gosstroyizdat Publ : 233-240.

Marmo,F. and Rosati L. (2017) *Reformulation and extension of the thrust network analysis*, Computers & Structures, Volume 182.

Mathieu, E. (1883) *Mémoire sur le movement vibratoire des cloches,* Journal de l'Ecole Polytechnique, 51st Cahier.

Muller-Breslau, H. (1891) *Beitrag zur Theorie des raumlichen Fachwerks,* Zentralblatt der Bauverwaltung, vol. 11.

Naghdi, P. M. (1964) *Further results in the derivation of the general equations of elastic shells,* International Journal of Engineering Science 2, no. 3: 269-273.

Nemish, Y. N. and Pelekh, B. L. (1969) *On the analogy between Timoshenko-type plate bending theory and the two-dimensional problem in moment theory of elasticity*, Soviet Applied Mechanics, 5(4), 440-443.

Novozhilov, V.V. (1947) *Teoriya Tonkikh Obolochek* (Theory of Thin Shells, in russian), Leningrad.

Novozhilov, V.V. (1959) *The Theory of Thin Shells*, Noordhoff, Groningen.

Novozhilov, V.V. (1964) *Thin Shell Theory,* Noordhoff, Groningen.

O'Dwyer, D. W. (1991) *Limit state analysis of masonry vaults*, M.Eng.Sc. thesis, University College, Galway, Ireland.

O'Dwyer, D. W. (1999) *Funicular Analysis of masonry vaults*, Comput. Struct., Vol. 73, No. 1-5, pp. 187-197.

Pavlović, M.N. (1985*) A simple model for thin shell theory*—Part 3: static-geometric analogy and the theorem of virtual work, Int J Mech Engng Educ.;13(4):281-7.

Pelekh, B. L. (1969), *Concerning the static-geometric analogy and the complex equations of Timoshenko-type shell theory*, Polymer Mechanics, 5(5), 839-841.

Pietraszkiewicz, W. (2016) *The resultant linear six-field theory of elastic shells: What it brings to the classical linear shell models?,* ZAMM-Journal of Applied Mathematics and Mechanics/Zeitschrift für Angewandte Mathematik und Mechanik, 96(8), 899-915.

Pippard, A.J.S. Tranter, E. Chitty, L. (1936) *The mechanics of the voussoir arch,* Journal of the ICE 1936;4:281±307.

Poisson, S.D. (1829) *Mémoire sur l'équilibre et le Mouvement des Corps élastiques*, Mémoires de l'Académie Royal des Sciencesde l'Institut de France 8, 357–570

Rosenbrock, H.H. (1960) *An automatic method for finding the greatest or least value of a function,* Computer Journal; 3:175-84.

Schek, H.J. (1974) *The force density method for form finding and computation of general networks*,

Computer Methods in Applied Mechanics and Engineering 3 (1), 115-134.

Steele, C.R. (1971) *A geometric optics solution for the thin shell equation*, International Journal of Engineering Science, 9(8), pp.681-704.

Simmonds, J. (1998) *Some comments on the status of shell theory at the end of the 20th century-complaints and correctives,* In 38th Structures, Structural Dynamics, and Materials Conference, p. 1074.

Taha, H.A. (1987) *Operations research: an introduction*, 4th ed. New York: MacMillan.

Timoshenko, S.P. (1940) *Theory of Plates and Shells*, McGraw-Hill Book Company.

Vasilenko, A.T. (1967) *The stress state of antisymmetrically loaded shells of revolution,* Soviet Applied Mechanics, 3(1), pp.35-39.

Visarion, V. and Stanescu, C. (1961) *An investigation of the quasi-invariants of the static-geometric analogy for thin elastic shells*, Journal of Applied Mathematics and Mechanics 25, no. 1: 93-104.

Williams, C. J. K. (1986) *Defining and designing curved exible tensile surface structures*, In J. A. Gregory (Ed.), The mathematics of surfaces, pp. 143-177.

Ringraziamenti

Ringrazio il Chiar.mo professor Alberto Carpinteri, per avermi guidato e supportato nella fase più importante del mio percorso accademico.

Un sentito grazie al professor Federico Accornero, correlatore di tesi, per il supporto costante e per i consigli indispensabili.

Ringrazio il Dott. Renato Caffarelli, per avermi dedicato del tempo ed aiutato nella realizzazione della tesi.

Grazie a Giulia, Sara e Roberta che mi hanno sopportato, oltre che supportato, in questa fase finale del mio percorso.

Infine, il più grande grazie lo dico a mia madre, che non ha mai smesso di credere in me.